

---

## Figures and tables

### Figures

(Figure A) Location of Geological Conservation Review (GCR) sites described in this volume.

(Figure B) A stratigraphical correlation of the Geological Conservation Review sites described in this volume. Sites appear more than once where they have multiple interests, or interests of different ages. Many of the ascriptions are highly provisional, and reference should be made to the individual site reports in this volume for a fuller discussion of the possible ages of the site evidence. Particular uncertainties are denoted by question marks.

(Figure 1.1) The oxygen isotope record, as represented in a borehole (Site 607) in the Mid-Atlantic at latitude *c.* 41°N. Numbered stages are shown at the top; even-numbered ones are relatively cold (more ice) and odd-numbered ones relatively warm (less ice). Note that the amplitude and wavelength of the curve increases at *c.* 0.7 million years ago (the  $\delta^{18}\text{O}$  scale is a ratio obtained by comparing the proportion of  $^{18}\text{O}$  to  $^{16}\text{O}$  in samples to that in a mean sea-water standard). (From Bridgland, 1994, compiled from data published by Ruddiman *et al.*, 1989).

(Figure 1.2) Portland Bill, Dorset, was chosen as a GCR site for its complex sequence of terrestrial and marine sediments. The site is exceptional in demonstrating raised beach deposits which can be assigned to two separate interglacials. These have been correlated with Stage 7 (*c.* 200 ka BP) and Stage 5e (*c.* 125 ka BP) of the deep-sea oxygen isotope record. The photograph shows the Stage 7 raised beach deposits, overlain by loam and head, on the west side of Portland Bill. (Photo: D.H. Keen.)

(Figure 2.1) The solid geology of South-West England. (Compiled from British Geological Survey sources.)

(Figure 2.2) The granite intrusions of South-West England: A, Isles of Scillies Granite; B, Land's End Granite; C, Cammellis Granite; D, St Austell Granite; E, Bodmin Moor Granite; F, Dartmoor Granite. (Adapted from Floyd *et al.*, 1993.)

(Figure 2.3) (a) Reconstructed Pleistocene maximum ice limits after Bowen (1994a) and Gray and Coxon (1991). (b) British glacial sediment systems. After Charlesworth (1957), and Bowen (1991). (But also see (Figure 8.4).)

(Figure 2.4) Brannam's Clay Pit in the 1960s, showing extensive working faces in the Fremington Clay. Although long held to be a 'Wolstonian' glacial deposit, the age and origin of the Clay remain highly controversial (Chapter 7). (Photo: N. Stephens.)

(Figure 2.5) Exposures in the Axe Valley terrace gravels at Kilmington Gravel Pit during the late 1960s. (Photo: N. Stephens.)

(Figure 2.6) The massive 'terrace' of raised beach, wind-blown sand ('sandrock') and periglacial head flanking Saunton Down in north Devon. (Photo: N. Stephens.)

(Figure 2.7) Quaternary coastal landforms and deposits around South-West England. (Adapted from Kidson, 1977.)

(Figure 2.8) Haytor Rocks, Dartmoor. Although tors such as these have evolved over an extremely protracted timescale, their final form, and that of the slopes around them, was fashioned by periglacial processes in the Devensian (Chapter 4). (Photo: S. Campbell.)

(Figure 2.9) Summary Holocene pollen diagrams from the Abbot's Way, Meare Heath and Sweet Track Factory sites in the Somerset Levels (selected taxa only). The vertical scale is based on dates in uncorrected radiocarbon years BP (before present 1950). (Adapted from Beckett and Hibbert, 1979.)

(Figure 3.1) (a) Southern and South-West England, showing localities referred to in the text, and selected geological outcrops. (b) Significant deposits and events in the geomorphological evolution of southern Britain. (Adapted from Green, 1985, with timescale based on Harland *et al.*, 1982.)

(Figure 3.2) Clay-filled chalk 'pipes' exposed along the northern working face of Beer Quarry in 1990.

(Figure 3.3) A large 'pipe' structure towards the western end of the north quarry face, showing the abrupt transition from chalk to the infill material (clay-with-flints). Even in monochrome, the profound darkening of the infill towards the pipe's margins can be seen clearly. (Photo: S. Campbell.)

(Figure 3.4) Detail of a typical pipe margin, showing the abrupt transition from chalk to clay-with-flints. (Photo: S. Campbell.)

(Figure 3.5) (a) Stratigraphic correlations of successions in the Bovey Basin, Newton Abbot bypass and Haldon Hills. (Adapted from Edwards, 1973, Hamblin, 1973b and Brunnsden *et al.*, 1976.) (b) Schematic representation (not to scale) of field relations of major lithostratigraphic units in the Sidmouth area. (Adapted from Isaac, 1981.)

(Figure 3.6) (a) The geology of the St Agnes and Beacon Cottage Farm outliers as interpreted by Walsh *et al.* (1987). The area between Cameron Quarry and the Beacon was regarded as problematic and has been re-mapped by Jowsey *et al.* (1992) (Figure 3.7); (b) Isopachs of combined Tertiary and Quaternary sediment. (Adapted from Walsh *et al.*, 1987.)

(Figure 3.7) (a) A revision of the St Agnes and Beacon Cottage Farm outliers by Jowsey *et al.* (1992). (b) Borehole and trench sections along line X–C (diagram a), adapted from Jowsey *et al.* (1992). (c) Stratigraphic sections along line D–C (diagram a), compiled from various sources. (d) Schematic reconstruction of the Beacon Cottage Farm and St Agnes outliers, based on Jowsey *et al.* (1992).

(Figure 3.8) Members of the Quaternary Research Association examine the sequence at St Agnes during the Annual Field Trip to west Cornwall in 1980. The sands are overlain unconformably by periglacial head. (Photo: S. Campbell.)

(Figure 4.1) Location of GCR sites in relation to: A, Isles of Scilly Granite; B, Land's End Granite; C, Carrunellis Granite; D, St Austell Granite; E, Bodmin Moor Granite; and F, Dartmoor Granite. (Adapted from Floyd *et al.*, 1993.)

(Figure 4.2) Linton's (1955) classic two-stage model of tor formation.

(Figure 4.3) A model of slope development for Dartmoor, after Waters (1964). Profiles: (a) Products of *in situ* weathering on a granite substrate; (b) Inversion of normal weathering profile following two separate periods of periglacial mass wasting; (c) and (d) Measured sections at Shilstone Pit [SX 659 902], Dartmoor. Many slope configurations, however, do not conform to this model (see text).

(Figure 4.4) A schematic composite representation of the main geomorphological features of Dartmoor. (After Gerrard, 1983.)

(Figure 4.5) Simplified geology of the Merrivale area. (Adapted from Gerrard, 1983.)

(Figure 4.6) Aerial photograph (scale c. 1:10 000) showing: (a) Cox Tor; (b) Roos Tor; (c) Great Staple Tor; (d) Middle Staple Tor; (e) Little Staple Tor; (f) Merrivale Quarry. Distinct 'boulder runs' of cater are particularly evident around the Staple Tors. (Cambridge University Collection: copyright reserved.)

(Figure 4.7) The geomorphology of Cox Tor and adjacent areas. (Adapted from Gerrard, 1983.)

(Figure 4.8) Great Staple Tor seen from Middle Staple Tor. The missing central portion or 'avenue' of Great Staple Tor can be seen clearly on the horizon. (Photo: S. Campbell.)

(Figure 4.9) Looking west through the 'avenue' of Great Staple Tor. (Photo: S. Campbell.)

(Figure 4.10) Great Staple Tor seen from Cox Tor, revealing a diverging anastomosing pattern of boulder runs on the west-facing slopes. (Photo: S. Campbell.)

(Figure 4.11) A profusion of earth hummocks on the east-facing slopes of Cox Tor, with Great Staple Tor and Middle Staple Tor on the horizon. (Photo: S. Campbell.)

(Figure 4.12) Granite alteration products and slope deposits at Believer Quarry being examined during the 1977 INQUA trip to the South-West. (Photo: N. Stephens.)

(Figure 4.13) A cross-section through the granite and associated alteration products at Two Bridges Quarry, Dartmoor, adapted from Campbell (1991).

(Figure 4.14) The section at Two Bridges Quarry, showing large intact granite masses, the unexhumed tors and adjacent deeply altered granite. (Photo: S. Campbell.)

(Figure 4.15) The disused china clay workings at Hawks Tor, Bodmin Moor. The altered granite or gowan is seen in the foreground faces, with the cliffed, but somewhat degraded, Devensian late-glacial and Holocene sequence along the lake edge behind. (Photo: S. Campbell.)

(Figure 4.16) A simplified composite section of the north-east face of the exposures at Hawks Tor as exposed in 1970–1971. Adapted from Brown (1977, 1980).

(Figure 4.17) The peat bog at the south-west end of Dozmary Pool, Bodmin Moor. (Photo: S. Campbell.)

(Figure 4.18) Blacklane Brook pollen site, southern Dartmoor. (Photo: S. Campbell.)

(Figure 4.19) Shallow peat sections exposed along Black Ridge Brook, northern Dartmoor. (Photo: C.J. Caseldine.)

(Figure 4.20) Simplified pollen diagram for Black Ridge Brook, adapted from Caseldine and Maguire (1986).

(Figure 5.1) (a) The principal localities where remains of Pleistocene mammals have been found in Devon, after Sutcliffe (1969). (b) Excavated caves in the Torbryan Valley, after Roberts (1996). The location of Berry Head 'sea caves' (Proctor, 1994, 1996) is also shown.

(Figure 5.2) Kent's Cavern, after Straw (1996). Distribution of: (a) Breccia; (b) Crystalline Stalagmite; (c) Cave Earth. (a)–(c) are shown as indicated in Reports to the British Association by W. Pengelly, 1865–1880. Cave outline is based on the survey by Proctor and Smart (1989).

(Figure 5.3) Plan of Pixie's Hole, after Collcutt (1984).

(Figure 5.4) Joint Mitnor Cave, Buckfastleigh: (a) General elevation and plan. (b) Detail of excavated section. (Based on the work of A.J. Sutcliffe and adapted from Sutcliffe's original drawing and Sutcliffe's (1974) simplified section.)

(Figure 6.1) (a) Quaternary deposits at Portland Bill, adapted from Davies and Keen (1985). (b) The Quaternary sequence at AUWE, adapted from Keen (1985). The cross-section follows line A–B shown in plan above.

(Figure 6.2) The Quaternary sequence at Hope's Nose. (Adapted from Mottershead *et al.*, 1987.)

(Figure 6.3) Coastal head deposits overlying a raised shore platform at Great Mattiscombe Sand [SX 816 369], 1.2 km west of Start Point. (Photo: D.H. Keen.)

(Figure 6.4) Coastal exposures at the western end of Pendower Beach, showing a compound shore platform cut across steeply dipping slates, overlain by cemented raised beach deposits and head. (Photo: S. Campbell.)

(Figure 6.5) A striking unconformity between the shore platform and overlying, cemented raised beach deposits at Pendower, viewed by members of the Quaternary Research Association in 1980. (Photo: S. Campbell.)

(Figure 6.6) The Giant's Rock at Porthleven, the South-West's most famous erratic — author for scale. (Photo: S. Campbell.)

(Figure 6.7) Boscawen GCR site (St Loy's Cove): solifluction deposits interbedded with organic sediments towards the base of the section. (Photo: J.D. Scourse.)

(Figure 6.8) Porth Nanven, west Cornwall: the spectacular 'raised boulder beach' overlain by solifluction deposits. (Photo: D.H. Keen.)

(Figure 6.9) Coastal exposures near Godrevy Cove, showing shore platform overlain by raised beach cobbles, sand and various head facies. (Photo: S. Campbell.)

(Figure 6.10) The Quaternary sequence at Trebetherick Point: Section 1 after Arkell (1943); Section 2 compiled by S. Campbell.

(Figure 7.1) The distribution and proposed stratigraphical relationships of Quaternary deposits around the Taw–Torrige Estuary. (After Kidson and Heyworth, 1977.)

(Figure 7.2) The extent of the Fremington 'boulder-clay' according to Maw (1864), and proposed stratigraphical relationships in the Fremington area. (After Maw, 1864, Mitchell, 1960 and Kidson and Wood, 1974.)

(Figure 7.3) The Quaternary sequence at Brannam's Clay Pit, Fremington. (a) Composite section of the former eastern and southern working faces, adapted from Stephens (1966a, 1966b, 1970a). (b) The succession recorded by Croot in 1987. (c) The sequence recorded by Croot *et al.* (1996).

(Figure 7.4) A reconstruction of the proposed Wolstonian (Saalian) glaciation of the Barnstaple Bay area, after Edmonds (1972), illustrating: (a) The development of ice-marginal drainage at the height of glaciation; (b) Present-day drainage.

(Figure 7.5) The Pleistocene sequence towards the western end of the Fremington Quay exposure. The vertical 'pipe' structures are infilled with lighter-coloured silt and clay, and penetrate beyond the base of the exposure: they may be frost or desiccation cracks (Wood, 1970). (Photo: S. Campbell.)

(Figure 7.6) The Quaternary sequence at the eastern end of the Fremington Quay exposure. (After Croot *et al.*, *in prep.*)

(Figure 7.7) Members of the Quaternary Research Association discuss possible evidence for glaciotectonism at the base of the Pleistocene succession towards the eastern end of the Fremington Quay exposures. (Photo: S. Campbell.)

(Figure 7.8) The Quaternary deposits and coastal morphology of the Croyde–Saunton Coast. (Adapted from Stephens, 1970a.)

(Figure 7.9) The Quaternary succession at: (a) Pencil Rock; (b) East of Pencil Rock, based on the work of R.M. Eve (1970) and adapted from Stephens (1974).

(Figure 7.10) Marine-cut platforms between Saunton and Baggy Point, based on the work of R.M. Eve (1970) and adapted from Stephens (1974). (See (Figure 7.8) for locations of cross-sections.)

(Figure 7.11) Saunton's famous 'pink granite' erratic, sealed beneath cemented sand and seen during the 1996 Annual Field Meeting of the Quaternary Research Association. (Photo: S. Campbell.)

(Figure 7.12) Extensively developed rock platforms at the western end of Saunton Down, looking north across Croyde Bay. (Photo: S. Campbell.)

(Figure 7.13) Thick cemented sand (marine and aeolian) and overlying head deposits near Saunton Sands Hotel. (Photo: S. Campbell.)



(Figure 7.14) Quaternary landforms and deposits at Westward Ho! (Adapted from Stephens 1970a.)

(Figure 7.15) The distribution of Holocene deposits at Westward Ho! (Adapted from Balaam *et al.*, 1987.)

(Figure 7.16) Plan and section of the midden 'island' at Westward Ho! (Adapted from Balaam *et al.*, 1987.)

(Figure 7.17) The Pleistocene sequence at Westward Ho!, showing the higher marine-cut platform overlain by raised 'cobble' beach and head deposits, with a lower platform extending into the distance. (Photo: S. Campbell.)

(Figure 7.18) (a) Landforms and Pleistocene deposits between Lynmouth and Woody Bay. (b) Profile of Pleistocene deposits within the Valley of Rocks and at Lee Abbey. (Adapted from Dalzell and Durrance, 1980.)

(Figure 7.19) The Valley of Rocks, looking east from Wringcliff Bay. (Photo: S. Campbell.)

(Figure 7.20) The evolution of the Valley of Rocks by: (a) Pre-Devensian glacial meltwaters; (b) Marine erosion and river capture. (Adapted from Mottershead, 1967, 1977c.)

(Figure 7.21) Tor-like buttresses and precipitous rock slopes on the northern margin of the Valley of Rocks, looking west. (Photo: S. Campbell.)

(Figure 7.22) (a) The location of the Doniford gravels. (b) Typical section through the Doniford gravels west of the footpath. (Adapted from Gilbertson and Mottershead, 1975.)

(Figure 7.23) The Doniford gravels overlying Liassic bedrock at the eastern end of Helwell Bay. (Photo: S. Campbell.)

(Figure 7.24) Quaternary deposits (mainly fluvial cobbly gravels; bed 2) exposed on the western bank of the Swill in 1980. (Photo: S. Campbell.)

(Figure 7.25) Selected pollen data and radiocarbon dates from a peat profile at The Chains, Exmoor. (Adapted from Merryfield and Moore 1974.)

(Figure 8.1) The Isles of Scilly: critical sites, exposures of the Scilly Till, the southern limit of the Hell Bay Gravel and Mitchell and Orme's (1967) glacial limit. (Adapted from Scourse, 1991.)

(Figure 8.2) Carn Morval on St Mary's (Figure 8.1) is one of five sites on the Isles of Scilly where organic sediments, which have yielded pollen evidence and radiocarbon dates, lie beneath or interbedded with periglacial head. Although yielding the most detailed of these palaeoenvironmental records, Carn Morval was not selected as a GCR site because coastal erosion has since removed much of the critical organic sequence. (Photo: J.D. Scourse.)

(Figure 8.3) A lithostratigraphic model for the Isles of Scilly. (Adapted from Scourse, 1991.)

(Figure 8.4) A reconstruction of the Celtic Sea ice lobe and glaciomarine terminus at 19 ka BP, adapted from Scourse *et al.* (1991). Dots represent vibrocoring sites which have yielded glacial sediment.

(Figure 8.5) The Pleistocene sequence at Watermill Cove. (Adapted from Scourse 1991.)

(Figure 8.6) (a) Variations in tor morphology. (b) Their distribution across the Isles of Scilly. (Adapted from Scourse 1986.)

(Figure 8.7) The spectacular development of horizontal tors (form (a); (Figure 8.6)) on the eastern side of Peninnis Head. (Photo: S. Campbell.)

(Figure 8.8) The Pleistocene sequence at Porth Seal: Sections 1 and 2 adapted from Scourse (1991); Section 3 is based on a field sketch made in 1965 by F.M. Syngé and subsequently figured in Stephens (1970a) and Kidson (1977).

(Figure 8.9) Richly organic sediments lying beneath periglacial head at Porth Seal, St Martin's. (Photo: J.D. Scourse.)

(Figure 8.10) The Pleistocene sequence at Bread and Cheese Cove. (Adapted from Scourse, 1991.)

(Figure 8.11) The Quaternary sequence at Chad Girt according to Barrow (1906). (Adapted from Scourse, 1986.)

(Figure 8.12) The Pleistocene Sequence at the Battery section. (Adapted from Scourse, 1986.)

(Figure 8.13) Quaternary sediments exposed in coastal cliffs at Castle Porth, Tresco. The Hell Bay Gravel at the northern end of the exposure (left) is rich in erratics, whereas erratics are absent at the southern end (right) of the section. (Photo: S. Campbell.)

(Figure 8.14) Selected pollen data and radiocarbon dates for a peat profile at Higher Moors, St Mary's. (Adapted from Scaife, 1984.)

(Figure 9.1) The Mendips and Somerset lowland, showing GCR sites described in this chapter, and selected GCR sites described in Chapters 7 and 10.

(Figure 9.2) A correlation of Pleistocene deposits in the Somerset lowland, Mendips, Bristol district and Avon Valley. (Adapted from Campbell *et al.*, in prep.)

(Figure 9.3) The Burtle Formation of the Somerset lowland. (Adapted from Kidson *et al.*, 1978 and Hunt, 1987.)

(Figure 9.4) An interpretation of the Quaternary sequence at Greylake No. 2 Quarry, adapted from Hughes (1980). Beds 1–15 are described in more detail in the text.

(Figure 9.5) A cross-section of the Pleistocene deposits at Portfield. (Adapted from Hunt, 1987.)

(Figure 9.6) The molluscan biostratigraphy of Pleistocene deposits at Portfield, adapted from Hunt (1987). Numbers 364 and 365 refer to boreholes shown in (Figure 9.5).

(Figure 9.7) The distribution of Quaternary deposits near Langport, Somerset. (Adapted from Hunt 1987.)

(Figure 9.8) The molluscan biostratigraphy of Pleistocene deposits at Low Ham. (Adapted from Hunt 1987.)

(Figure 9.9) (a) The topographic setting of the Axe Valley and the distribution of plateau-gravel sites. (b) The principal exposures of the Axe Valley terrace gravels. (Adapted from Stephens, 1977 and Green *et al.*, in prep.)

(Figure 9.10) The long-profile of the modern River Axe, and the height-range and distribution of the principal terrace gravel outcrops. (Adapted from Green *et al.*, in prep.)

(Figure 9.11) Extensive exposures at Chard Junction through the Axe Valley terrace gravels in 1985. (Photo: S. Campbell.)

(Figure 9.12) (a) Location of the Broom Gravel Pits, adapted from Green *et al.* (in prep.). (b) Schematic section of the Broom gravels, adapted from Reid Moir (1936) and Hawkes (1943). (c) An interpretation of a section of the Broom gravels, adapted from J.F.N. Green (1947) and Calkin and Green (1949). (d) A schematic composite section of the Broom gravels, adapted from Shakesby and Stephens (1984).

(Figure 9.13) 'Cherry' gravels with sand lenses, seen in the south-east faces of the disused Railway Pit at Broom in 1985. (Photo: S. Campbell.)

(Figure 9.14) Acheulian hand-axes from Broom, seen during the 1977 INQUA visit to South-West England. (Photo: N. Stephens.)

(Figure 9.15) Quaternary deposits at Swallow Cliff, Middle Hope, simplified from Gilbertson and Hawkins (1977).

(Figure 9.16) The Quaternary sequence at Brean Down, simplified from ApSimon *et al.* (1961).

(Figure 9.17) The Pleistocene sequence at Brean Down. (Photo: S. Campbell.)

(Figure 9.18) Schematic cross-section of the Buffington fan at Bourne, showing the aggradational components of the fan and their relationship to the Bourne section. (Adapted from Pounder and Macklin, 1985.)

(Figure 9.19) The Quaternary sequence exposed in the old railway cutting at Wookey Station. (Adapted from Macklin and Hunt, 1988.)

(Figure 10.1) The Avon Valley and Bristol district, showing GCR sites described in this chapter.

(Figure 10.2) Schematic cross-section through Quaternary sediments in the 'col-gully' at Court Hill. (Adapted from Gilbertson and Hawkins, 1978b.)

(Figure 10.3) A four-stage model to explain the formation of the Court Hill 'col-gully'. (Adapted from Gilbertson and Hawkins, 1978b.)

(Figure 10.4) The Pleistocene sequence at Nightingale Valley, adapted from Hunt (in prep.).

(Figure 10.5) The Quaternary sequence at Kennpier. (Adapted from Andrews *et al.*, 1984.)

(Figure 10.6) The commonest marine dinoflagellate cyst in the Kennpier interglacial deposit (bed 3) - *Achomosphaera andalousiense* Jan du Chene — seen at a magnification of *c.* x 1000 by UV fluorescence microscopy. (Photo: S.A.V. Hall.)

(Figure 10.7) Pollen diagram for Kennpier. (Adapted from Hunt, 1981.)

(Figure 10.8) The Quaternary sequence at Weston-in-Gordano. (Adapted from ApSimon and Donovan, 1956.)

(Figure 10.9) The Quaternary sequence at Holly Lane, Clevedon. (Adapted from Gilbertson and Hawkins, 1974.)

## Tables

(Table 7.1) Radiocarbon dates from the outer peat.

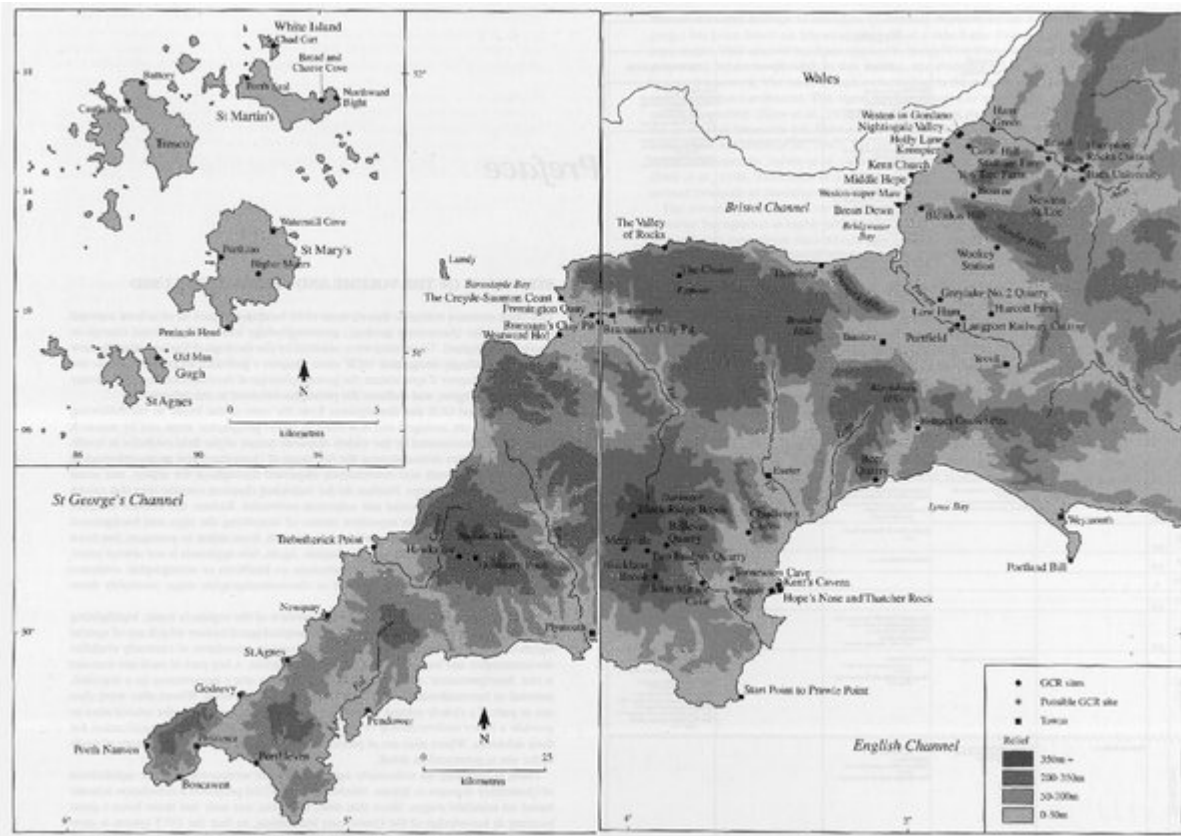
(Table 9.1) Fossil molluscs from the Chadbrick Gravel.

(Table 10.1) Fossil molluscs from three profiles through the interglacial channel-fill at Kennpier Footbridge (after Gilbertson and Hawkins, 1978a).

(Table 10.2) Fossil molluscs from the interglacial deposit at Yew Tree Farm (after Gilbertson and Hawkins, 1978a).

(Table 10.3) Molluscs from the interglacial deposit at Kenn Church (after Gilbertson, 1974; Gilbertson and Hawkins, 1978a).

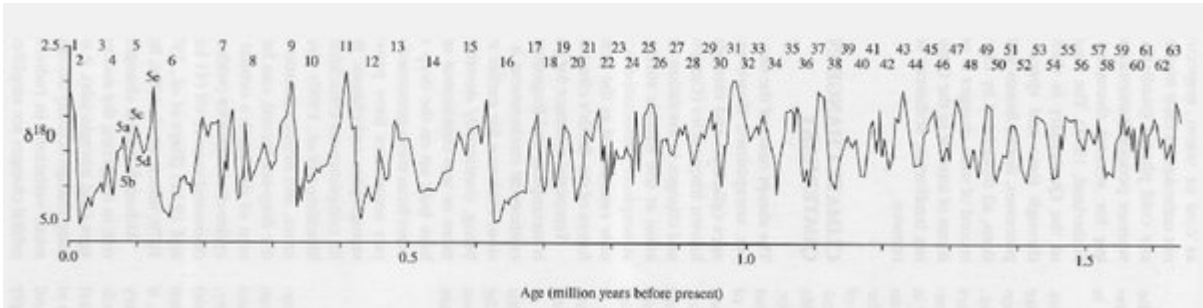
## [References](#)



(Figure A) Location of Geological Conservation Review (GCR) sites described in this volume.

Oxygen Isotope Stage Age (Ma BP)	Region				
	Isles of Scilly	Cornwall (mainland)	Devon	Dorset	Somerset & Avon
1 10	Higher Moor pass	Winkle Tor and Bosbury Field pass Godfrey pass	Merrivale road (mainland) Black Ridge Brook pass Kend's Cairns (mainland) Westward Hill (pass)		The Chalk and Groveley No. 2 Quarry sites Husley Station (mainland) Kempsey (mainland) New Free Farm (mainland)
2 24	Portlino (mainland) Watermill Cove (mainland) Old Man (mainland) Preston's Head (sea) Porth Seal (mainland) Boswell & Chase Cove (sea) Chad Cliff (mainland) Northward Right (mainland) Bosbury (mainland) Castle Park (mainland)	Winkle Tor (sea) Penderon (mainland) Boswell (mainland) Porth Nannon (mainland) Godfrey (mainland) Tretterbeck Point (mainland)	Merrivale (sea) Belver Quarry (mainland) Two Bridges Quarry (mainland) Kend's Cairns (sea) Boswell (sea) Chadleigh Cove (sea) Hep's Nose & Thimble Rock (sea) Sturt Point to Frowle Point (sea) Boswell (sea) Croyde-Saxton Coast (sea) Westward Hill (sea) The Valley of Rocks (sea)	Portland Hill (mainland)	Portfield (sea) Boswell (sea) Husley Station (sea) Bully Lane (sea)
3 59	Watermill Cove (sea) Porth Seal (sea) Boswell & Chase Cove (sea)	Boswell (sea)	Kend's Cairns (sea) Boswell (sea)		Boswell (sea)
4 71	Porth Seal (sea)	Penderon (sea) Boswell (sea) Tretterbeck Point (sea)	Boswell (sea) Croyde-Saxton Coast (sea)	Portland Hill (sea)	Boswell (sea) Bully Lane (sea)
5a-d 116					Low Ham (sea)
5e 128	Portlino (sea) Watermill Cove (sea) Porth Seal (sea) Chad Cliff (sea) Northward Right (sea)	Penderon (sea) Porth Nannon (sea) Godfrey (sea) Tretterbeck Point (sea)	Kend's Cairns (sea) Boswell (sea) Chadleigh Cove (sea) Jane Minnor (sea) Hep's Nose & Thimble Rock (sea) The Valley of Rocks (sea) Croyde-Saxton Coast (sea) Westward Hill (sea)	Portland Hill (sea) Portland Hill (sea)	Langport Railway Cutting (sea) Groveley No. 2 Quarry (sea) Mable Hope (sea) Boswell (sea) Hampton Rocks Cutting (sea)
6 185		Penderon (sea) Godfrey (sea)	Boswell (sea) Croyde-Saxton Coast (sea)	Portland Hill (sea) Boswell (sea)	Portfield (sea) Boswell (sea) Hampton Rocks Cutting (sea)
7 245		Penderon (sea) Porth Nannon (sea) Godfrey (sea)	Boswell (sea) Hep's Nose & Thimble Rock (sea) Croyde-Saxton Coast (sea)	Portland Hill (sea) Boswell (sea)	Groveley No. 2 Quarry (sea) Portfield (sea) Boswell (sea)
8 301			Hep's Nose & Thimble Rock (sea)		Langport Railway Cutting (sea) Sixham Farm (sea)
9 379			Kend's Cairns (sea)		Hampton Rocks (sea)
10 423			Kend's Cairns (sea)		Hampton Rocks (sea)
11 478			Boswell (sea) The Valley of Rocks (sea) Fremington Quay (sea)		Hampton Rocks (sea)
13-21		Portland Hill (sea)	Kend's Cairns (sea) Boswell (sea) Boswell (sea)		Portland Hill (sea) Boswell (sea) Boswell (sea) Boswell (sea) Boswell (sea) Boswell (sea) Boswell (sea) Boswell (sea) Boswell (sea) Boswell (sea) Boswell (sea)
Pre-Pleistocene	Preston's Head (sea)	St Agnes Beach (sea) St Agnes Beach (sea)	Portlino (sea) Merrivale (sea) Belver Quarry (sea) Two Bridges Quarry (sea)		

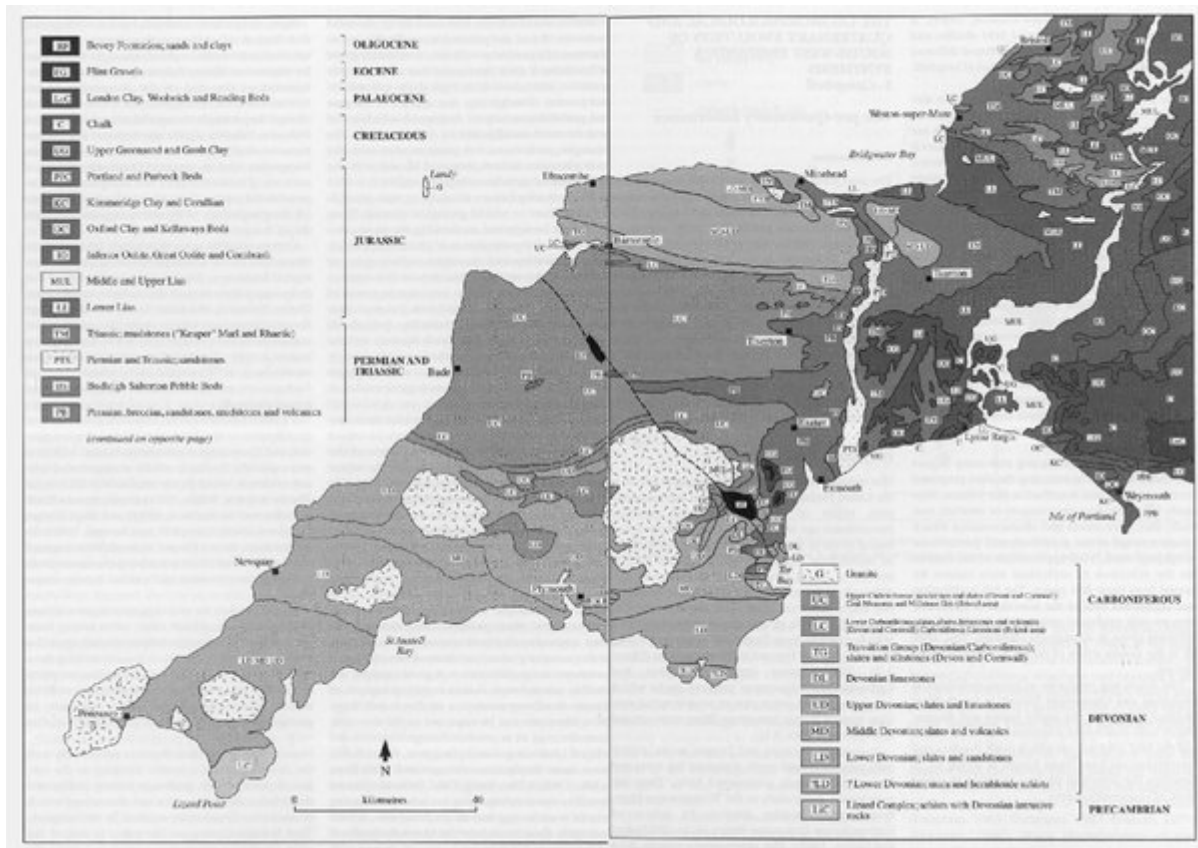
(Figure B) A stratigraphical correlation of the Geological Conservation Review sites described in this volume. Sites appear more than once where they have multiple interests, or interests of different ages. Many of the ascriptions are highly provisional, and reference should be made to the individual site reports in this volume for a fuller discussion of the possible ages of the site evidence. Particular uncertainties are denoted by question marks.



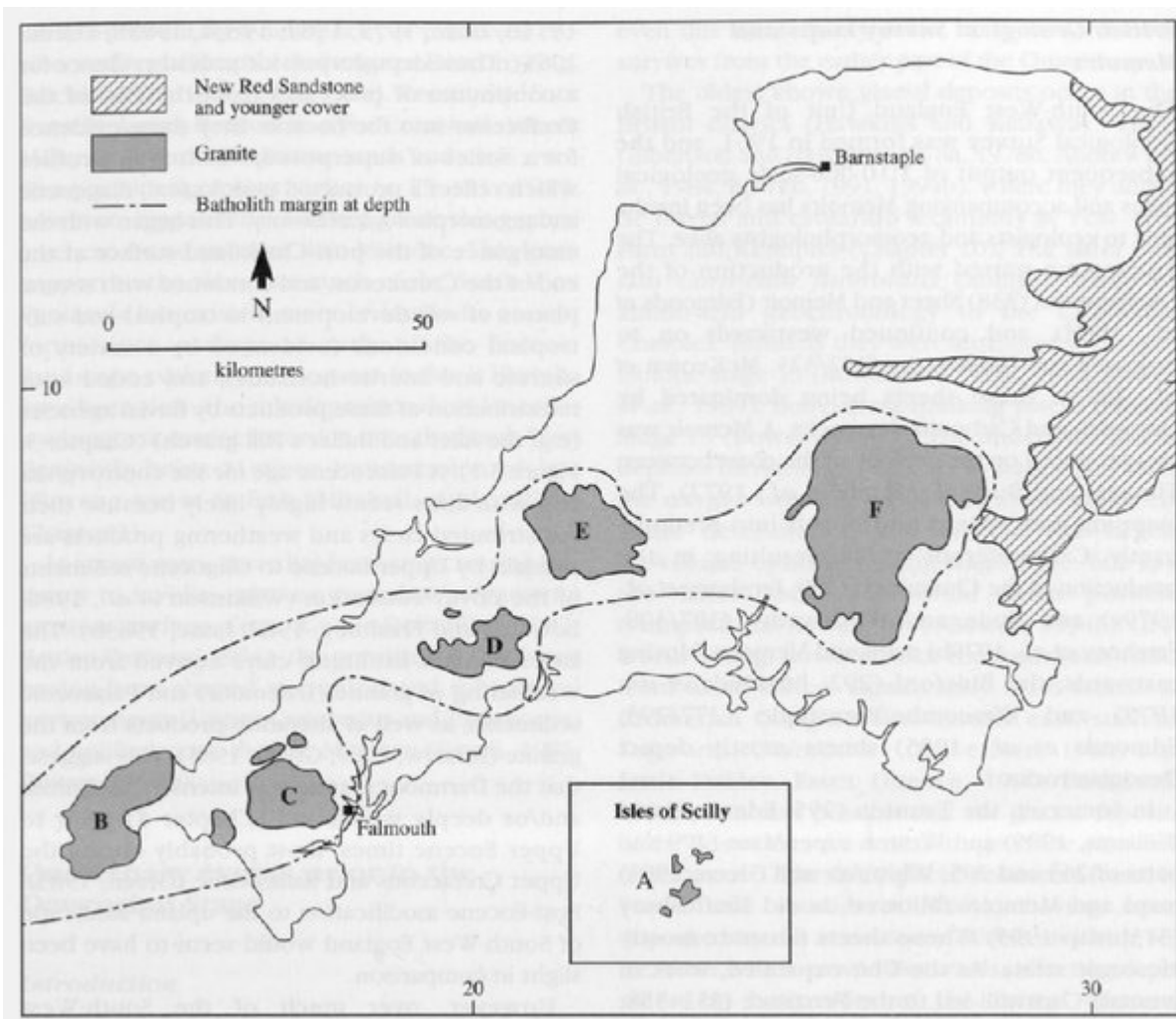
(Figure 1.1) The oxygen isotope record, as represented in a borehole (Site 607) in the Mid-Atlantic at latitude c. 41°N. Numbered stages are shown at the top; even-numbered ones are relatively cold (more ice) and odd-numbered ones relatively warm (less ice). Note that the amplitude and wavelength of the curve increases at c. 0.7 million years ago (the  $\delta^{18}\text{O}$  scale is a ratio obtained by comparing the proportion of  $^{18}\text{O}$  to  $^{16}\text{O}$  in samples to that in a mean sea-water standard). (From Bridgland, 1994, compiled from data published by Ruddiman et al., 1989).



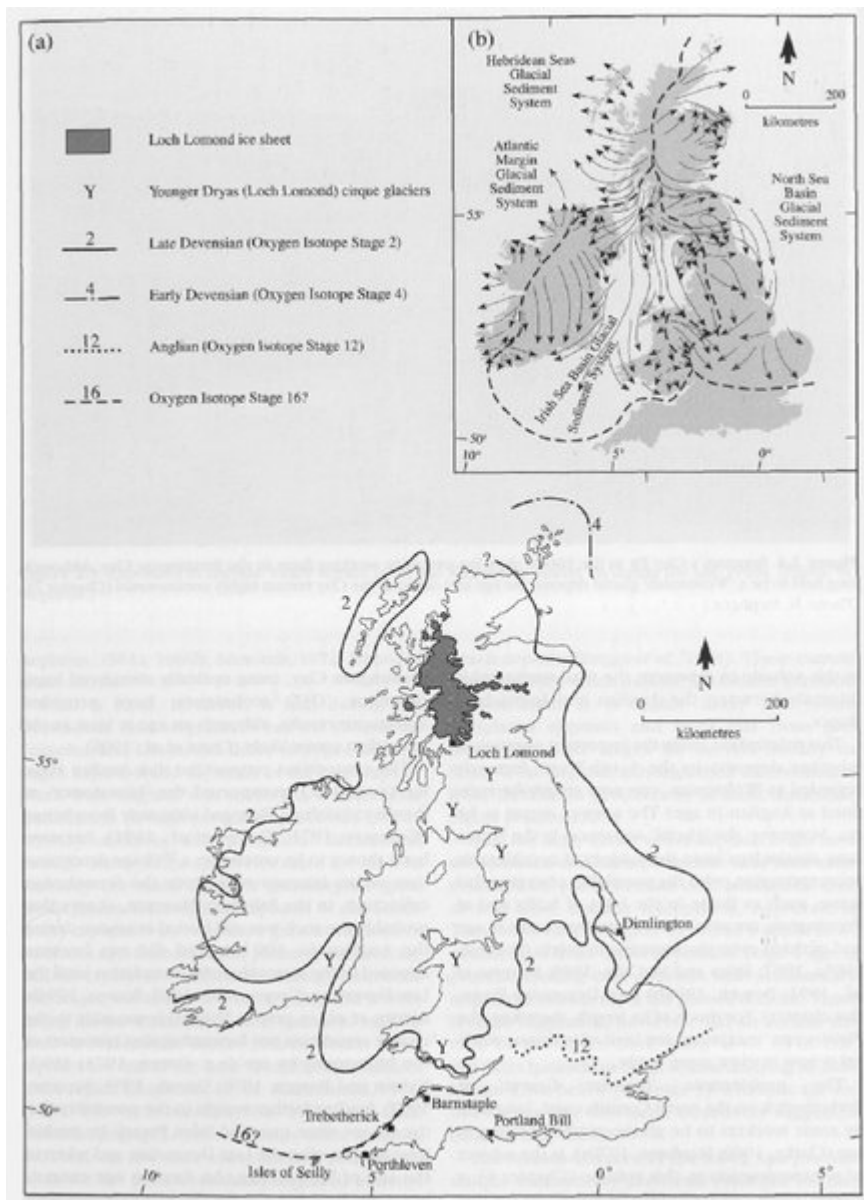
(Figure 1.2) Portland Bill, Dorset, was chosen as a GCR site for its complex sequence of terrestrial and marine sediments. The site is exceptional in demonstrating raised beach deposits which can be assigned to two separate interglacials. These have been correlated with Stage 7 (c. 200 ka BP) and Stage 5e (c. 125 ka BP) of the deep-sea oxygen isotope record. The photograph shows the Stage 7 raised beach deposits, overlain by loam and head, on the west side of Portland Bill. (Photo: D.H. Keen.)



(Figure 2.1) The solid geology of South-West England. (Compiled from British Geological Survey sources.)

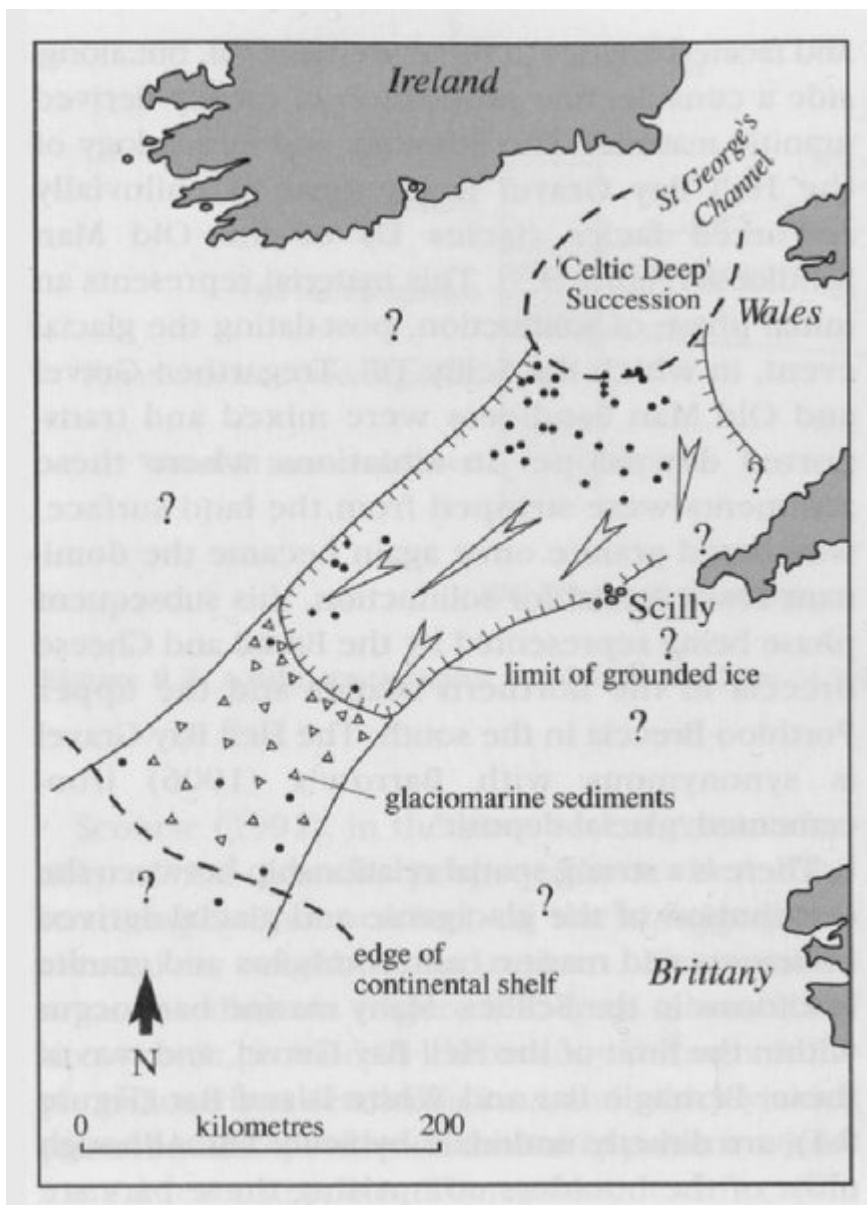


(Figure 2.2) The granite intrusions of South-West England: A, Isles of Scillies Granite; B, Land's End Granite; C, Cammellis Granite; D, St Austell Granite; E, Bodmin Moor Granite; F, Dartmoor Granite. (Adapted from Floyd et al., 1993.)



(Figure 2.3) (a) Reconstructed Pleistocene maximum ice limits after Bowen (1994a) and Gray and Coxon (1991). (b) British glacial sediment systems. After Charlesworth (1957), and Bowen (1991). (But also see (Figure 8.4).)

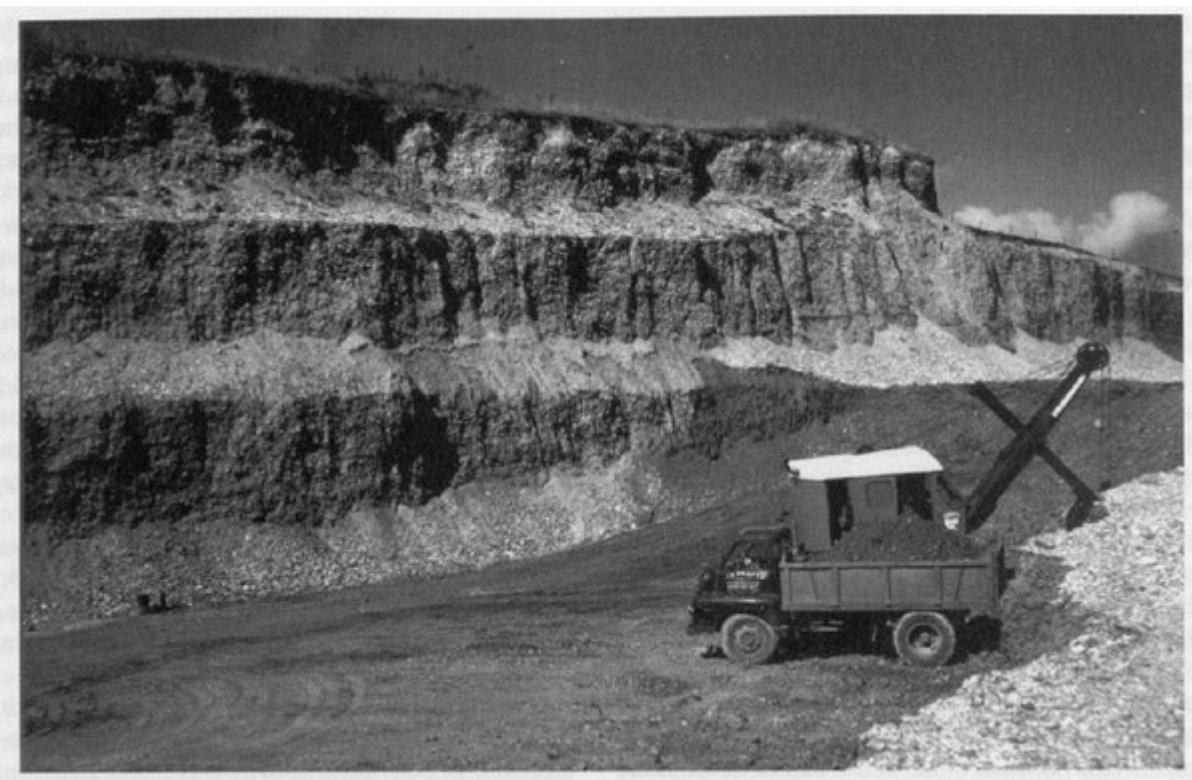




(Figure 8.4) A reconstruction of the Celtic Sea ice lobe and glaciomarine terminus at 19 ka BP, adapted from Scourse et al. (1991). Dots represent vibrocoring sites which have yielded glaciogenic sediment.



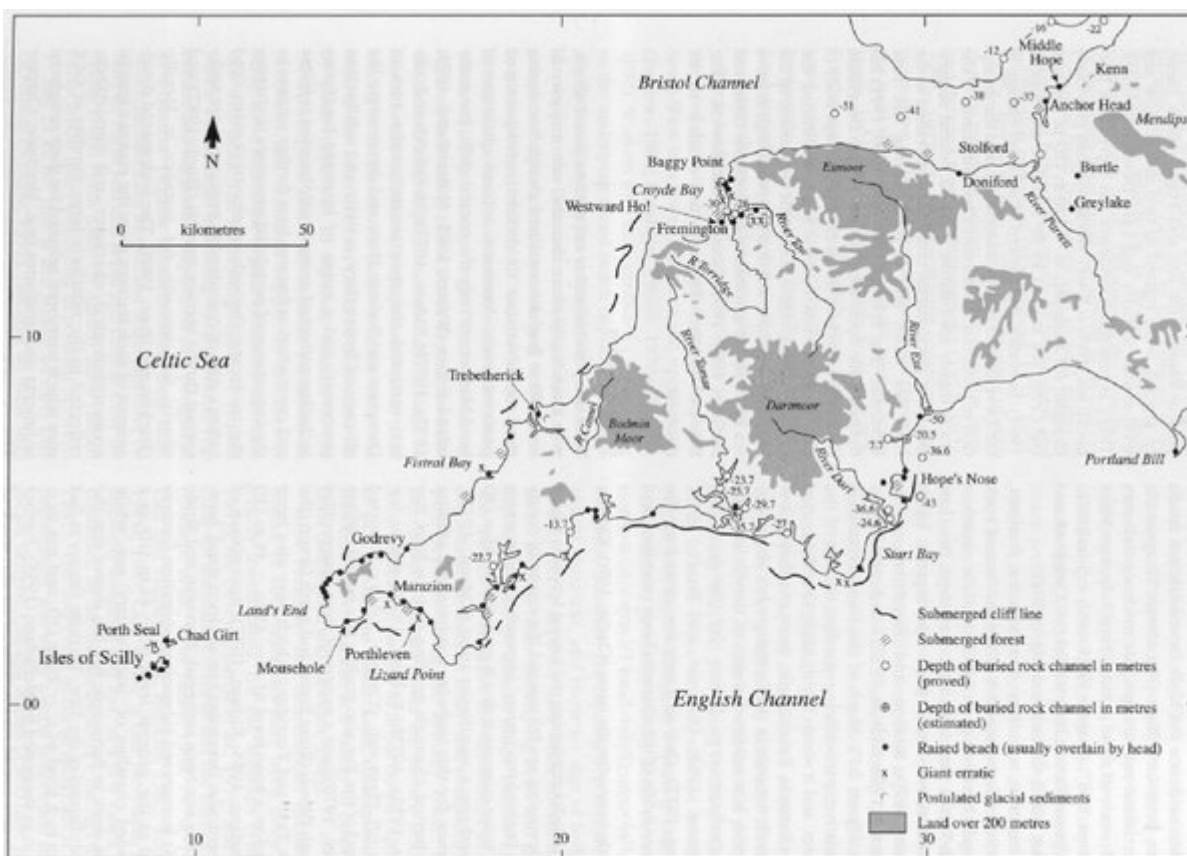
*(Figure 2.4) Brannam's Clay Pit in the 1960s, showing extensive working faces in the Fremington Clay. Although long held to be a 'Wolstonian' glacial deposit, the age and origin of the Clay remain highly controversial (Chapter 7). (Photo: N. Stephens.)*



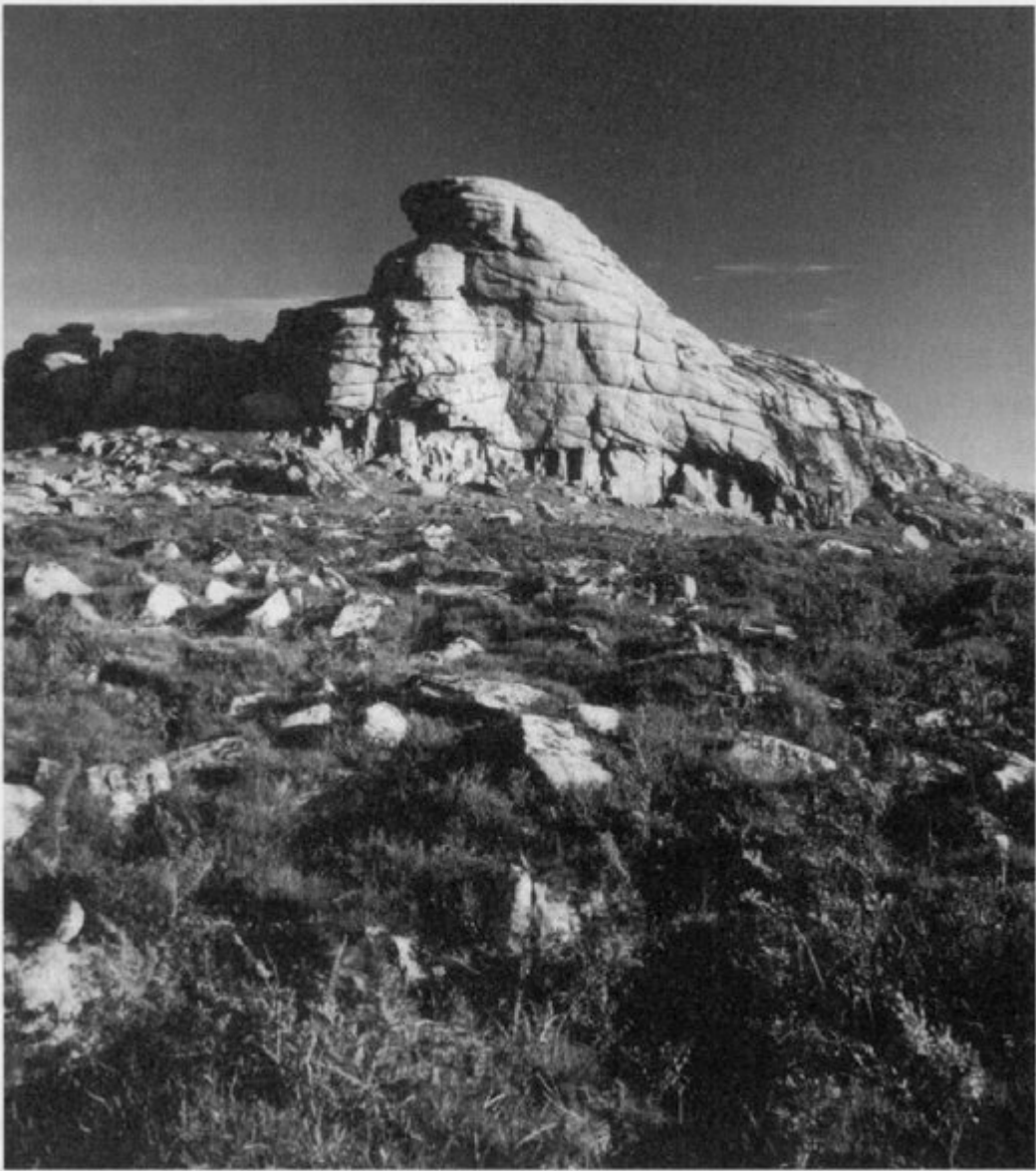
*(Figure 2.5) Exposures in the Axe Valley terrace gravels at Kilmington Gravel Pit during the late 1960s. (Photo: N. Stephens.)*



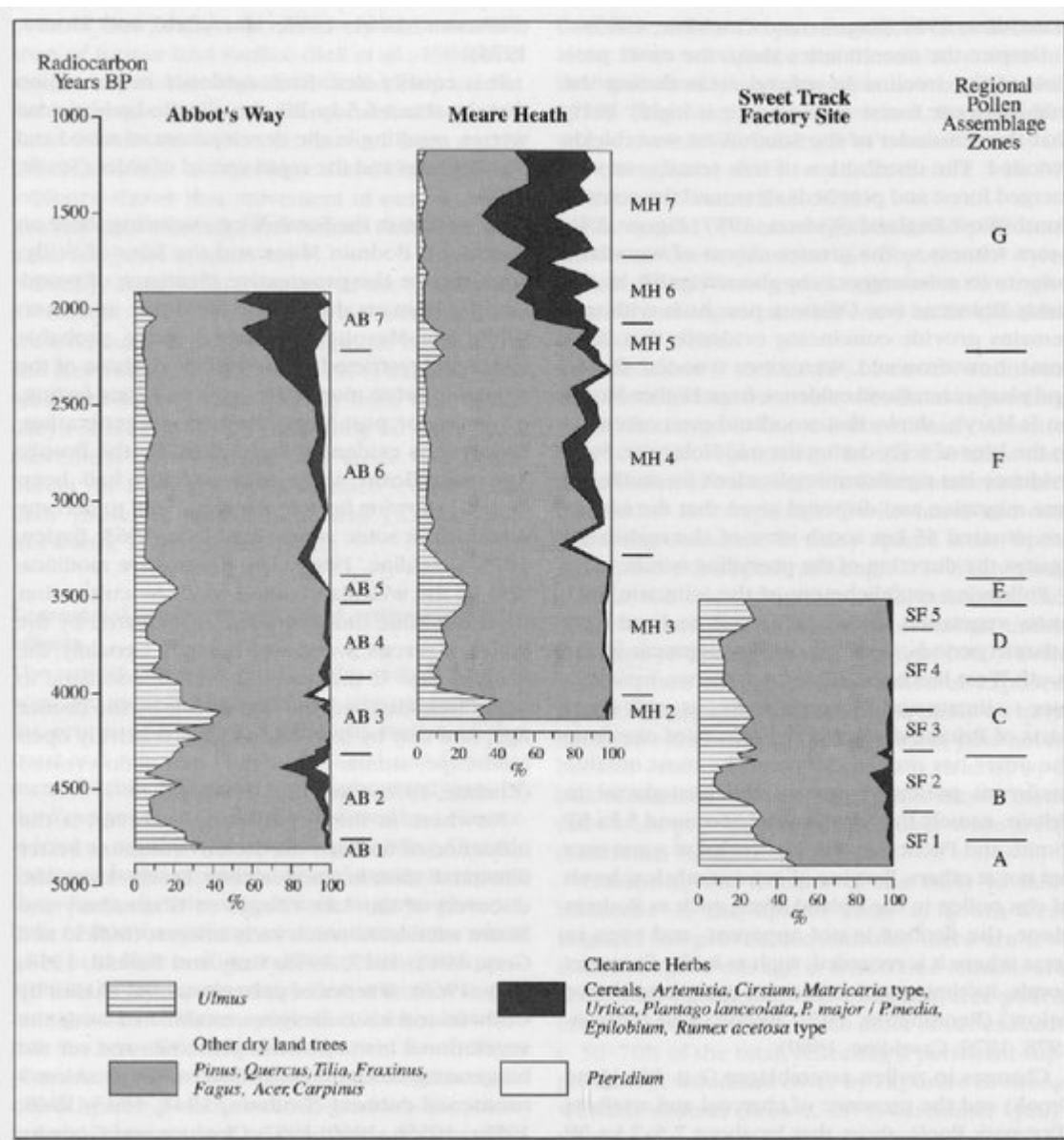
(Figure 2.6) The massive 'terrace' of raised beach, wind-blown sand ('sandrock') and periglacial head flanking Saunton Down in north Devon. (Photo: N. Stephens.)



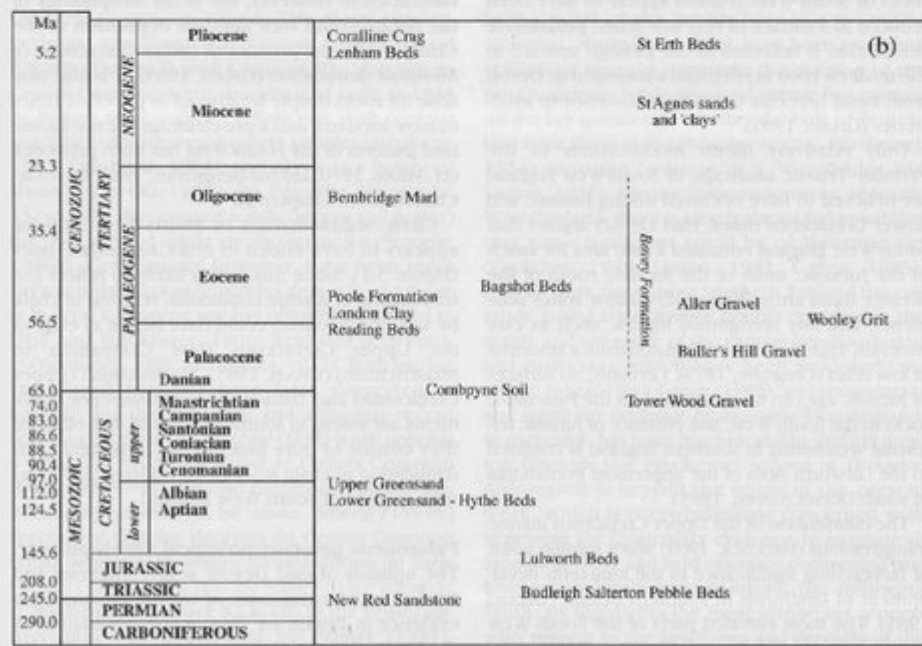
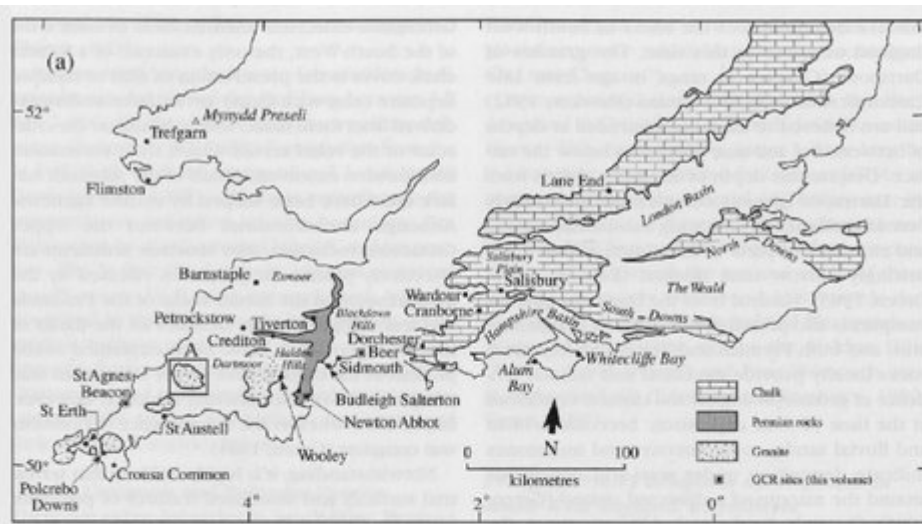
(Figure 2.7) Quaternary coastal landforms and deposits around South-West England. (Adapted from Kidson, 1977.)



*(Figure 2.8) Haytor Rocks, Dartmoor. Although tors such as these have evolved over an extremely protracted timescale, their final form, and that of the slopes around them, was fashioned by periglacial processes in the Devensian (Chapter 4). (Photo: S. Campbell.)*

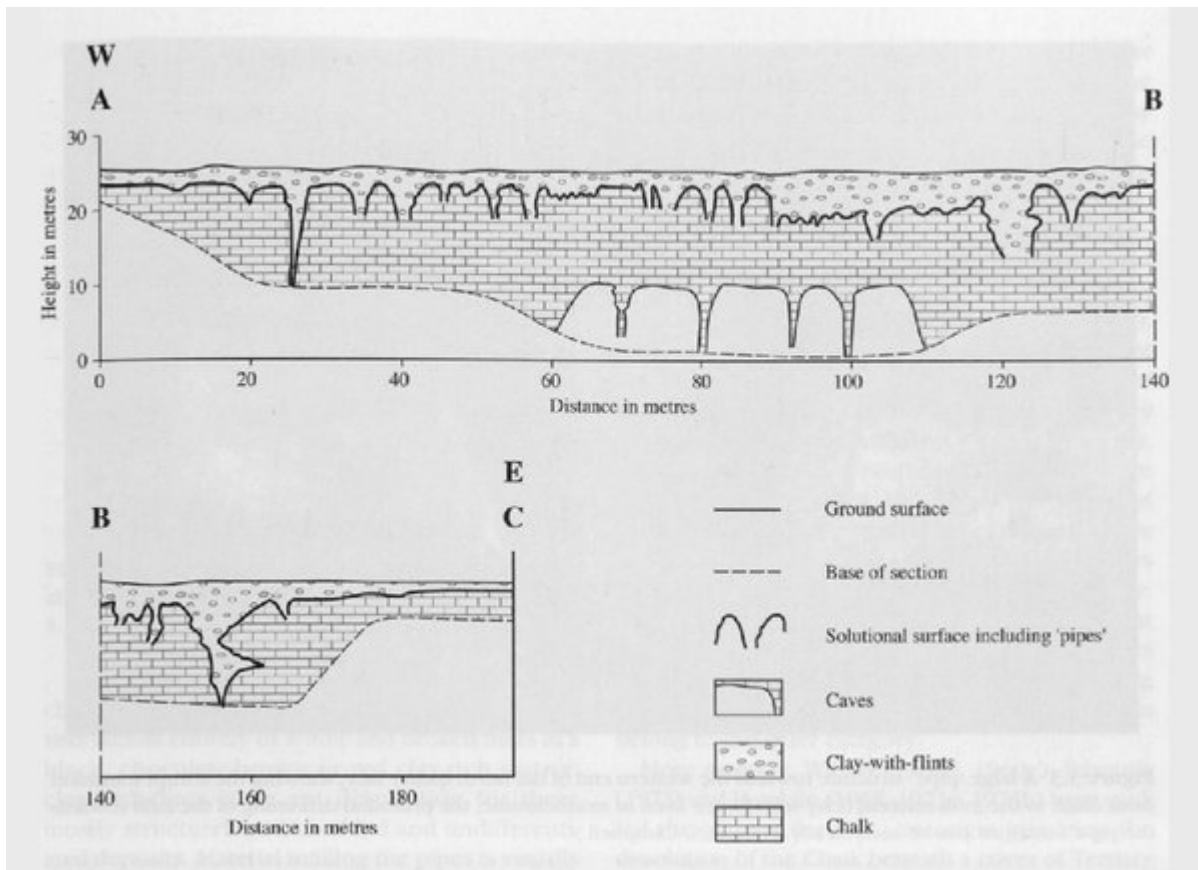


(Figure 2.9) Summary Holocene pollen diagrams from the Abbot's Way, Meare Heath and Sweet Track Factory sites in the Somerset Levels (selected taxa only). The vertical scale is based on dates in uncorrected radiocarbon years BP (before present 1950). (Adapted from Beckett and Hibbert, 1979.)

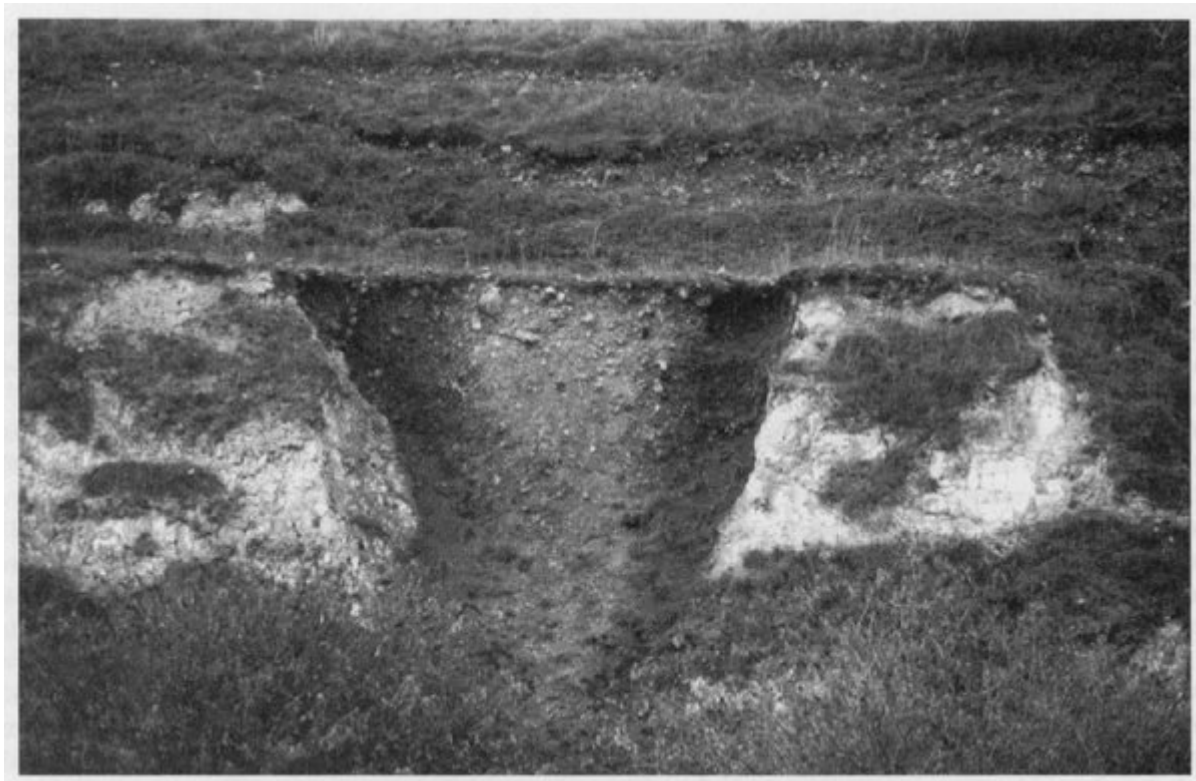


(Figure 3.1) (a) Southern and South-West England, showing localities referred to in the text, and selected geological outcrops. (b) Significant deposits and events in the geomorphological evolution of southern Britain. (Adapted from Green, 1985, with timescale based on Harland et al., 1982.)

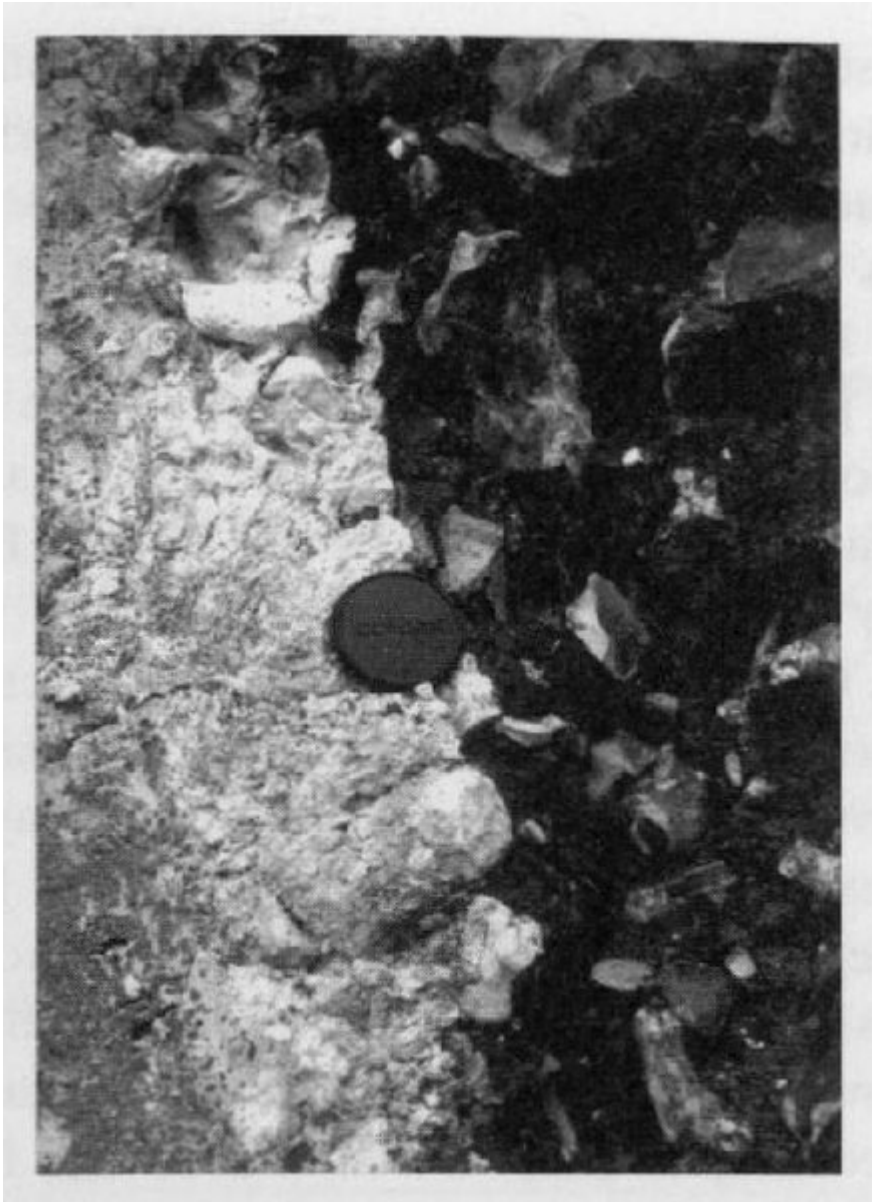




(Figure 3.2) Clay-filled chalk 'pipes' exposed along the northern working face of Beer Quarry in 1990.

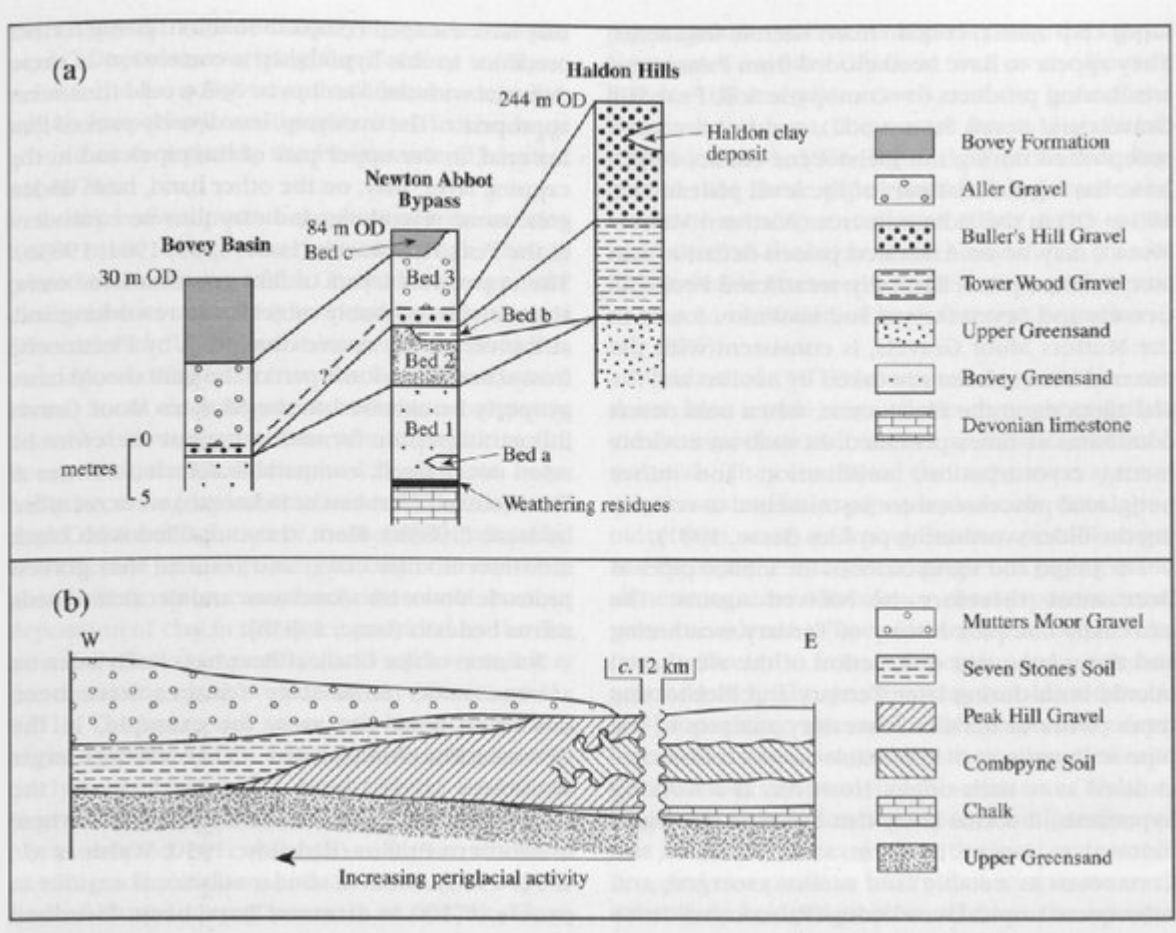


(Figure 3.3) A large 'pipe' structure towards the western end of the north quarry face, showing the abrupt transition from chalk to the infill material (clay-with-flints). Even in monochrome, the profound darkening of the infill towards the pipe's margins can be seen clearly. (Photo: S. Campbell.)

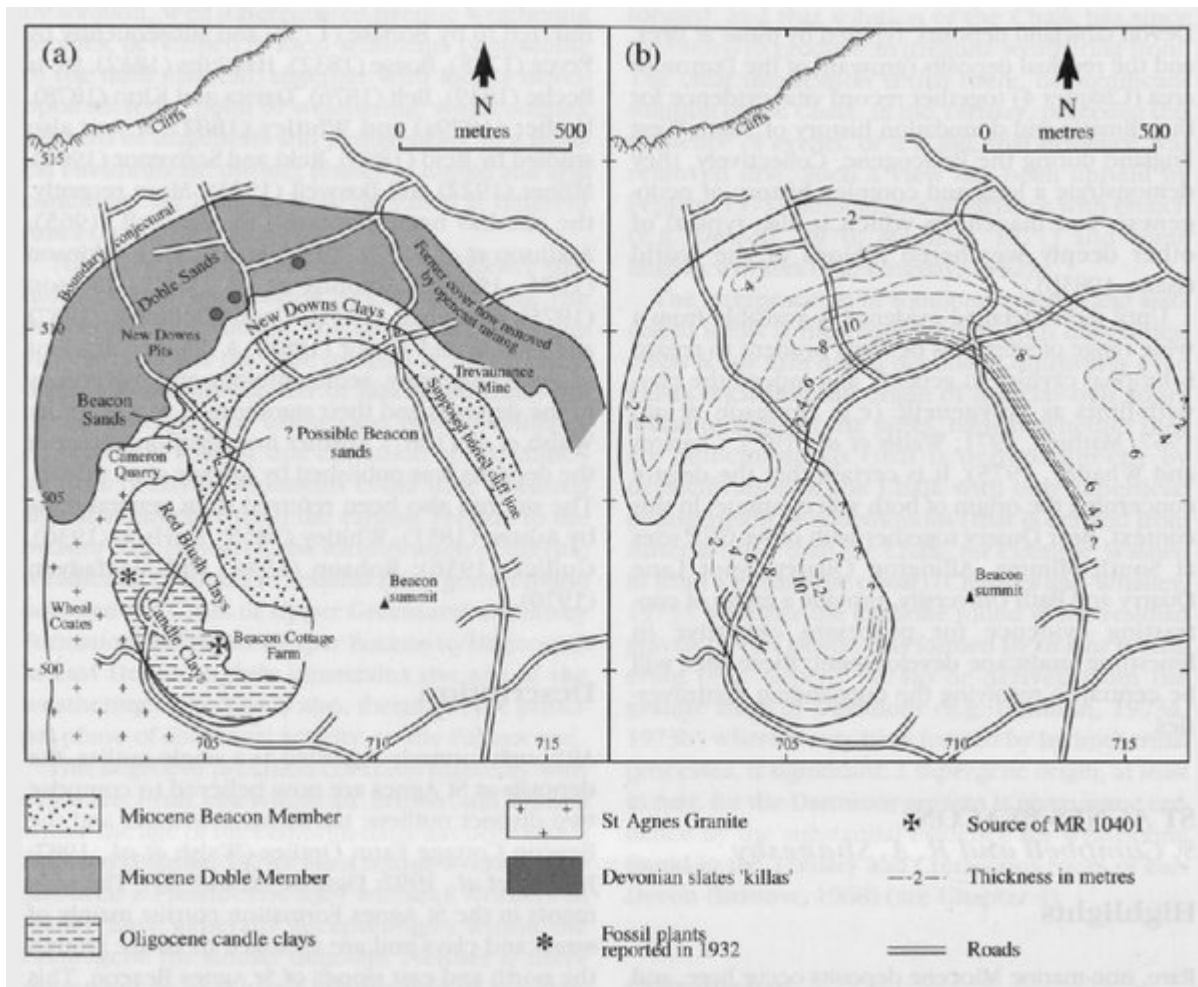


*(Figure 3.4) Detail of a typical pipe margin, showing the abrupt transition from chalk to clay-with-flints. (Photo: S. Campbell.)*

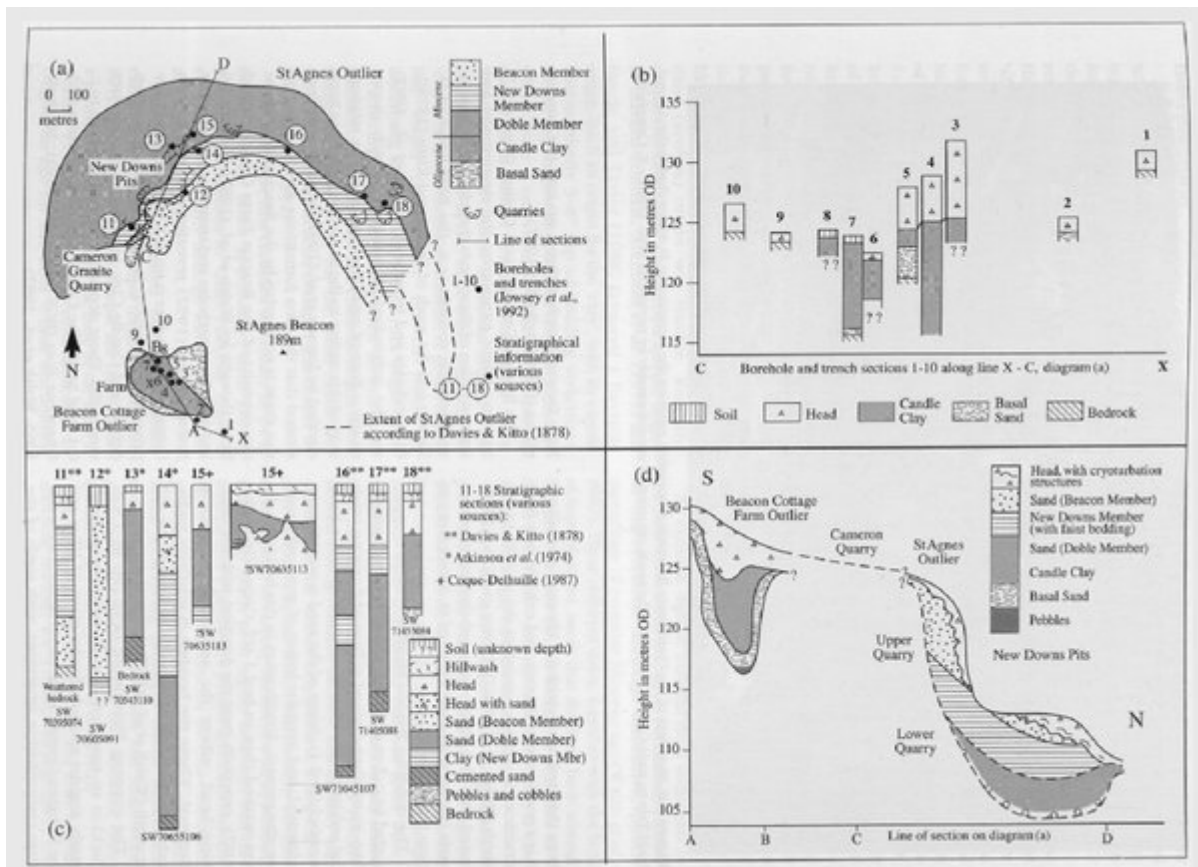




(Figure 3.5) (a) Stratigraphic correlations of successions in the Bovey Basin, Newton Abbot bypass and Haldon Hills. (Adapted from Edwards, 1973, Hamblin, 1973b and Brunsdon et al., 1976.) (b) Schematic representation (not to scale) of field relations of major lithostratigraphic units in the Sidmouth area. (Adapted from Isaac, 1981.)



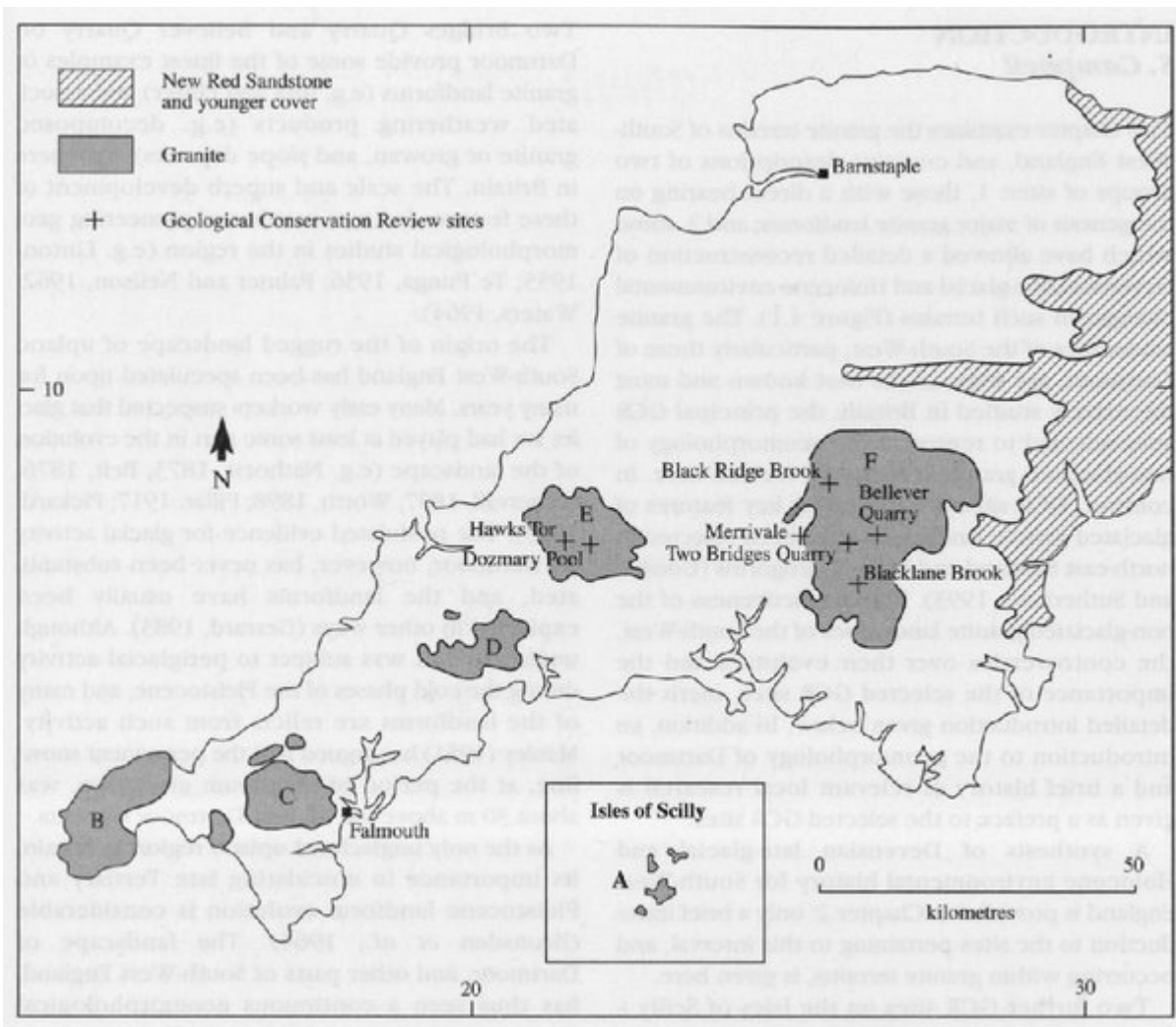
(Figure 3.6) (a) The geology of the St Agnes and Beacon Cottage Farm outliers as interpreted by Walsh et al. (1987). The area between Cameron Quarry and the Beacon was regarded as problematic and has been re-mapped by Jowsey et al. (1992) (Figure 3.7); (b) Isopachs of combined Tertiary and Quaternary sediment. (Adapted from Walsh et al., 1987.)



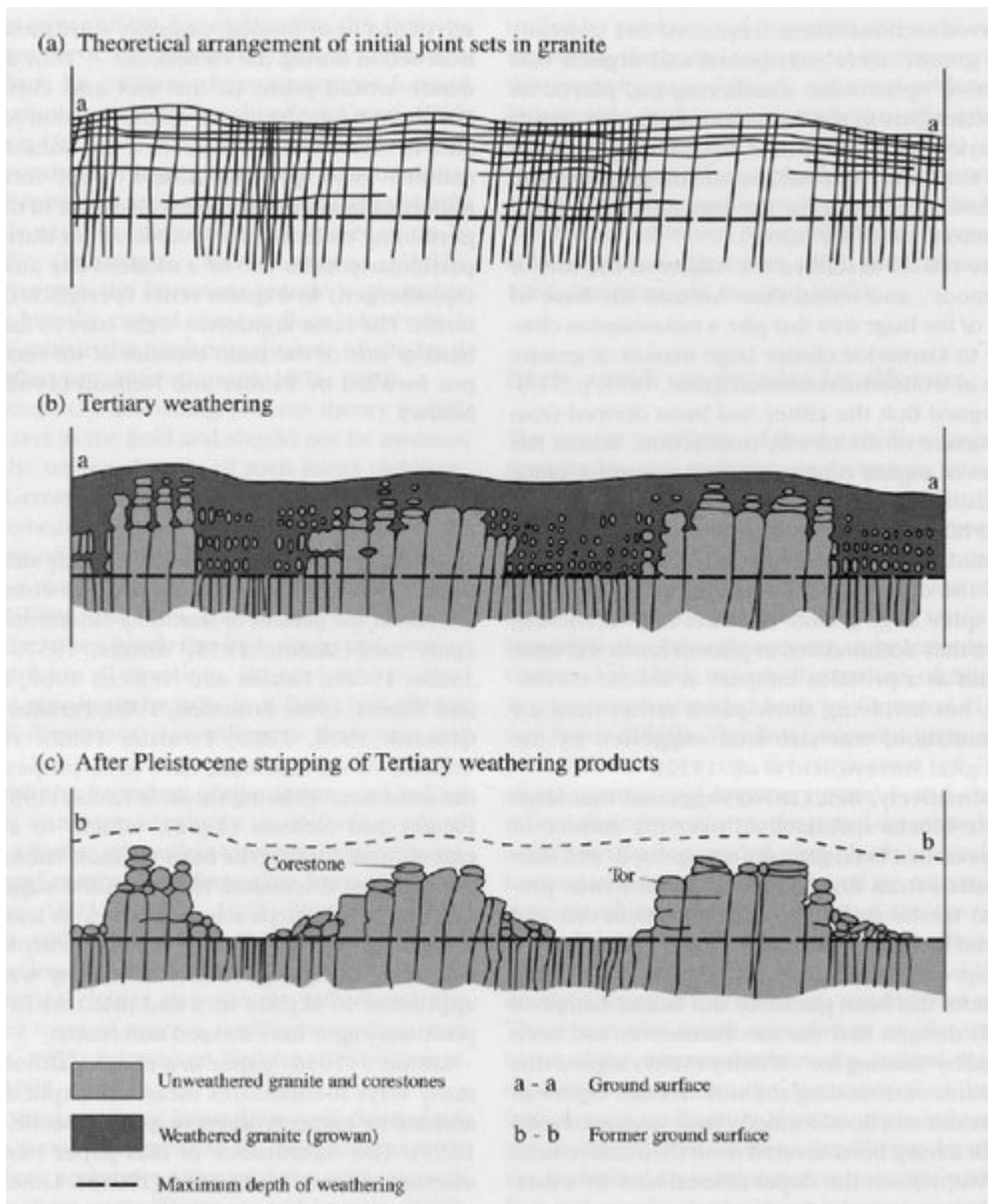
(Figure 3.7) (a) A revision of the St Agnes and Beacon Cottage Farm outliers by Jowsey et al. (1992). (b) Borehole and trench sections along line X–C (diagram a), adapted from Jowsey et al. (1992). (c) Stratigraphic sections along line D–C (diagram a), compiled from various sources. (d) Schematic reconstruction of the Beacon Cottage Farm and St Agnes outliers, based on Jowsey et al. (1992).



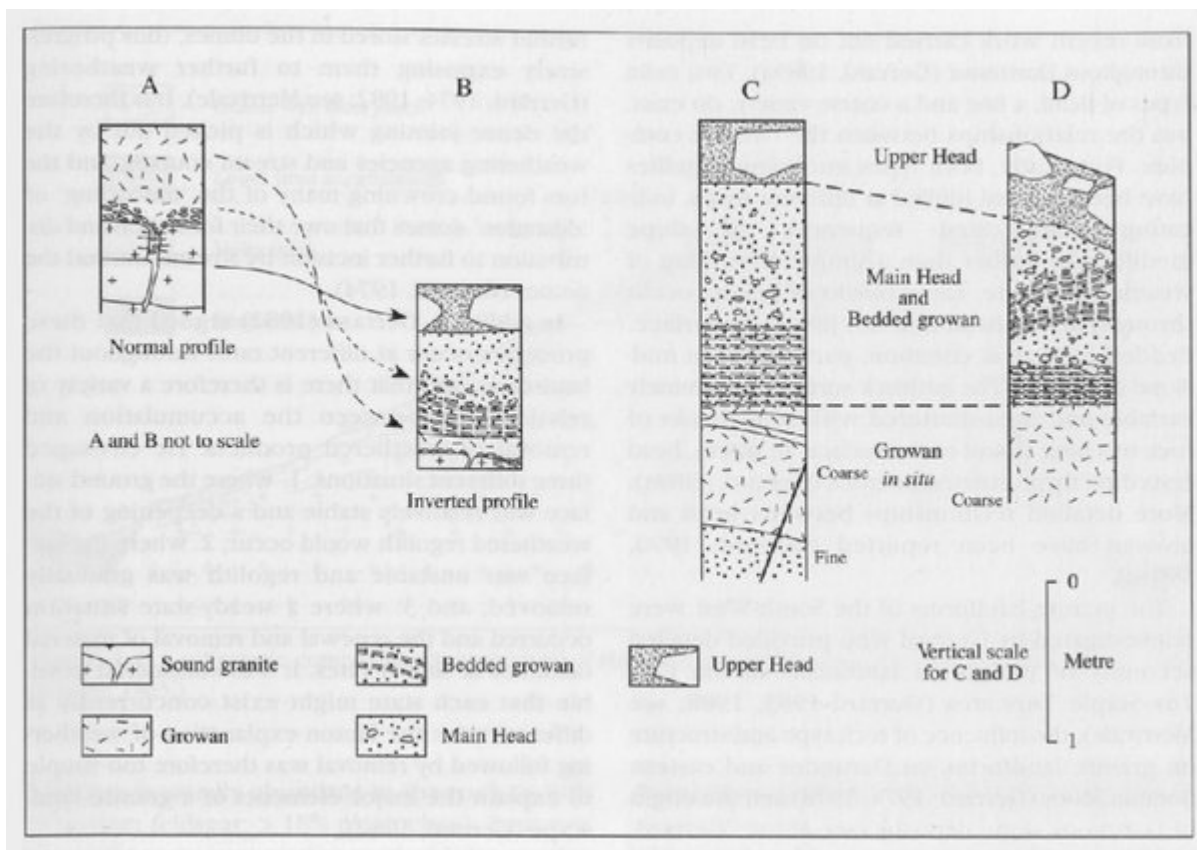
(Figure 3.8) Members of the Quaternary Research Association examine the sequence at St Agnes during the Annual Field Trip to west Cornwall in 1980. The sands are overlain unconformably by periglacial head. (Photo: S. Campbell.)



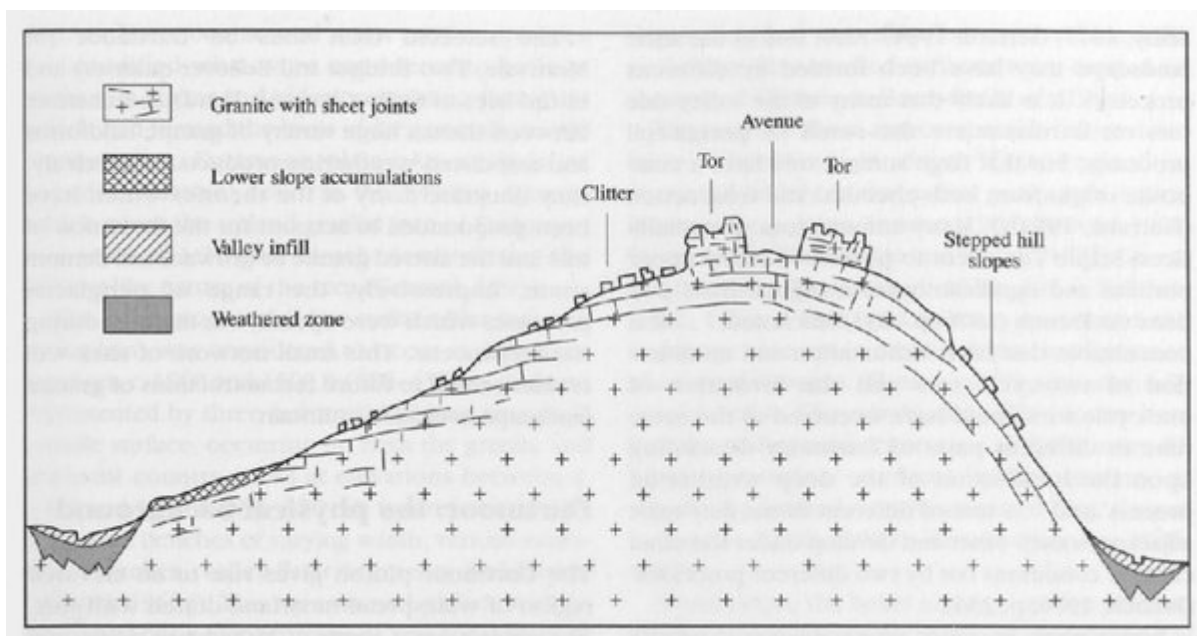
(Figure 4.1) Location of GCR sites in relation to: A, Isles of Scilly Granite; B, Land's End Granite; C, Carrunellis Granite; D, St Austell Granite; E, Bodmin Moor Granite; and F, Dartmoor Granite. (Adapted from Floyd et al., 1993.)



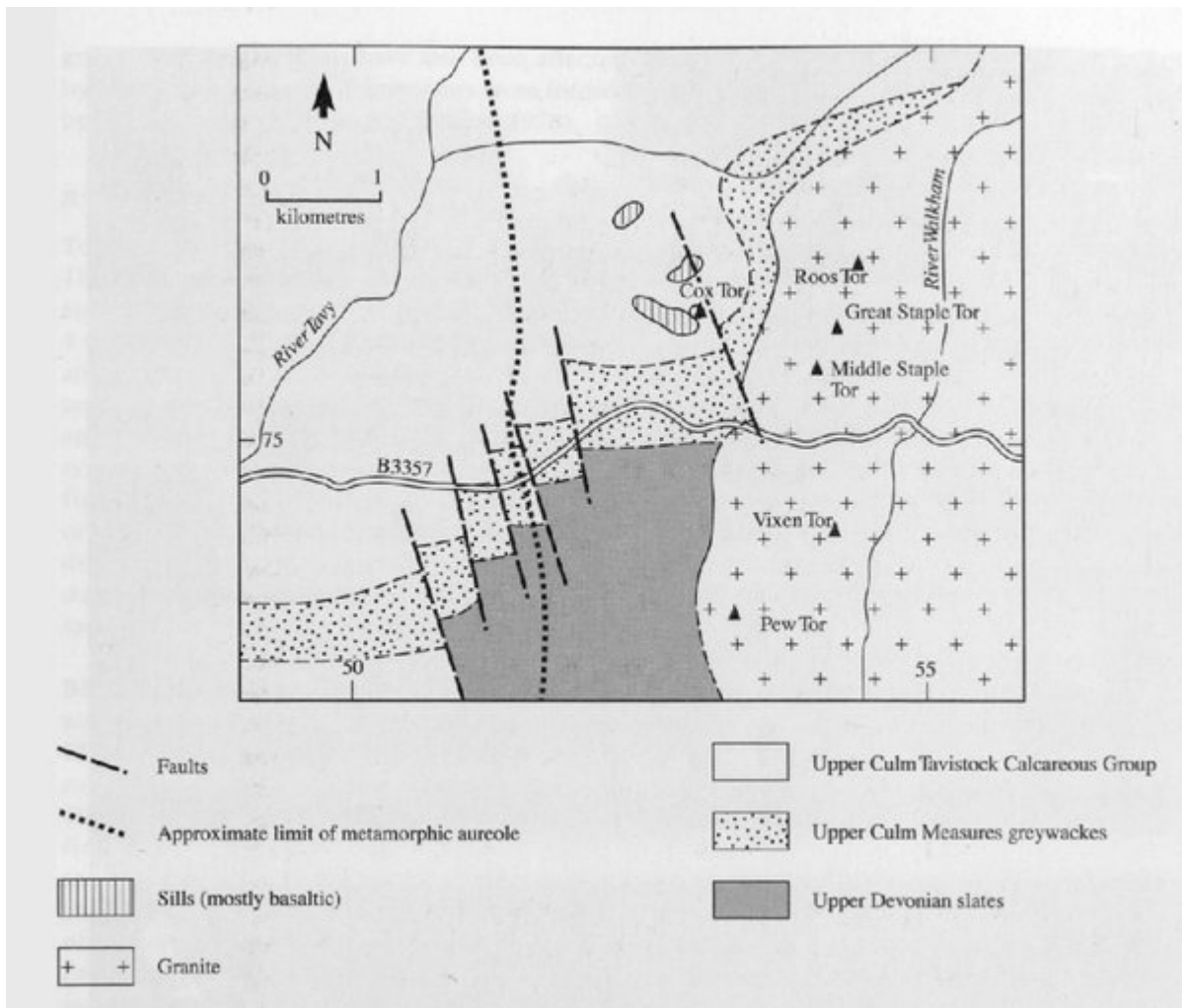
(Figure 4.2) Linton's (1955) classic two-stage model of tor formation.



(Figure 4.3) A model of slope development for Dartmoor, after Waters (1964). Profiles: (a) Products of in situ weathering on a granite substrate; (b) Inversion of normal weathering profile following two separate periods of periglacial mass wasting; (c) and (d) Measured sections at Shilstone Pit [SX 659 902], Dartmoor. Many slope configurations, however, do not conform to this model (see text).

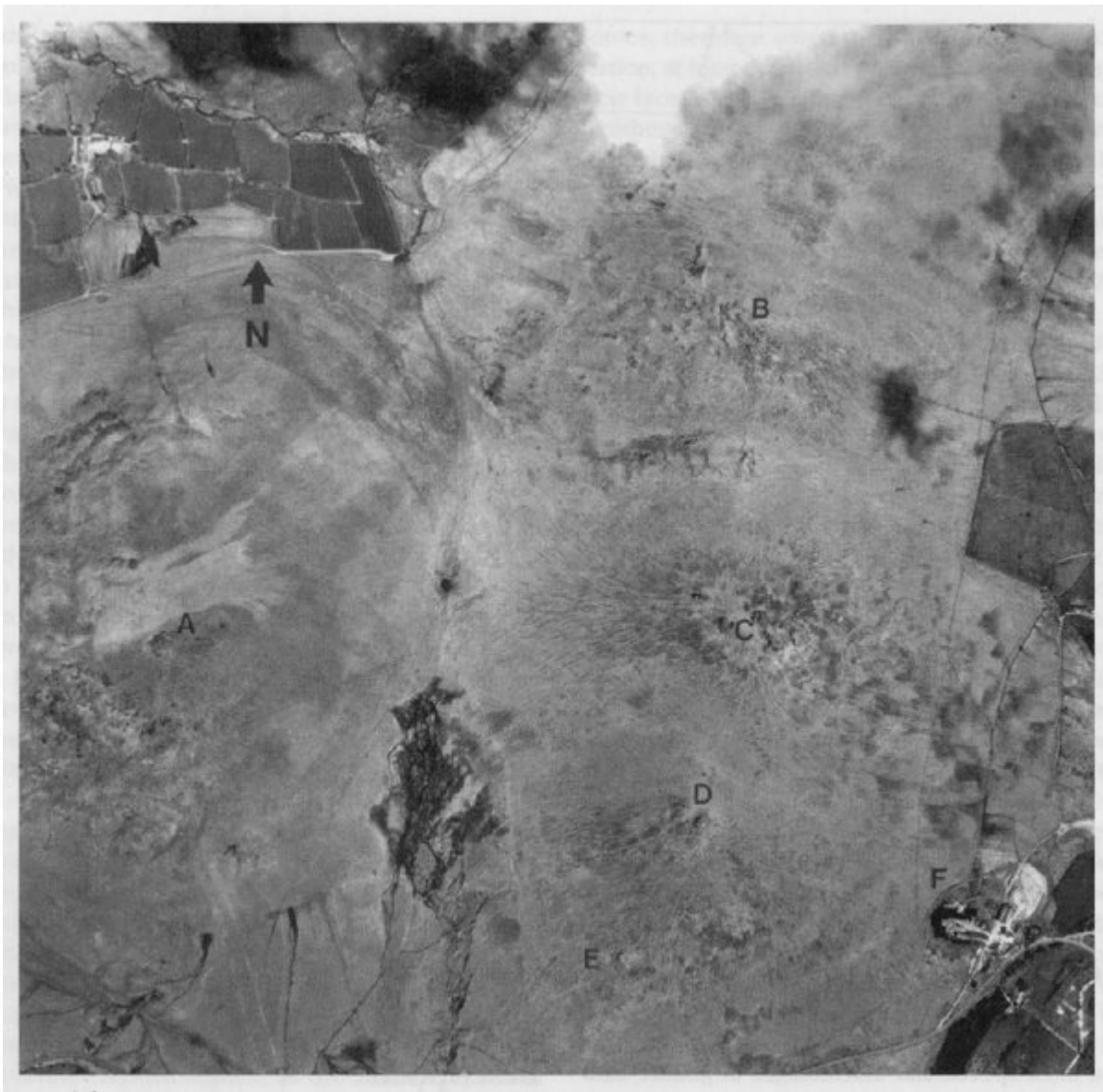


(Figure 4.4) A schematic composite representation of the main geomorphological features of Dartmoor. (After Gerrard, 1983.)



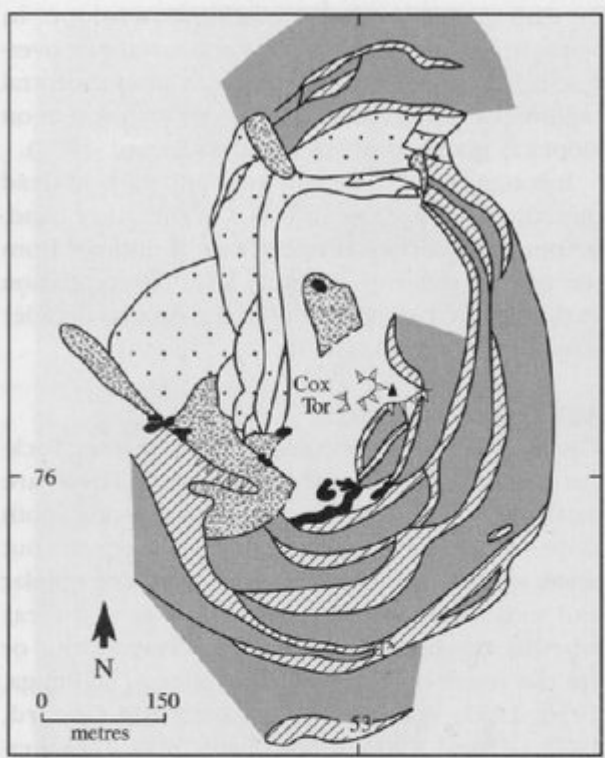
(Figure 4.5) Simplified geology of the Merrivale area. (Adapted from Gerrard, 1983.)






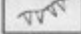




(Figure 4.6) Aerial photograph (scale c. 1:10 000) showing: (a) Cox Tor; (b) Roos Tor; (c) Great Staple Tor; (d) Middle Staple Tor; (e) Little Staple Tor; (f) Merrivale Quarry. Distinct 'boulder runs' of cater are particularly evident around the Staple Tors. (Cambridge University Collection: copyright reserved.)



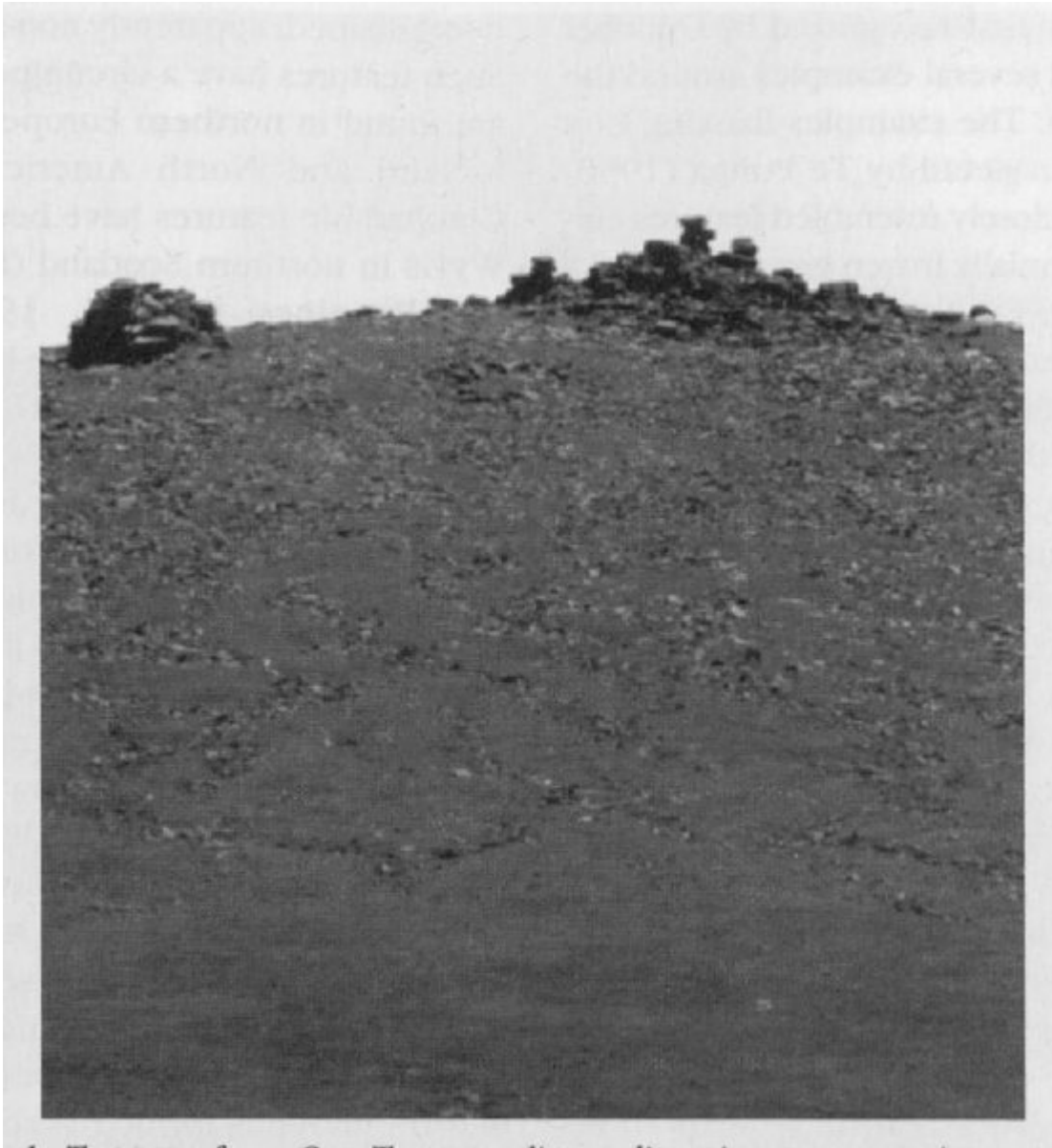


-  Altiplanation terrace 'treads'
-  Altiplanation terrace 'risers'
-  Boulder lobes and banks
-  Concentrated boulder 'runs'
-  Upstanding rock exposures
-  Rock scarps

(Figure 4.7) The geomorphology of Cox Tor and adjacent areas. (Adapted from Gerrard, 1983.)



*(Figure 4.8) Great Staple Tor seen from Middle Staple Tor. The missing central portion or 'avenue' of Great Staple Tor can be seen clearly on the horizon. (Photo: S. Campbell.)*



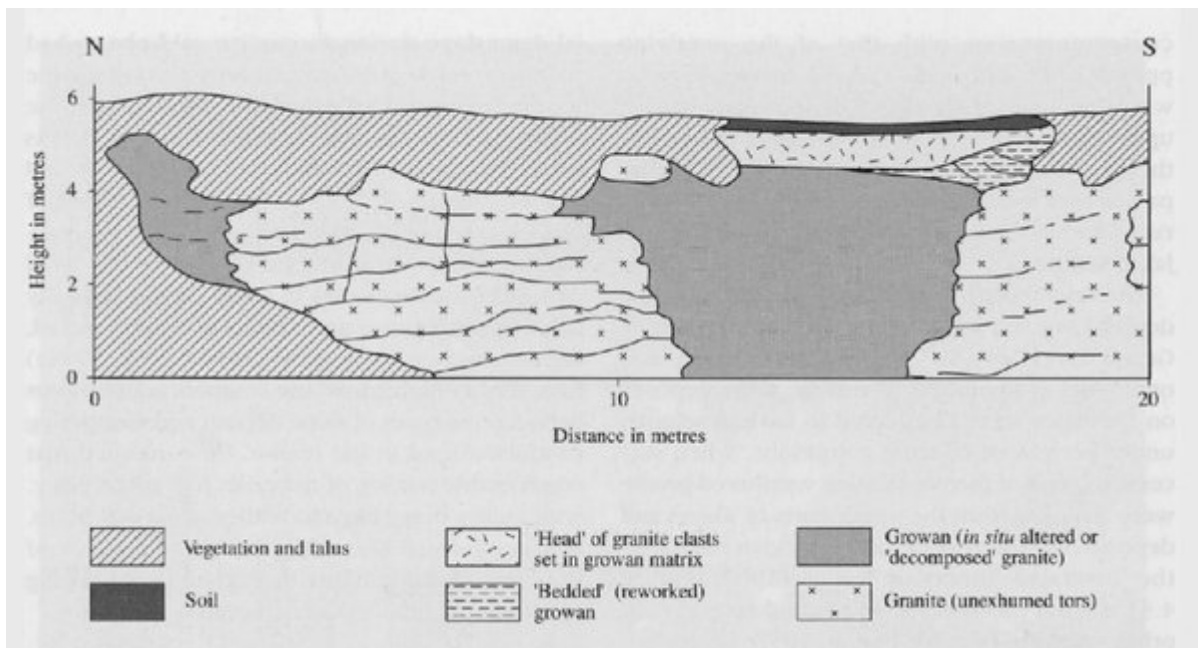
*(Figure 4.9) Looking west through the 'avenue' of Great Staple Tor. (Photo: S. Campbell.)*



*(Figure 4.10) Great Staple Tor seen from Cox Tor, revealing a diverging anastomosing pattern of boulder runs on the west-facing slopes. (Photo: S. Campbell.)*



(Figure 4.11) A profusion of earth hummocks on the east-facing slopes of Cox Tor, with Great Staple Tor and Middle Staple Tor on the horizon. (Photo: S. Campbell.)



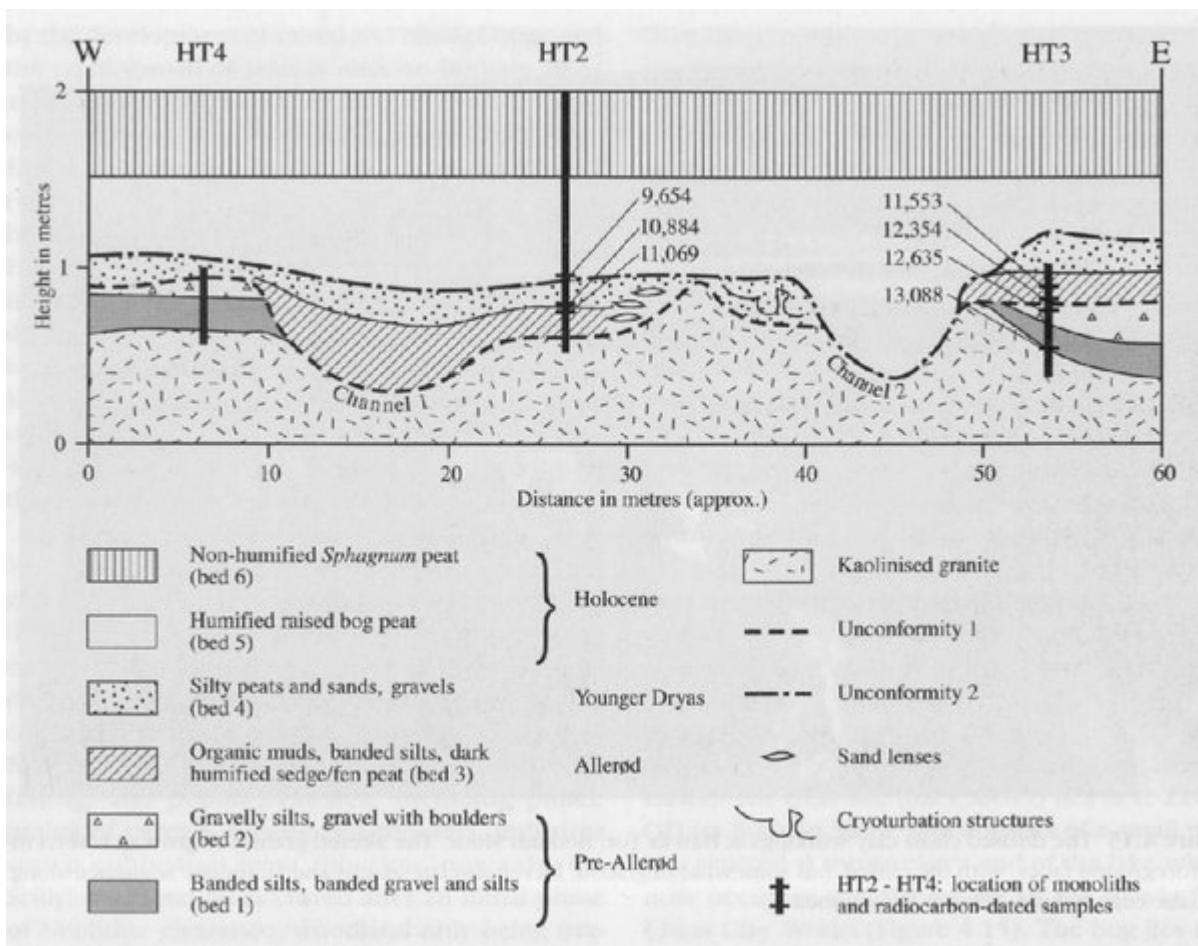
(Figure 4.12) Granite alteration products and slope deposits at Believer Quarry being examined during the 1977 INQUA trip to the South-West. (Photo: N. Stephens.)



*(Figure 4.13) A cross-section through the granite and associated alteration products at Two Bridges Quarry, Dartmoor, adapted from Campbell (1991).*



*(Figure 4.14) The section at Two Bridges Quarry, showing large intact granite masses, the unexhumed tors and adjacent deeply altered granite. (Photo: S. Campbell.)*



(Figure 4.15) The disused china clay workings at Hawks Tor, Bodmin Moor. The altered granite or growan is seen in the foreground faces, with the cliffed, but somewhat degraded, Devensian late-glacial and Holocene sequence along the lake edge behind. (Photo: S. Campbell.)



(Figure 4.16) A simplified composite section of the north-east face of the exposures at Hawks Tor as exposed in 1970–1971. Adapted from Brown (1977, 1980).



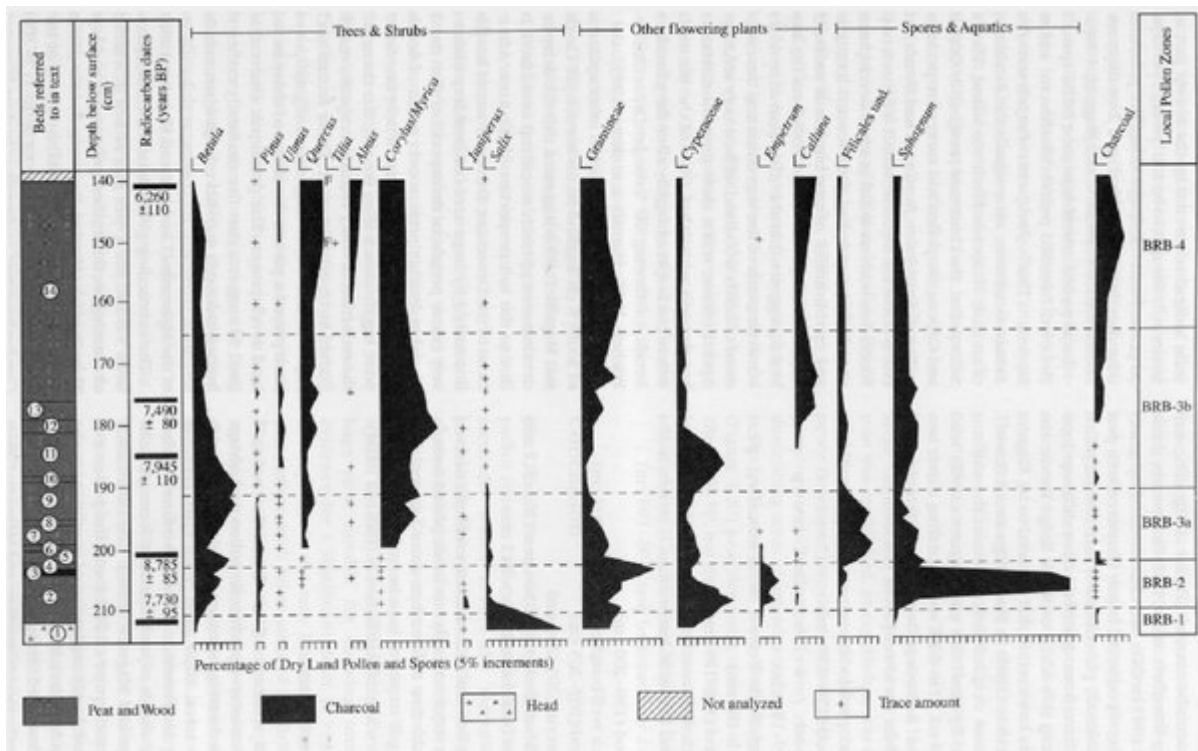


*(Figure 4.17) The peat bog at the south-west end of Dozmary Pool, Bodmin Moor. (Photo: S. Campbell.)*

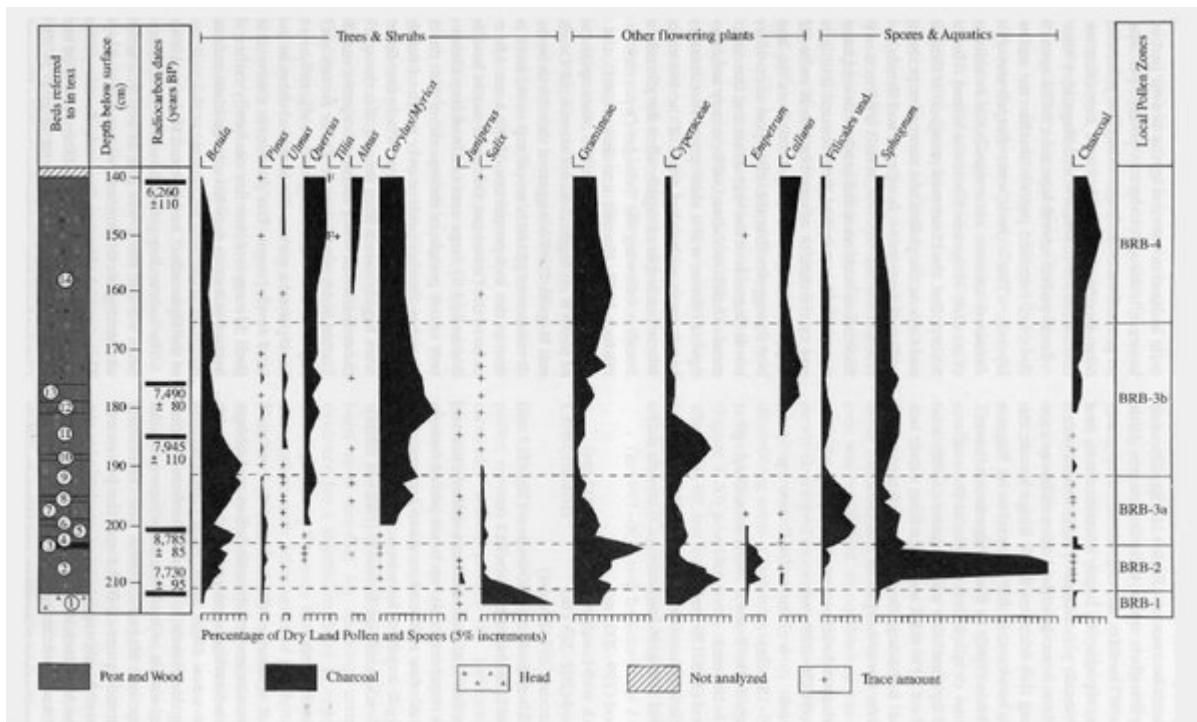




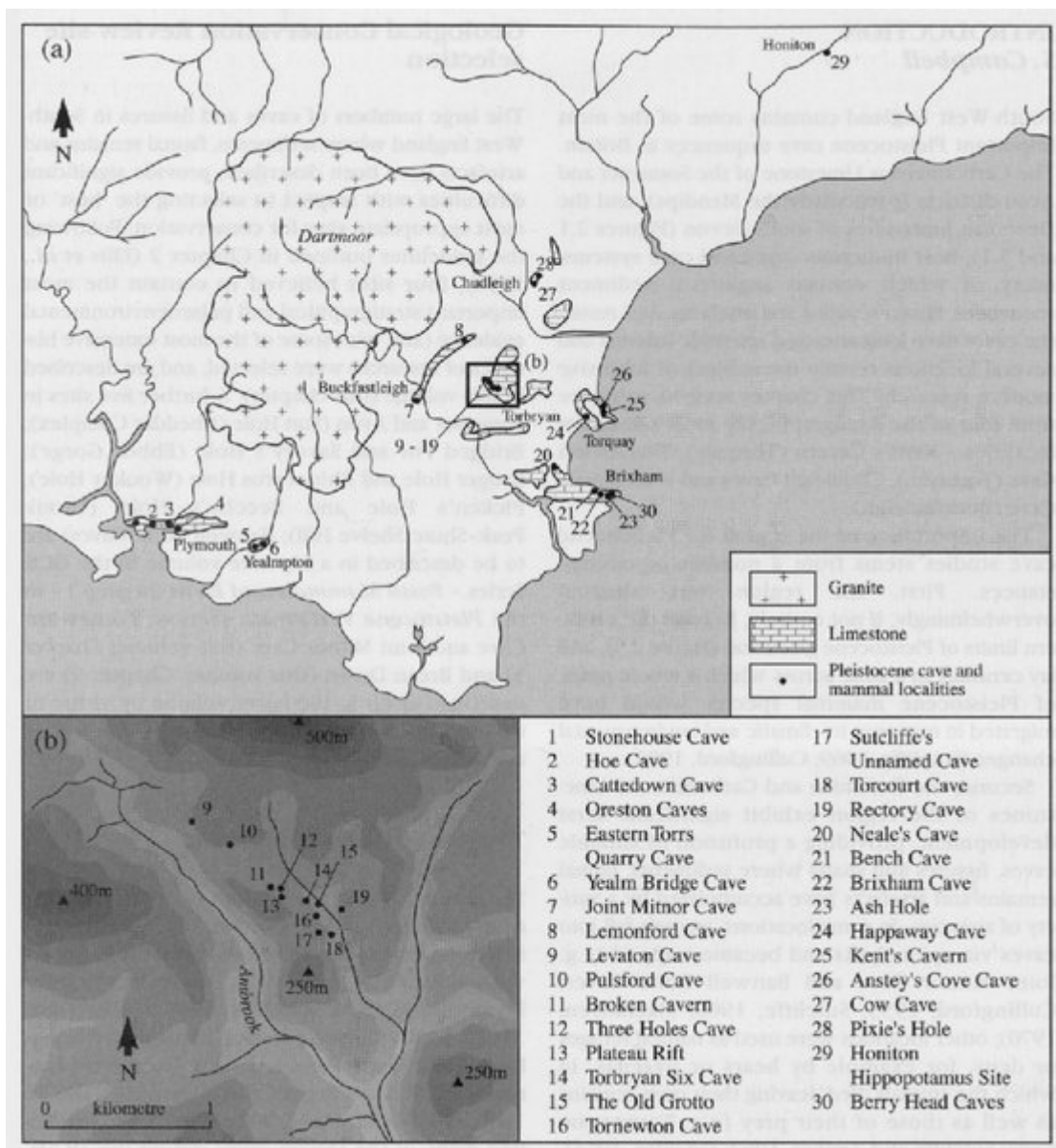
(Figure 4.18) Blacklane Brook pollen site, southern Dartmoor. (Photo: S. Campbell.)



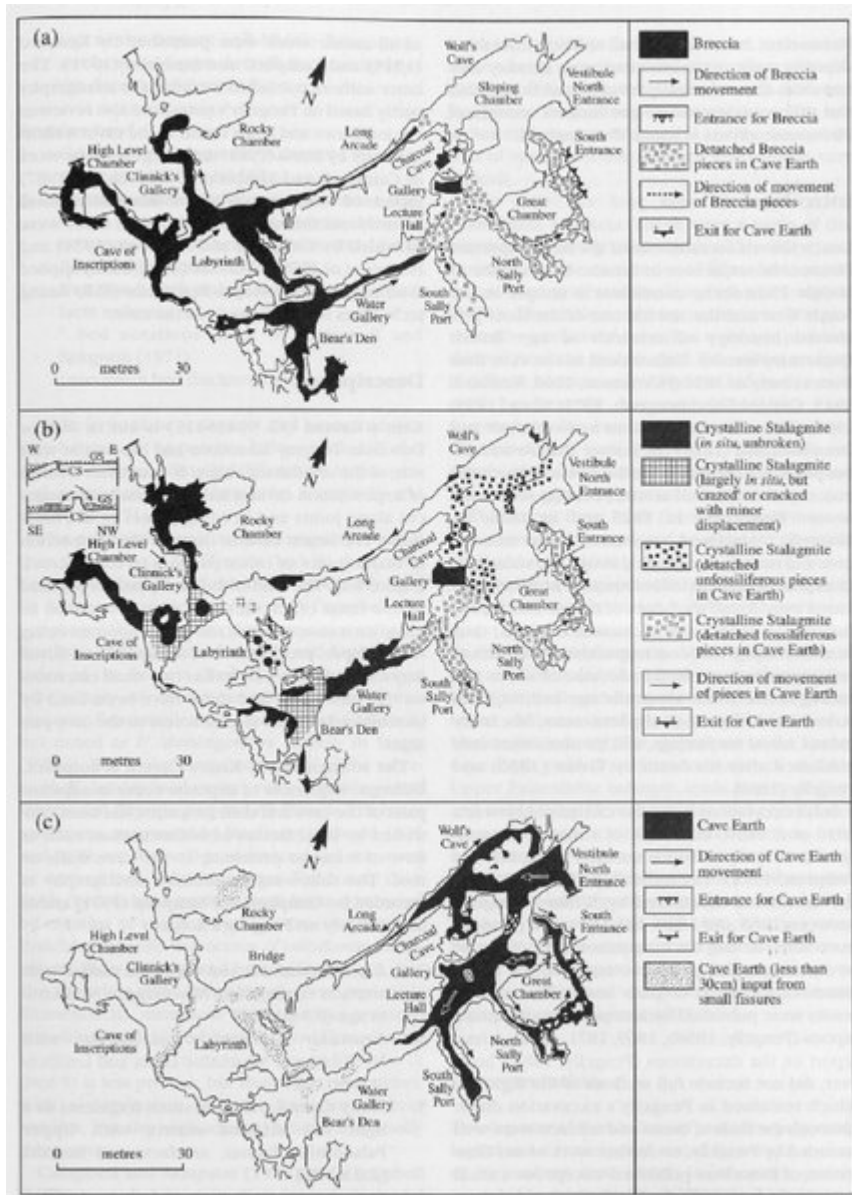
(Figure 4.19) Shallow peat sections exposed along Black Ridge Brook, northern Dartmoor. (Photo: C.J. Caseldine.)



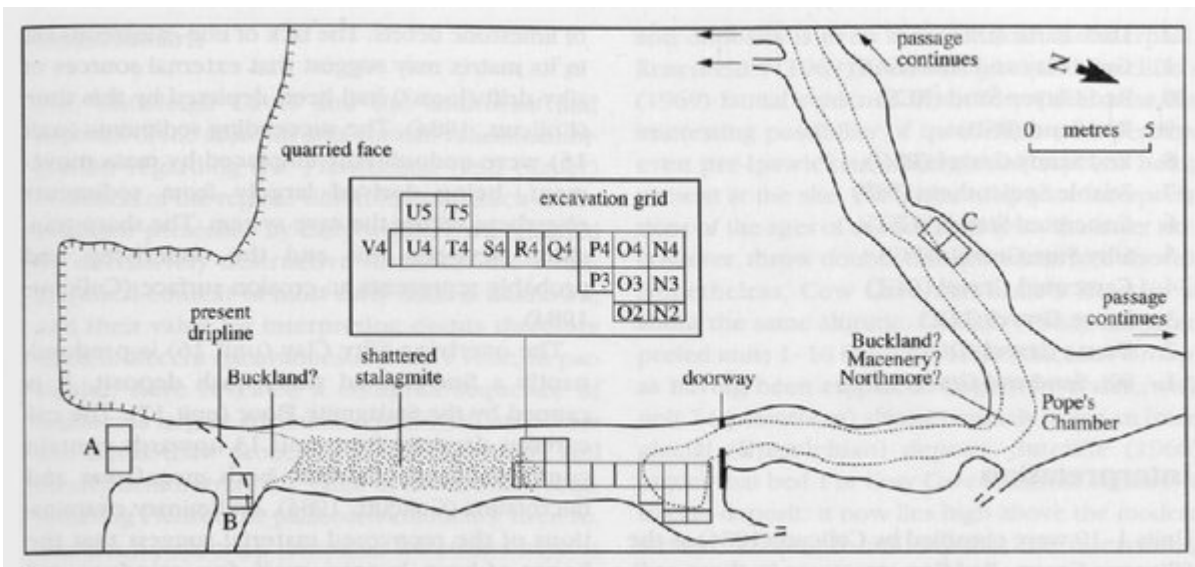
(Figure 4.20) Simplified pollen diagram for Black Ridge Brook, adapted from Caseldine and Maguire (1986).



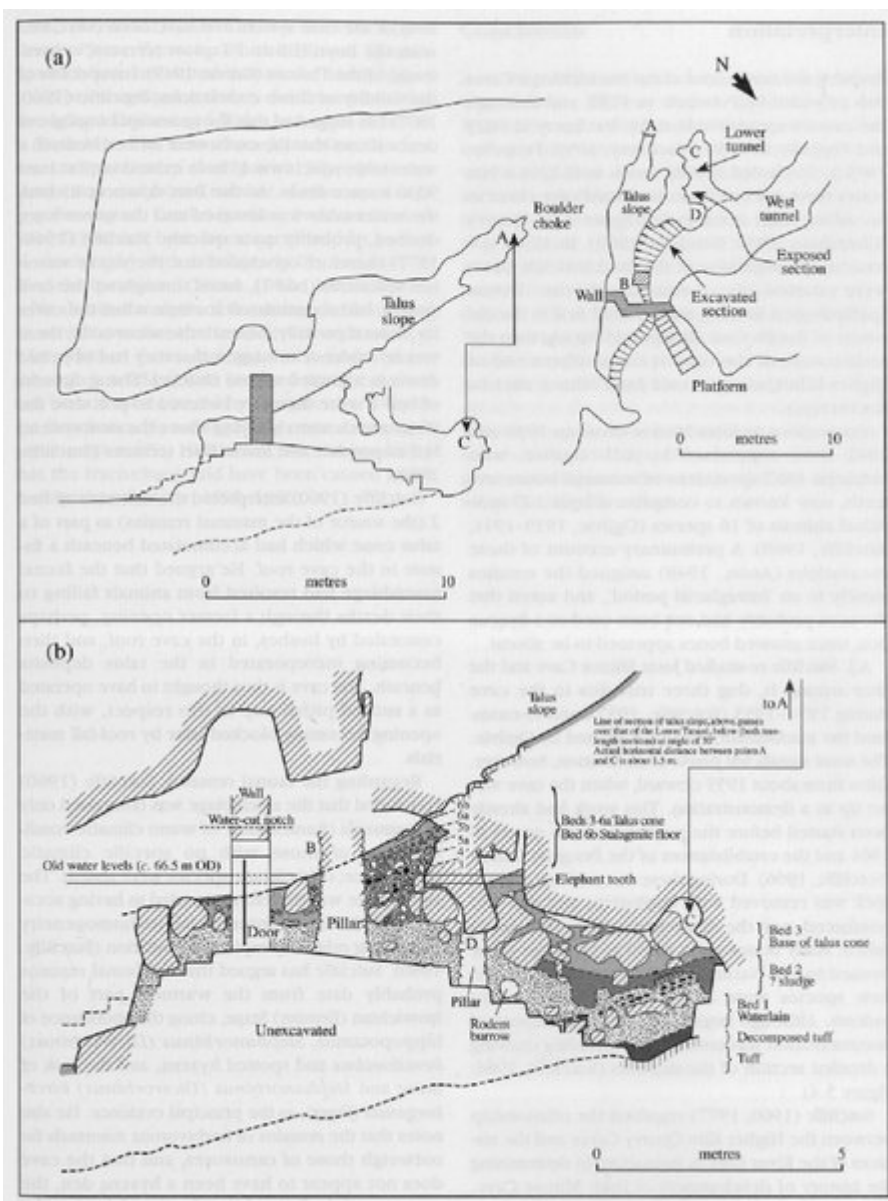
(Figure 5.1) (a) The principal localities where remains of Pleistocene mammals have been found in Devon, after Sutcliffe (1969). (b) Excavated caves in the Torbryan Valley, after Roberts (1996). The location of Berry Head 'sea caves' (Proctor, 1994, 1996) is also shown.



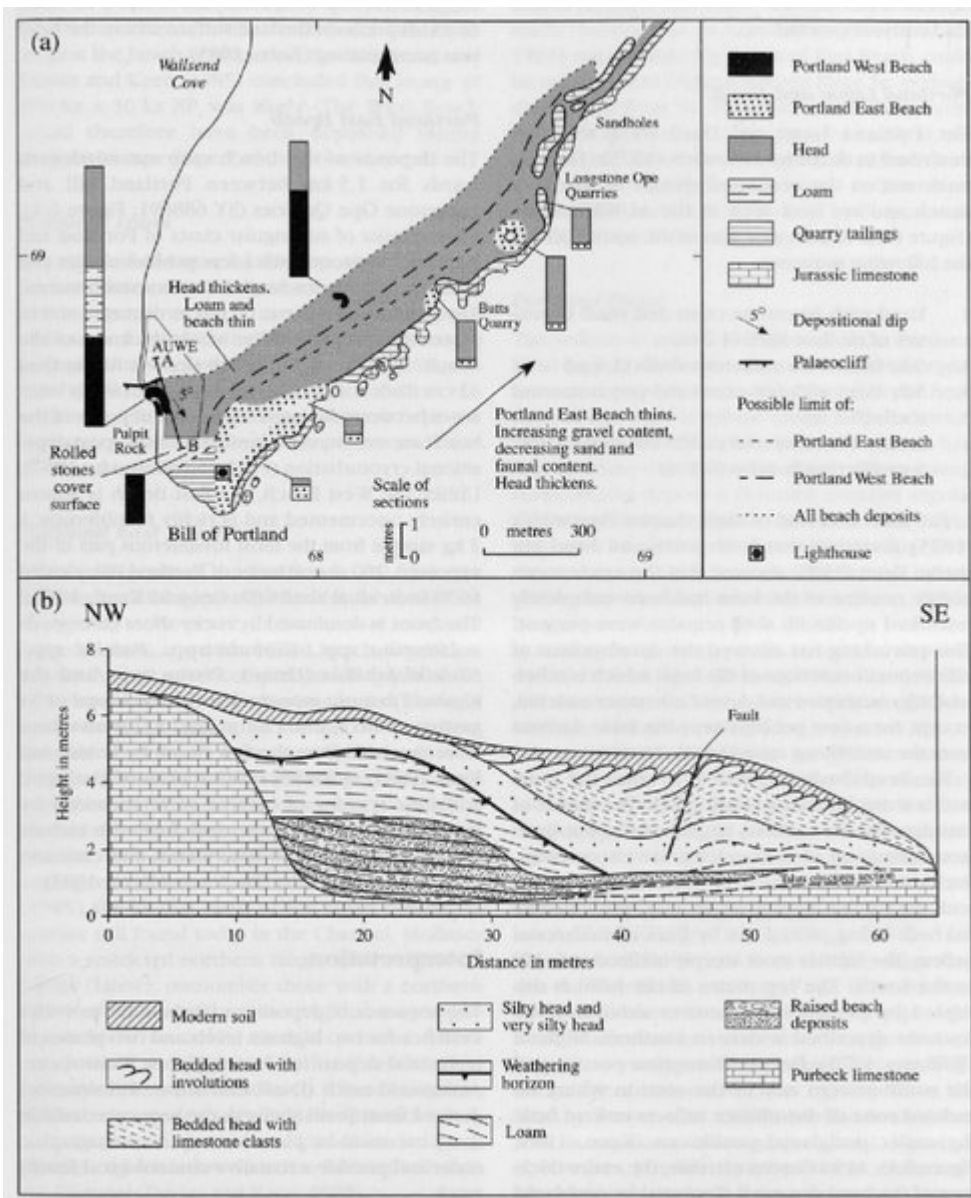
(Figure 5.2) Kent's Cavern, after Straw (1996). Distribution of: (a) Breccia; (b) Crystalline Stalagmite; (c) Cave Earth. (a)–(c) are shown as indicated in Reports to the British Association by W. Pengelly, 1865–1880. Cave outline is based on the survey by Proctor and Smart (1989).



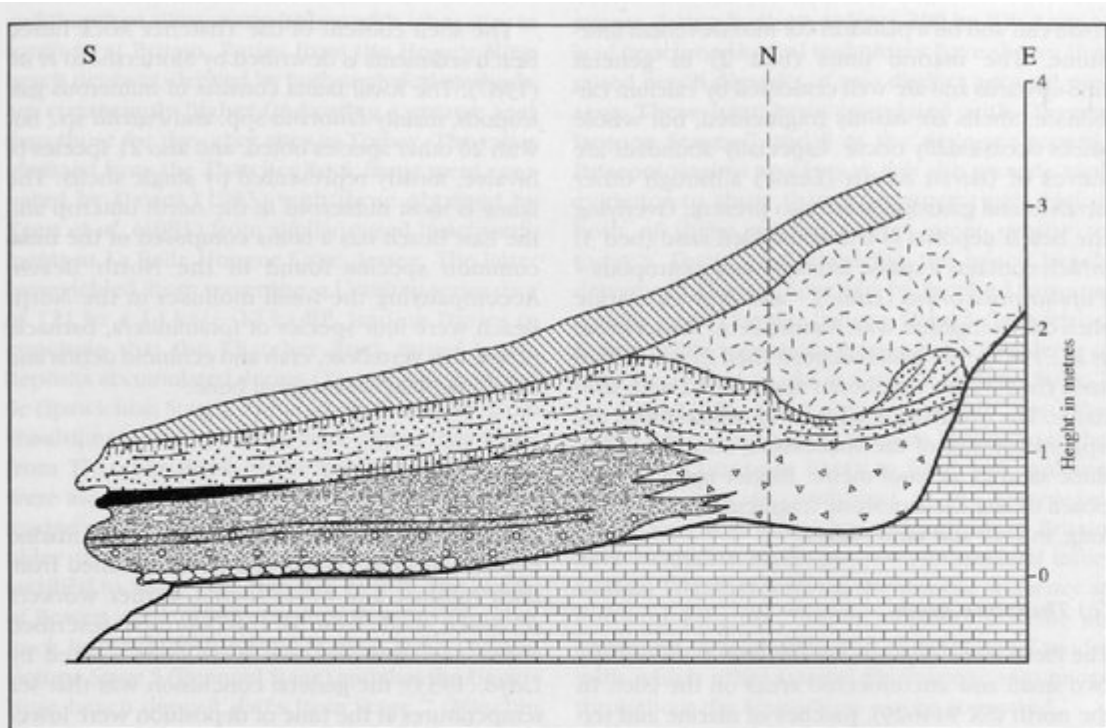
(Figure 5.3) Plan of Pixie's Hole, after Collcutt (1984).







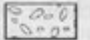






(Figure 5.4) Joint Mitnor Cave, Buckfastleigh: (a) General elevation and plan. (b) Detail of excavated section. (Based on the work of A.J. Sutcliffe and adapted from Sutcliffe's original drawing and Sutcliffe's (1974) simplified section.)



(Figure 6.1) (a) Quaternary deposits at Portland Bill, adapted from Davies and Keen (1985). (b) The Quaternary sequence at AUWE, adapted from Keen (1985). The cross-section follows line A–B shown in plan above.



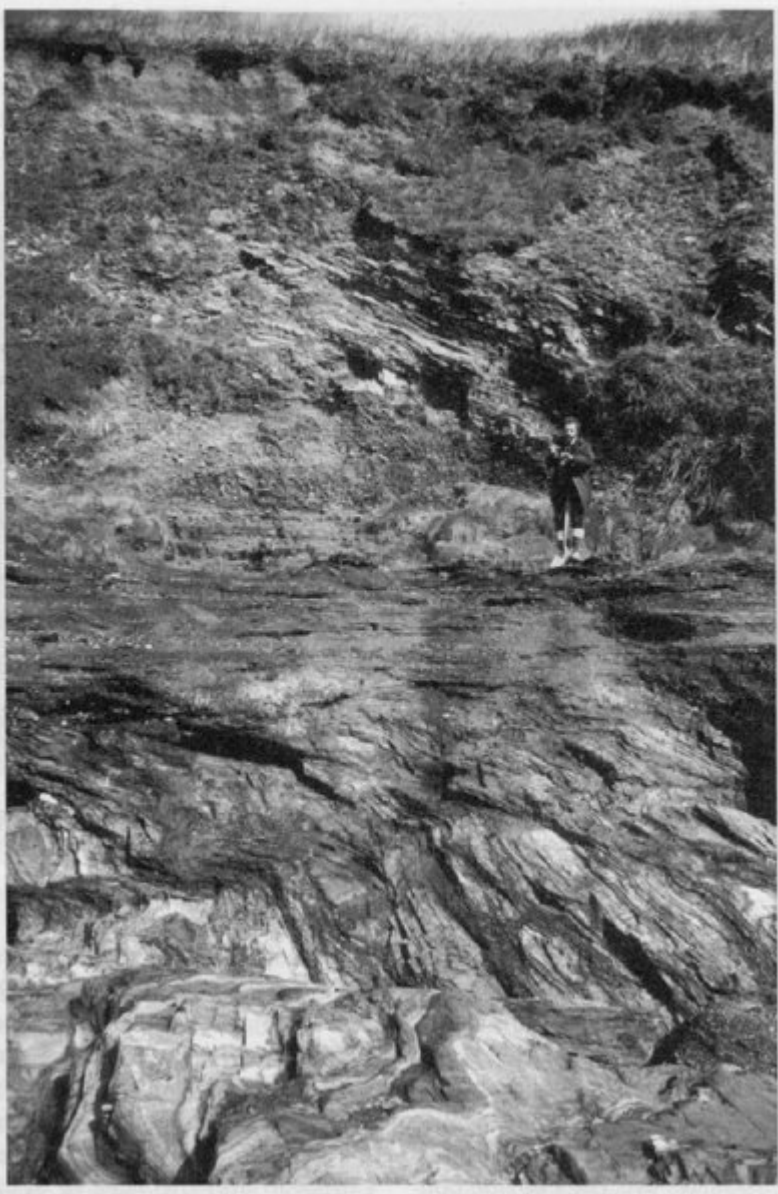
- |   |  |   |  |
|---|--|---|--|
|    | Red-brown silt loam (Upper Head)               |    | Sand and pebbles with abundant shells of <i>Ostrea edulis</i> (marine) |
|    | Coarse angular limestone fragments (Main Head) |    | Boulder bed (marine)   |
|  | Cross-bedded coarse sand (dune sand)           |  | Angular blocky limestone fragments (Lower Head)                        |
|  | Boulder layer                                  |  | Devonian limestone (shore platform)                                    |
|  | Coarse sand with shell debris (marine)         |  | Weathering horizons  |
|  | Coarse sand with pebbles and shells (marine)   |   |  |

(Figure 6.2) The Quaternary sequence at Hope's Nose. (Adapted from Mottershead et al., 1987.)





*(Figure 6.3) Coastal head deposits overlying a raised shore platform at Great Mattiscombe Sand [SX 816 369], 1.2 km west of Start Point. (Photo: D.H. Keen.)*

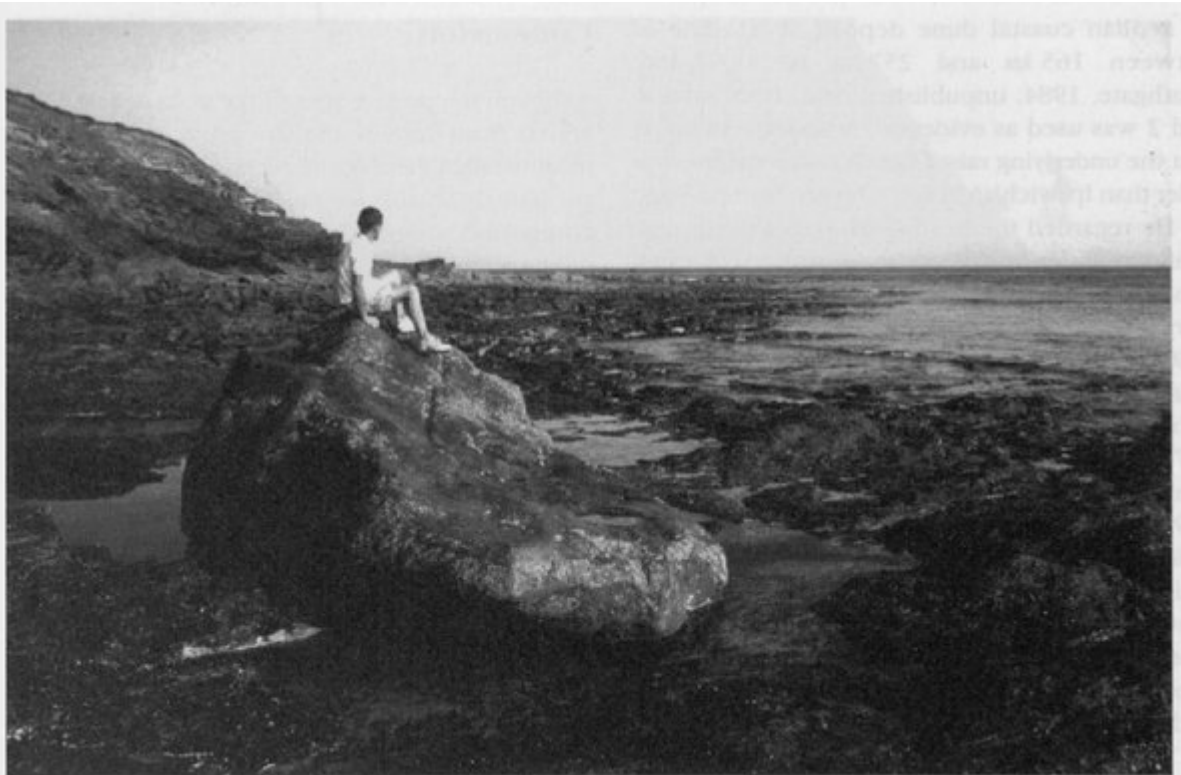


*(Figure 6.4) Coastal exposures at the western end of Pendower Beach, showing a compound shore platform cut across steeply dipping slates, overlain by cemented raised beach deposits and head. (Photo: S. Campbell.)*





*(Figure 6.5) A striking unconformity between the shore platform and overlying, cemented raised beach deposits at Pendower, viewed by members of the Quaternary Research Association in 1980. (Photo: S. Campbell.)*



*(Figure 6.6) The Giant's Rock at Porthleven, the South-West's most famous erratic — author for scale. (Photo: S. Campbell.)*



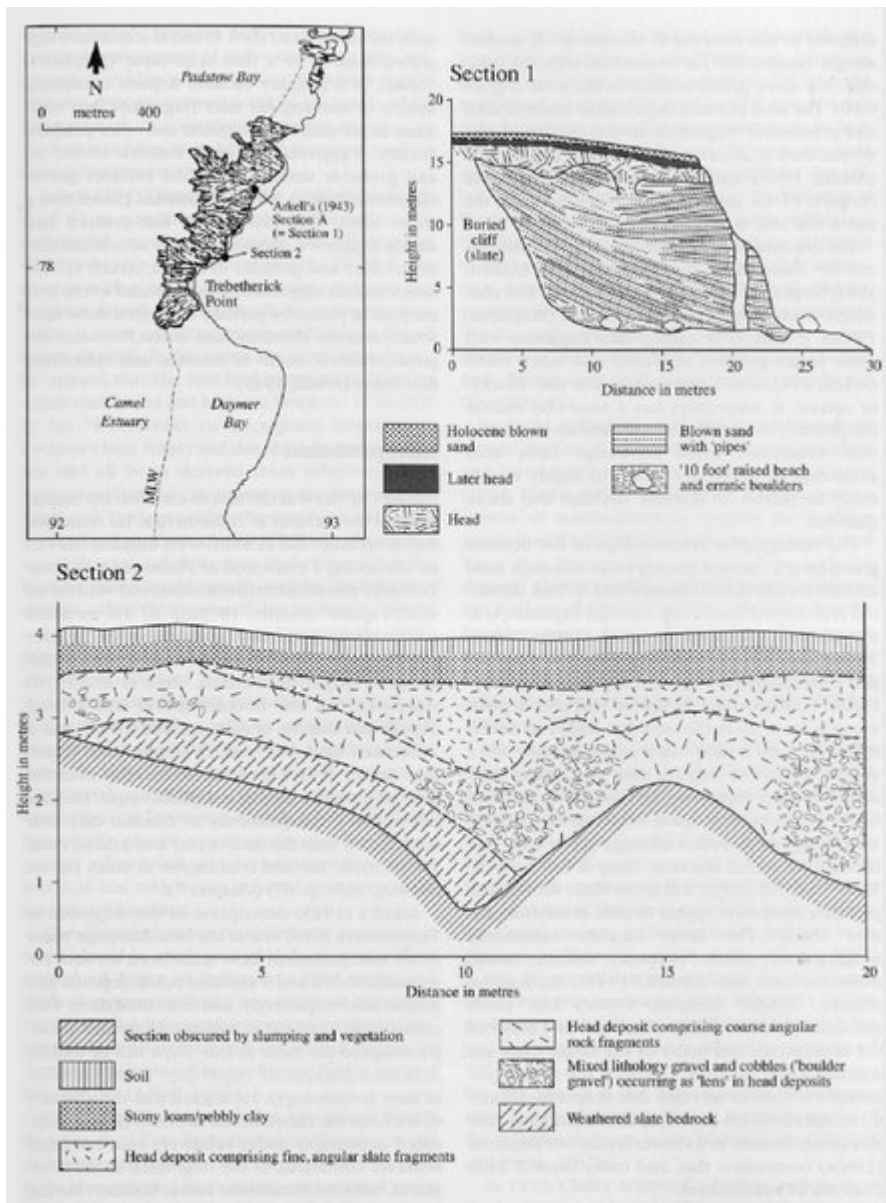
*(Figure 6.7) Boscawen GCR site (St Loy's Cove): solifluction deposits interbedded with organic sediments towards the base of the section. (Photo: J.D. Scourse.)*



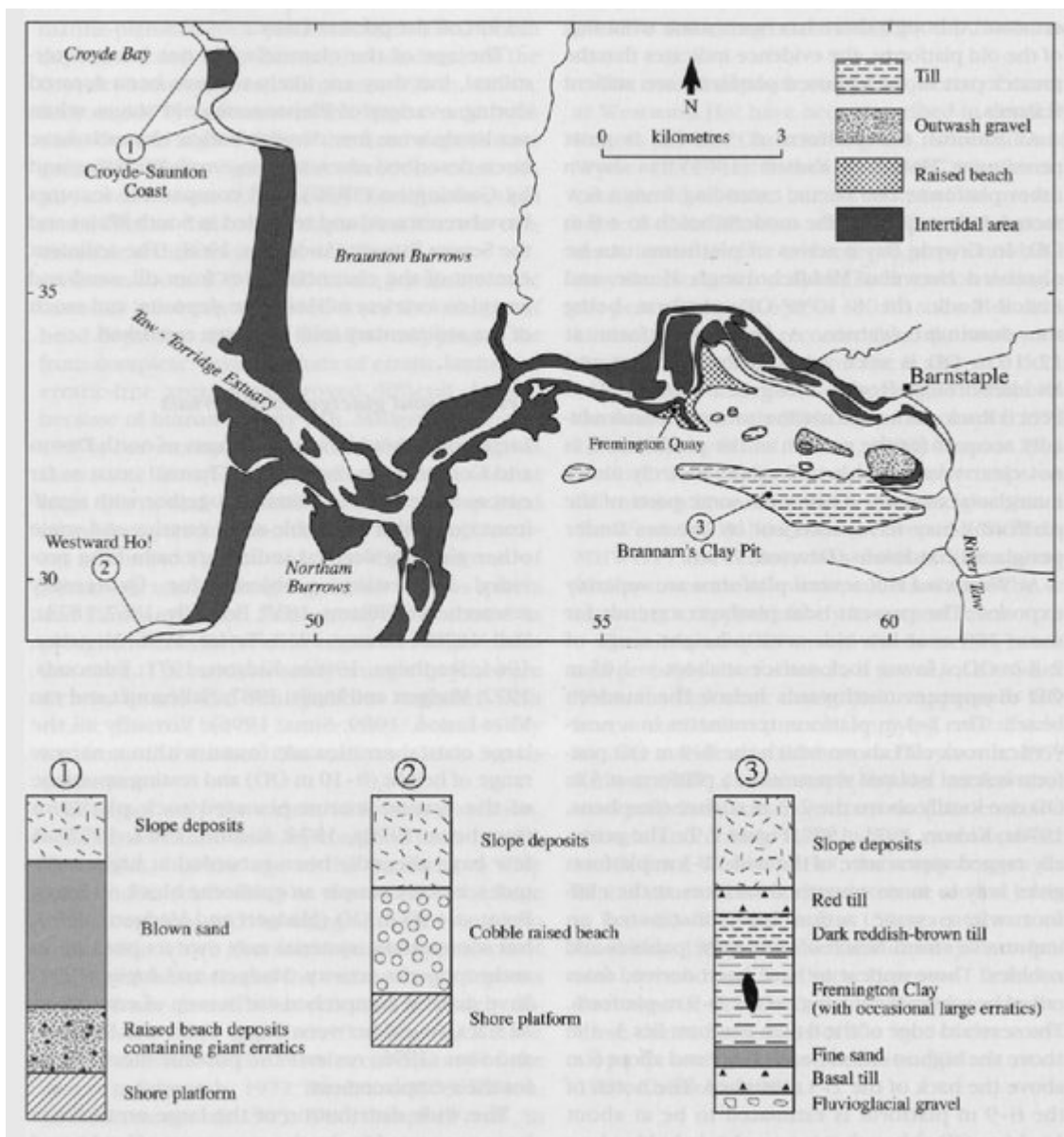
*(Figure 6.8) Porth Nanven, west Cornwall: the spectacular 'raised boulder beach' overlain by solifluction deposits. (Photo: D.H. Keen.)*



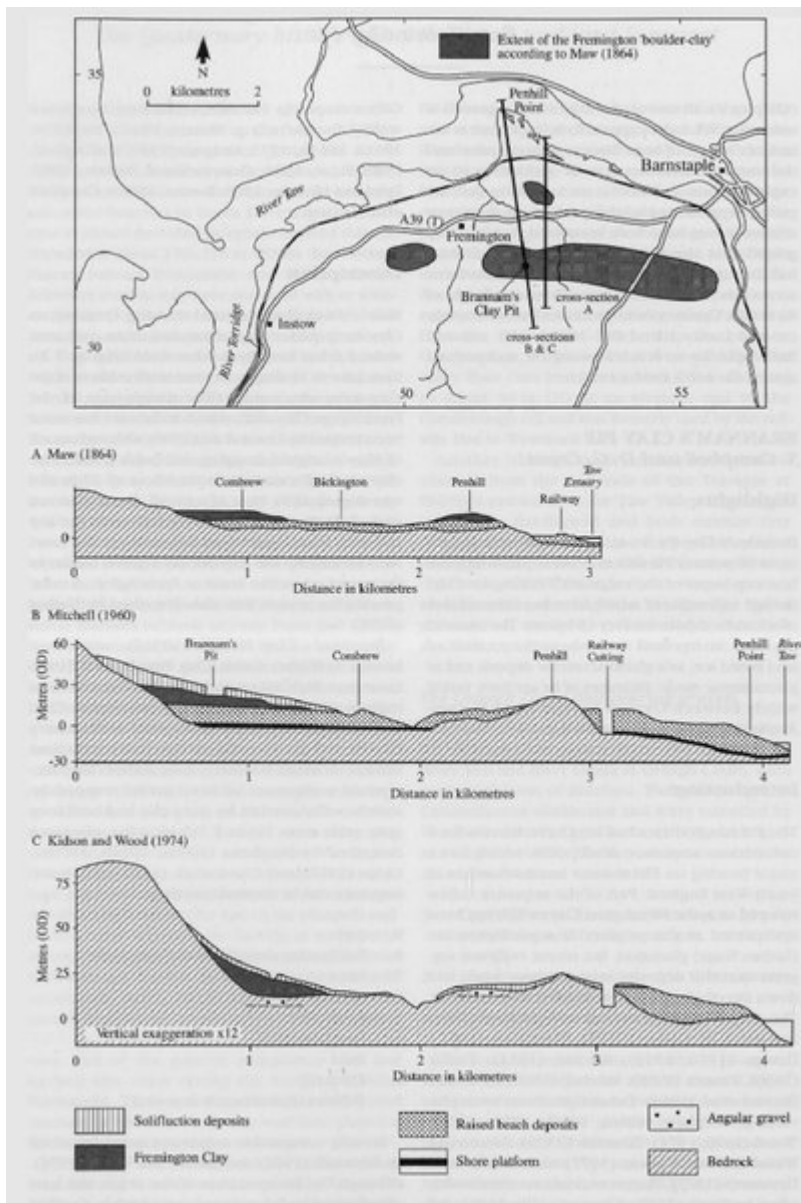
*(Figure 6.9) Coastal exposures near Godrevy Cove, showing shore platform overlain by raised beach cobbles, sand and various head facies. (Photo: S. Campbell.)*



(Figure 6.10) The Quaternary sequence at Trebetherick Point: Section 1 after Arkell (1943); Section 2 compiled by S. Campbell.

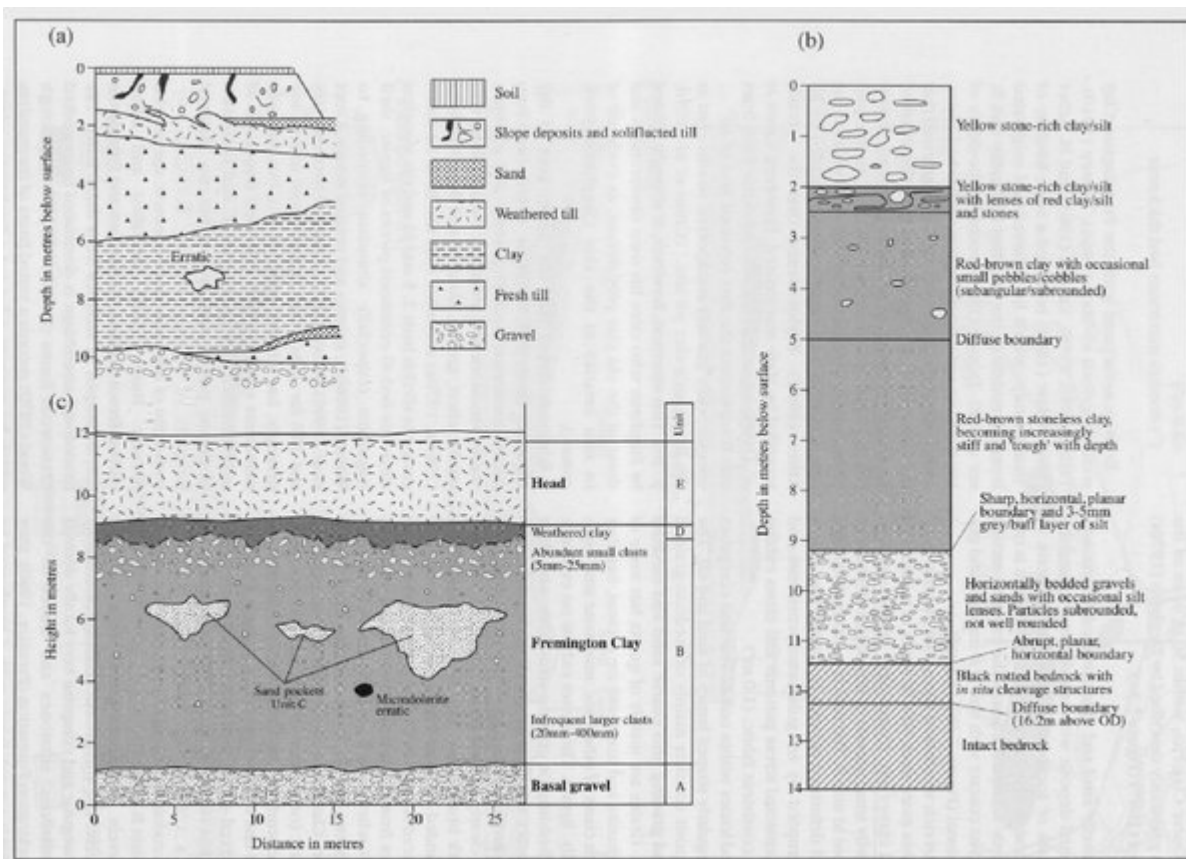


(Figure 7.1) The distribution and proposed stratigraphical relationships of Quaternary deposits around the Taw-Torrige Estuary. (After Kidson and Heyworth, 1977.)



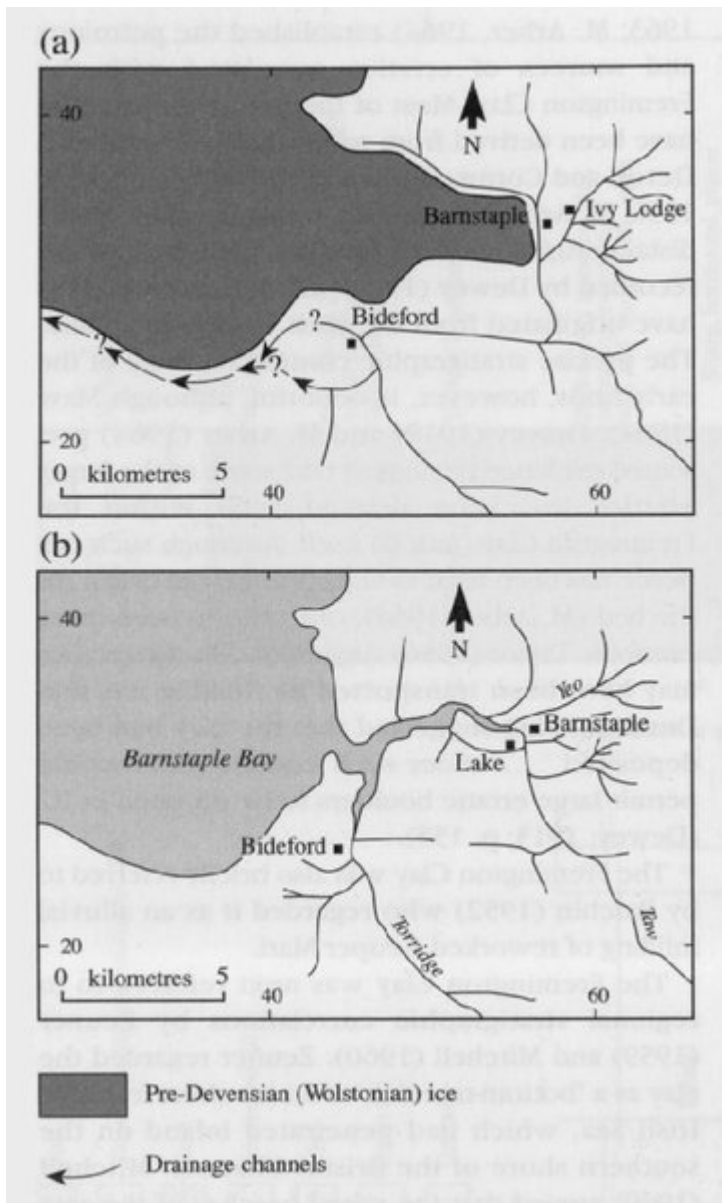
(Figure 7.2) The extent of the Fremington 'boulder-clay' according to Maw (1864), and proposed stratigraphical relationships in the Fremington area. (After Maw, 1864, Mitchell, 1960 and Kidson and Wood, 1974.)





(Figure 7.3) The Quaternary sequence at Brannam's Clay Pit, Fremington. (a) Composite section of the former eastern and southern working faces, adapted from Stephens (1966a, 1966b, 1970a). (b) The succession recorded by Croot in 1987. (c) The sequence recorded by Croot et al. (1996).

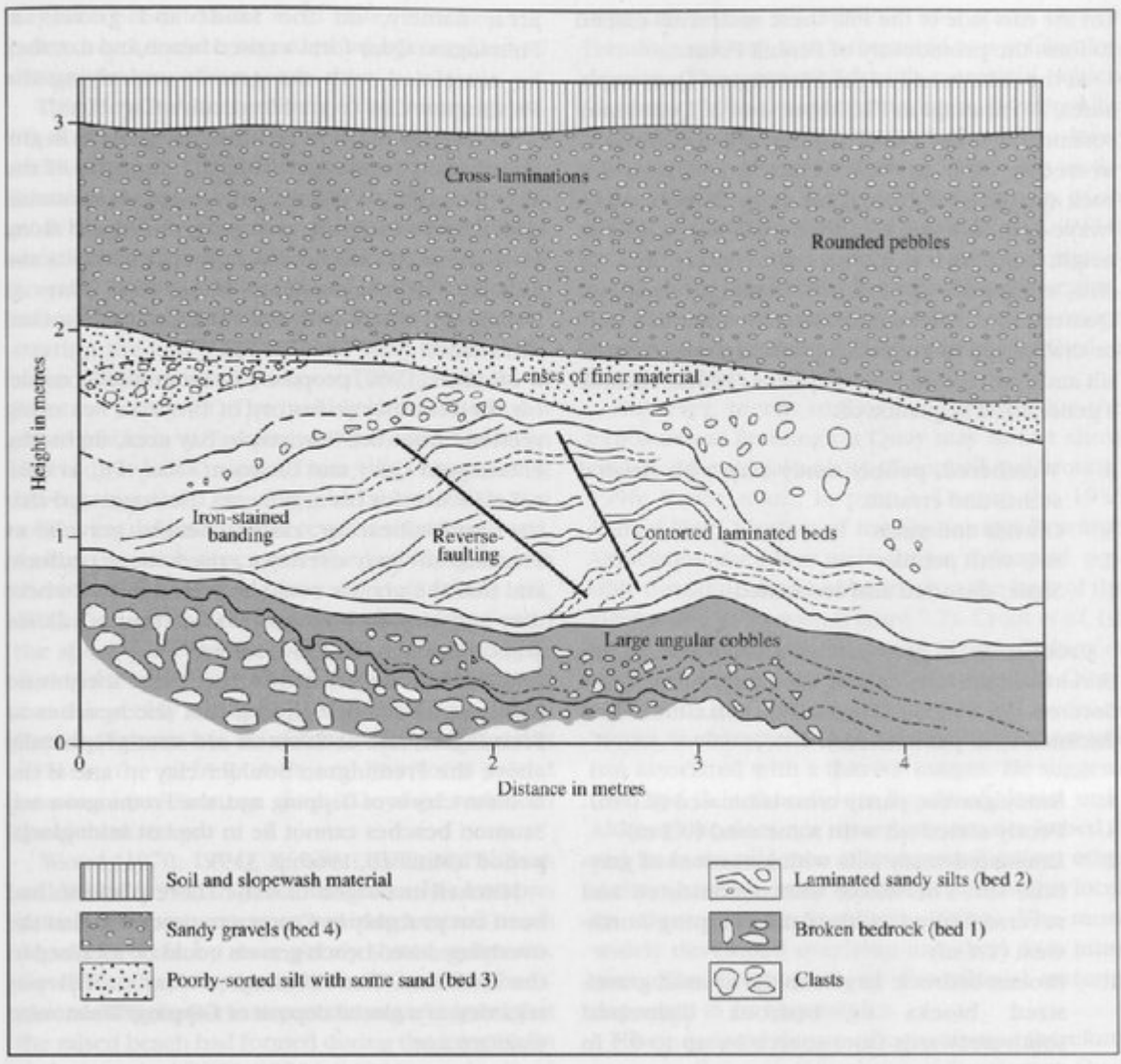




(Figure 7.4) A reconstruction of the proposed Wolstonian (Saalian) glaciation of the Barnstaple Bay area, after Edmonds (1972), illustrating: (a) The development of ice-marginal drainage at the height of glaciation; (b) Present-day drainage.



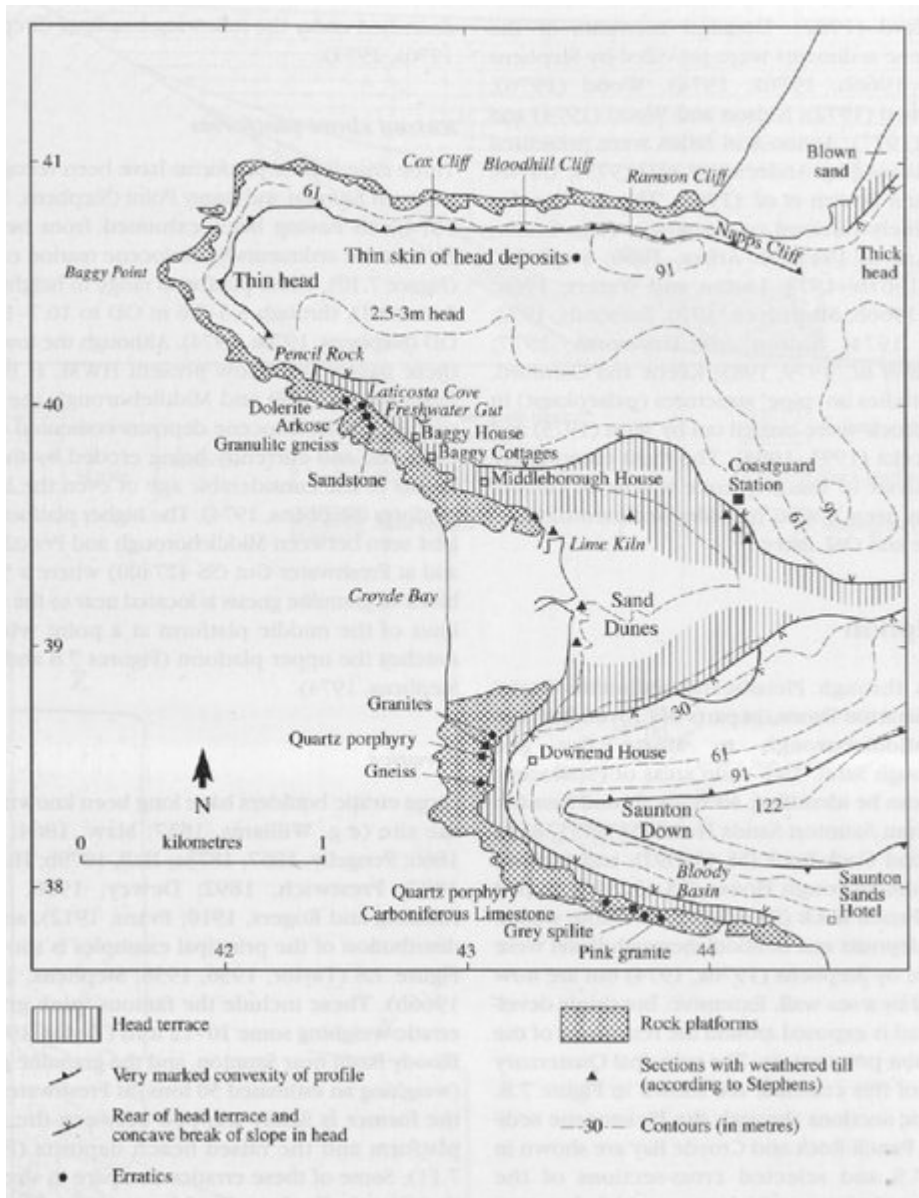
*(Figure 7.5) The Pleistocene sequence towards the western end of the Fremington Quay exposure. The vertical 'pipe' structures are infilled with lighter-coloured silt and clay, and penetrate beyond the base of the exposure: they may be frost or desiccation cracks (Wood, 1970). (Photo: S. Campbell.)*



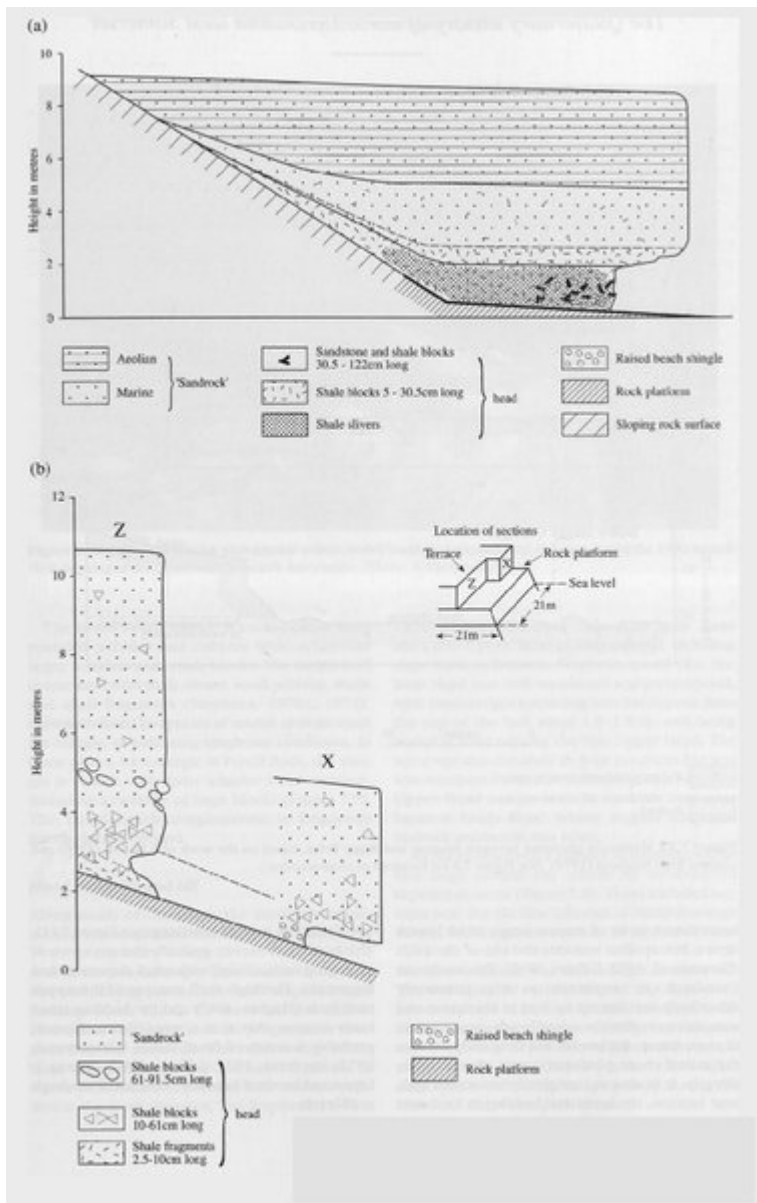
(Figure 7.6) The Quaternary sequence at the eastern end of the Fremington Quay exposure. (After Croot et al., in prep.)



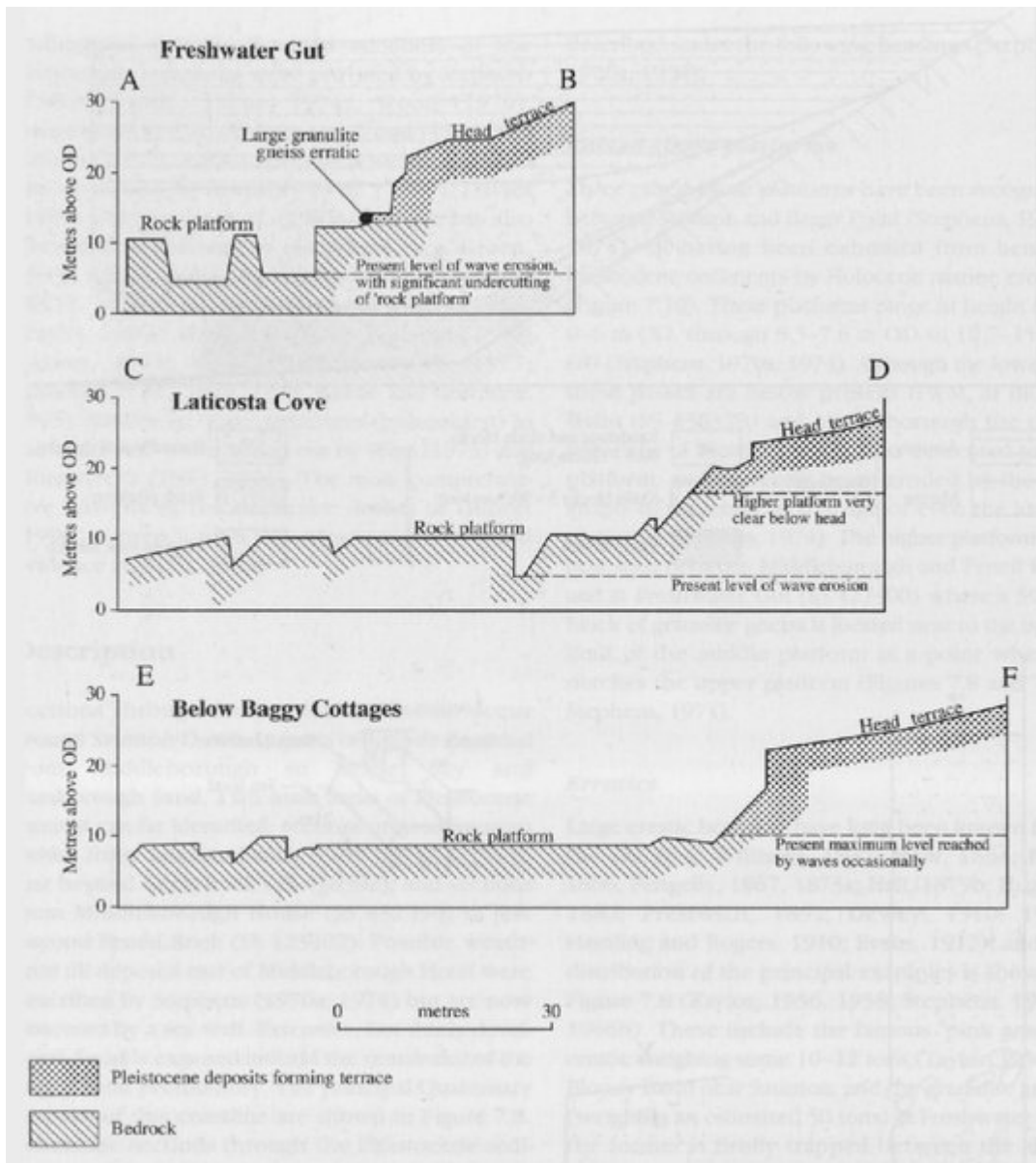
(Figure 7.7) Members of the Quaternary Research Association discuss possible evidence for glaciotectonism at the base of the Pleistocene succession towards the eastern end of the Fremington Quay exposures. (Photo: S. Campbell.)



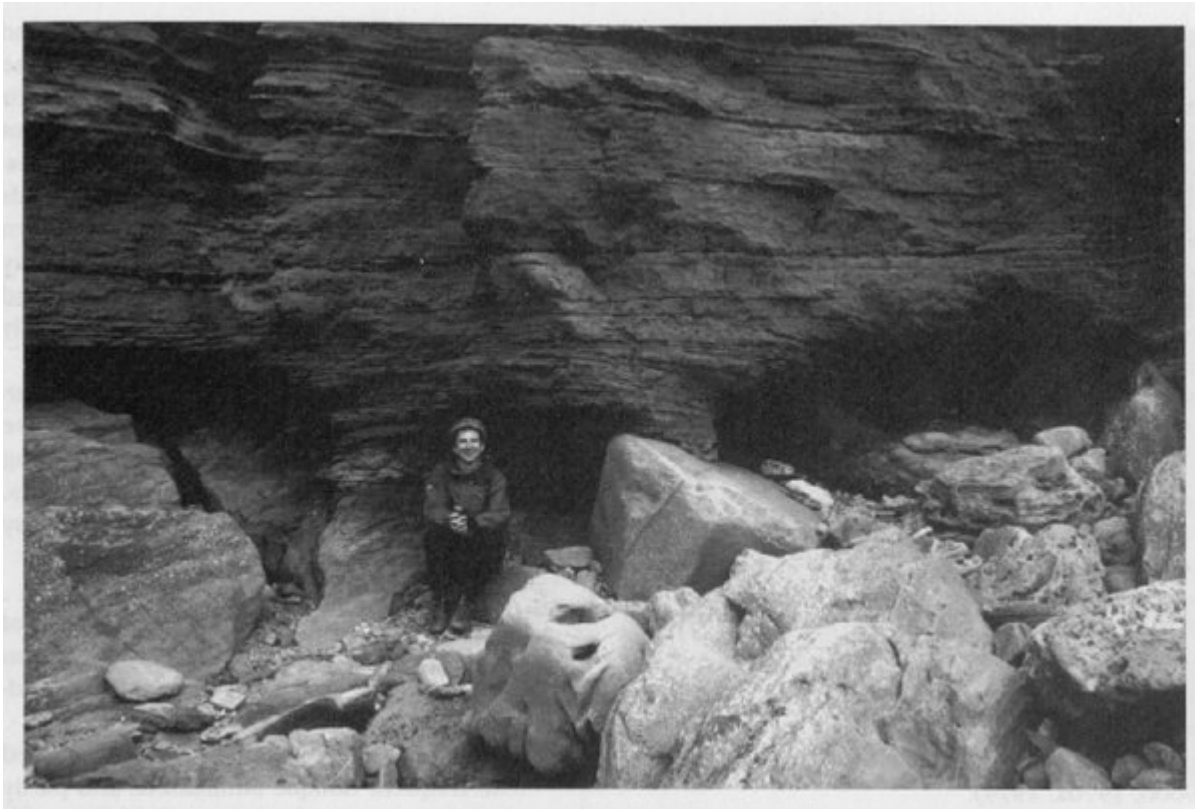
(Figure 7.8) The Quaternary deposits and coastal morphology of the Croyde-Saunton Coast. (Adapted from Stephens, 1970a.)



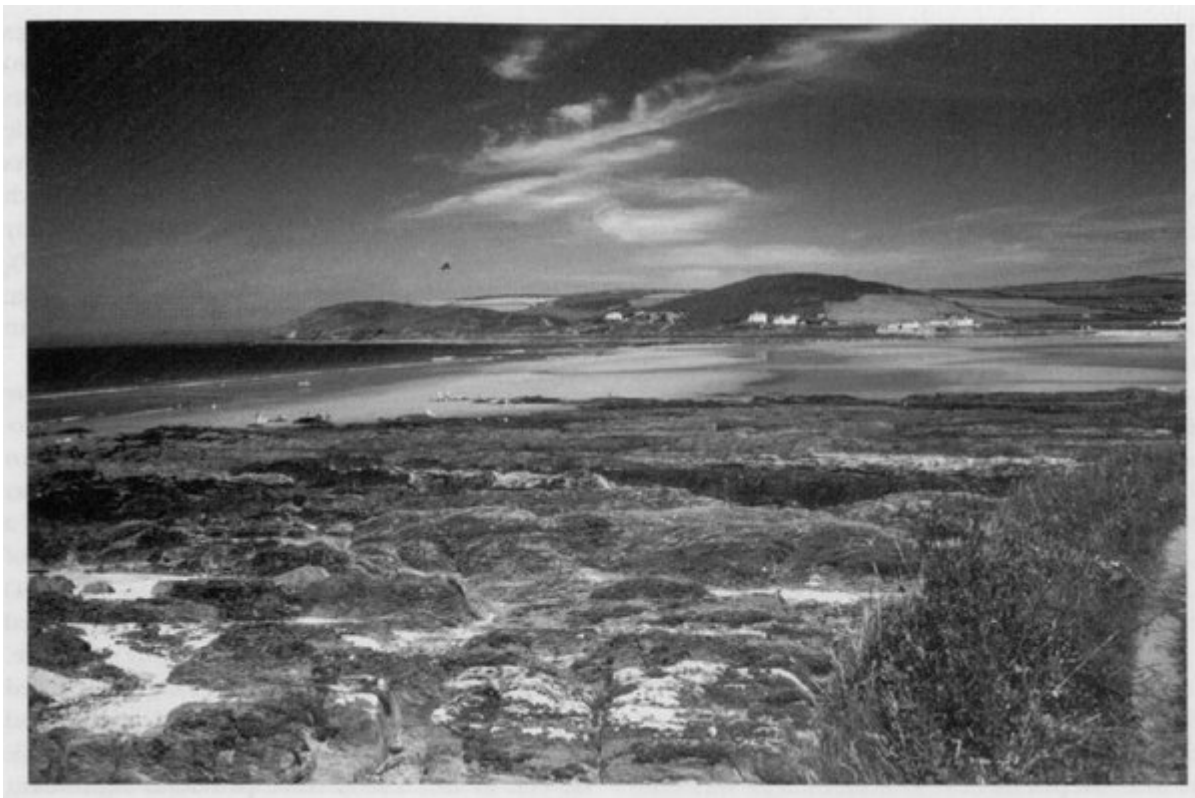
(Figure 7.9) The Quaternary succession at: (a) Pencil Rock; (b) East of Pencil Rock, based on the work of R.M. Eve (1970) and adapted from Stephens (1974).



(Figure 7.10) Marine-cut platforms between Saunton and Baggy Point, based on the work of R.M. Eve (1970) and adapted from Stephens (1974). (See (Figure 7.8) for locations of cross-sections.)

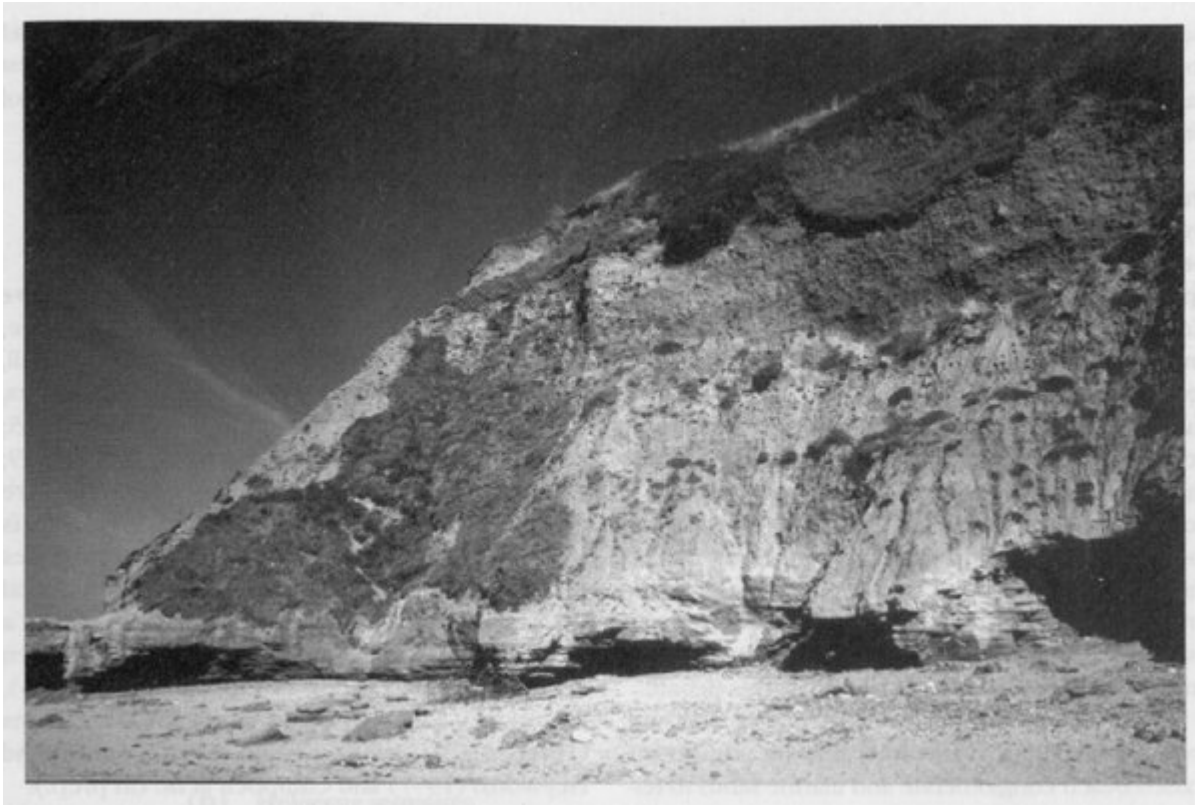


*(Figure 7.11) Saunton's famous 'pink granite' erratic, sealed beneath cemented sand and seen during the 1996 Annual Field Meeting of the Quaternary Research Association. (Photo: S. Campbell.)*



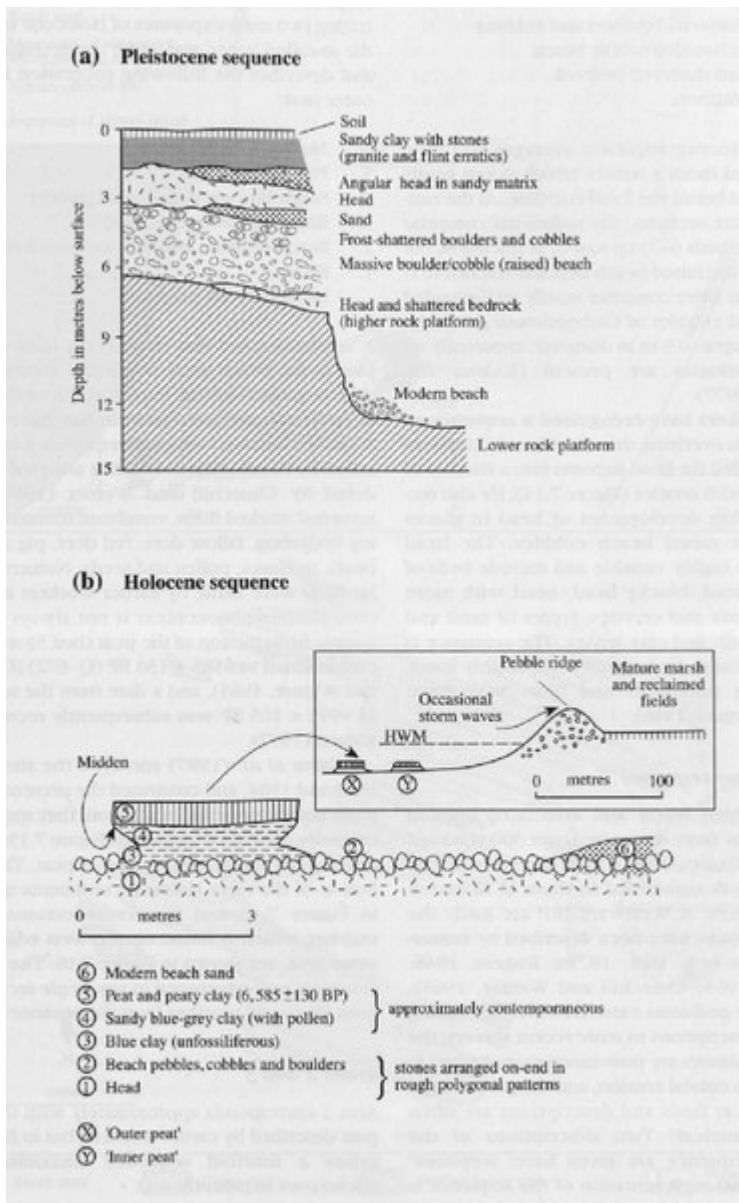
*(Figure 7.12) Extensively developed rock platforms at the western end of Saunton Down, looking north across Croyde Bay. (Photo: S. Campbell.)*



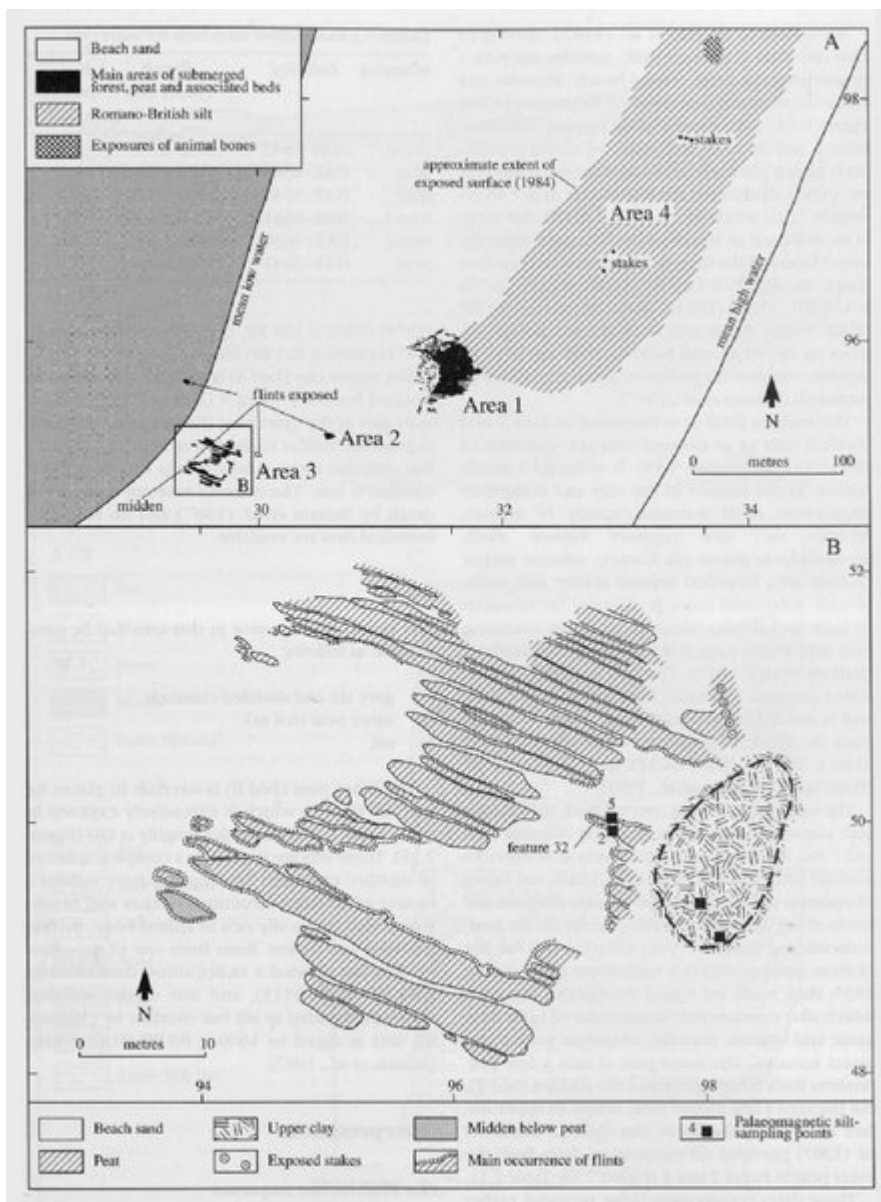


*(Figure 7.13) Thick cemented sand (marine and aeolian) and overlying head deposits near Saunton Sands Hotel. (Photo: S. Campbell.)*

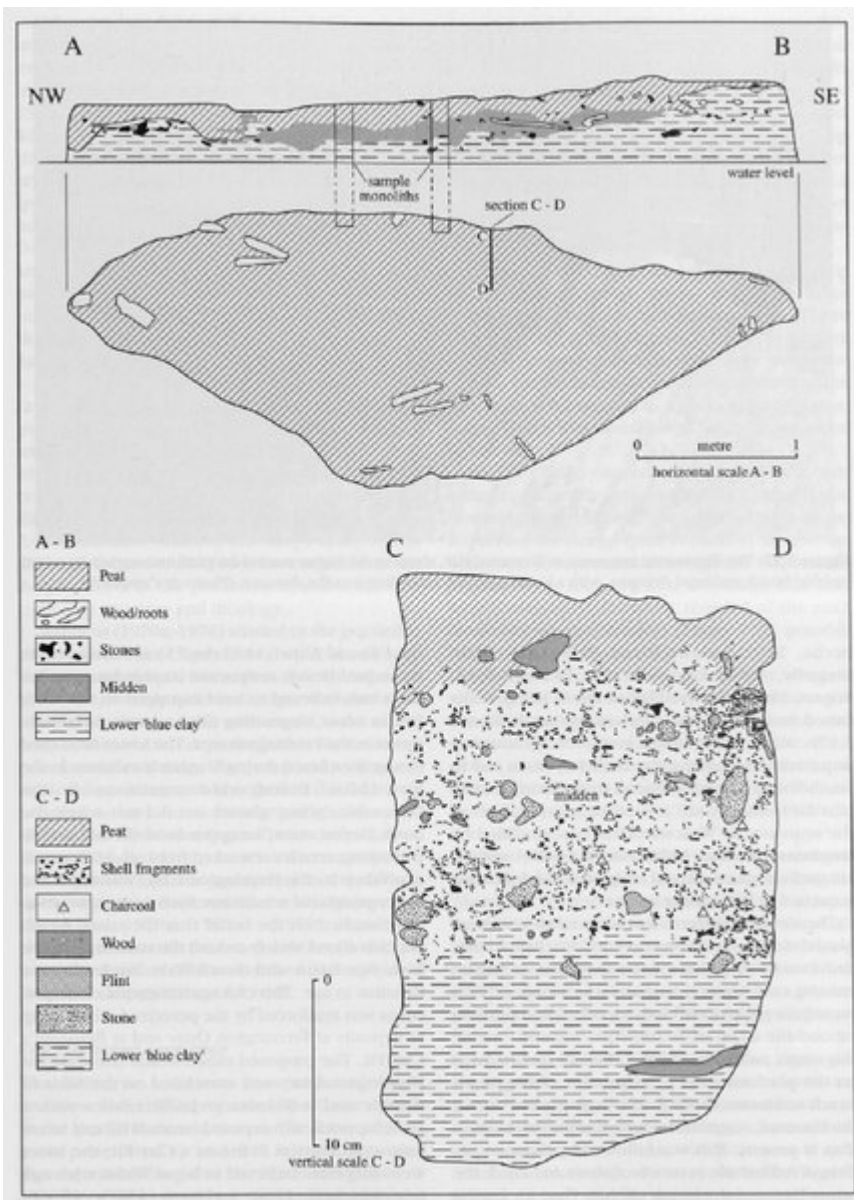




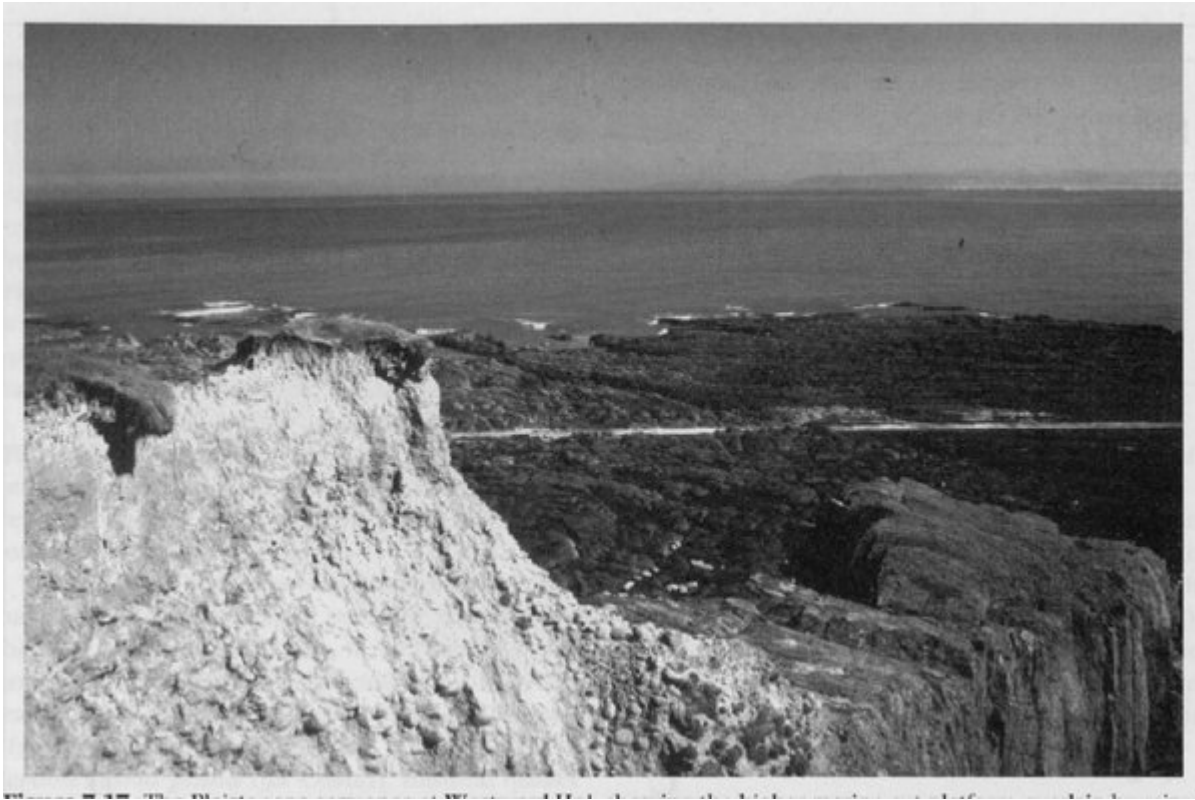
(Figure 7.14) Quaternary landforms and deposits at Westward Ho! (Adapted from Stephens 1970a.)



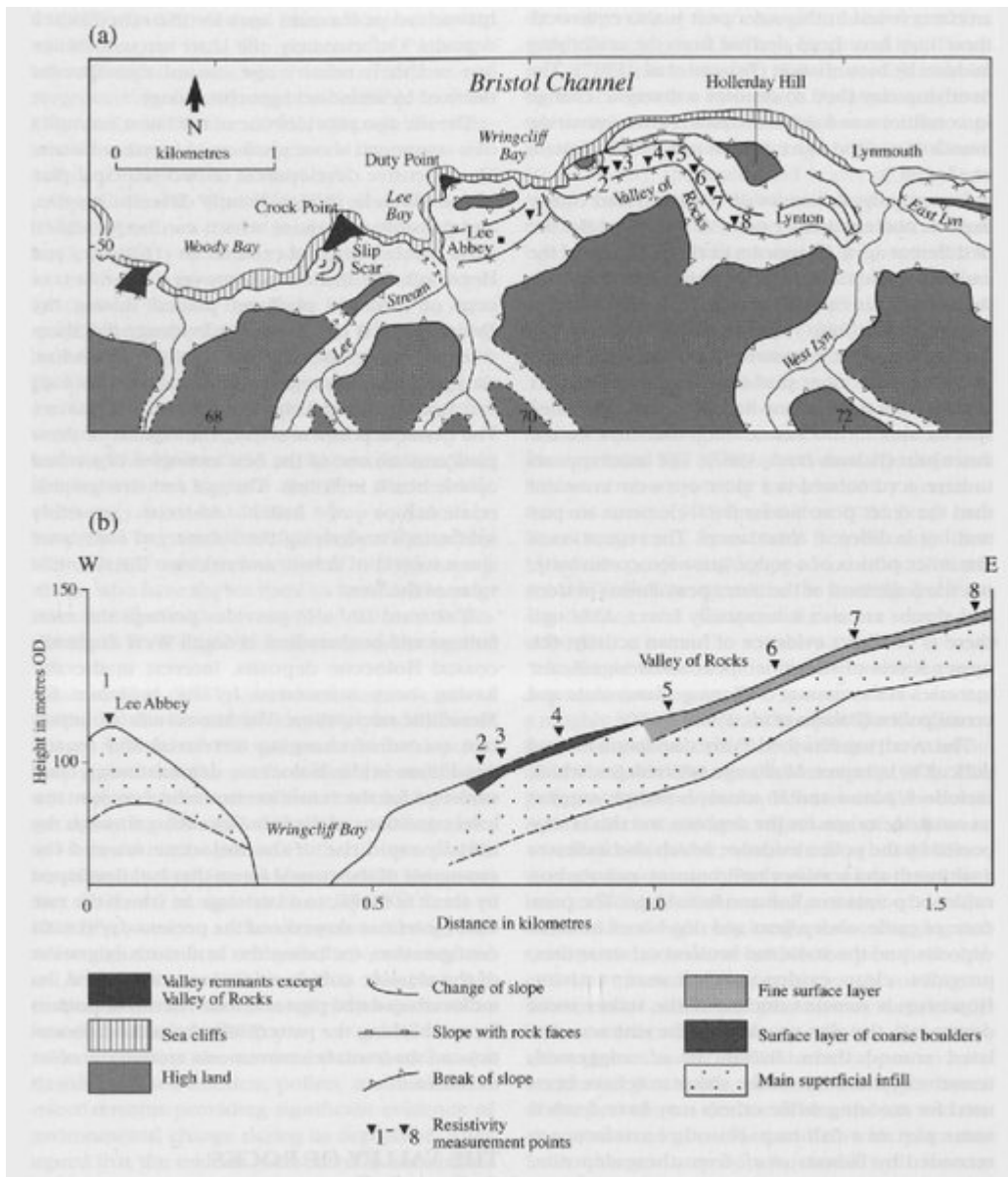
(Figure 7.15) The distribution of Holocene deposits at Westward Ho! (Adapted from Balaam et al., 1987.)



(Figure 7.16) Plan and section of the midden 'island' at Westward Ho! (Adapted from Balaam et al., 1987.)



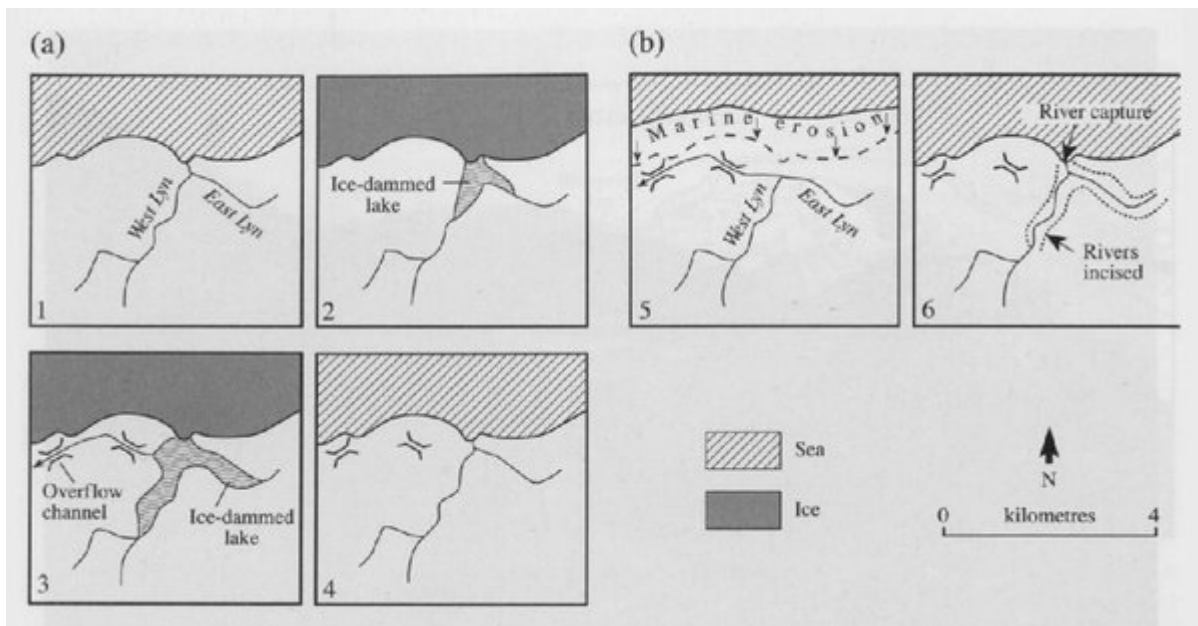
*(Figure 7.17) The Pleistocene sequence at Westward Ho!, showing the higher marine-cut platform overlain by raised 'cobble' beach and head deposits, with a lower platform extending into the distance. (Photo: S. Campbell.)*



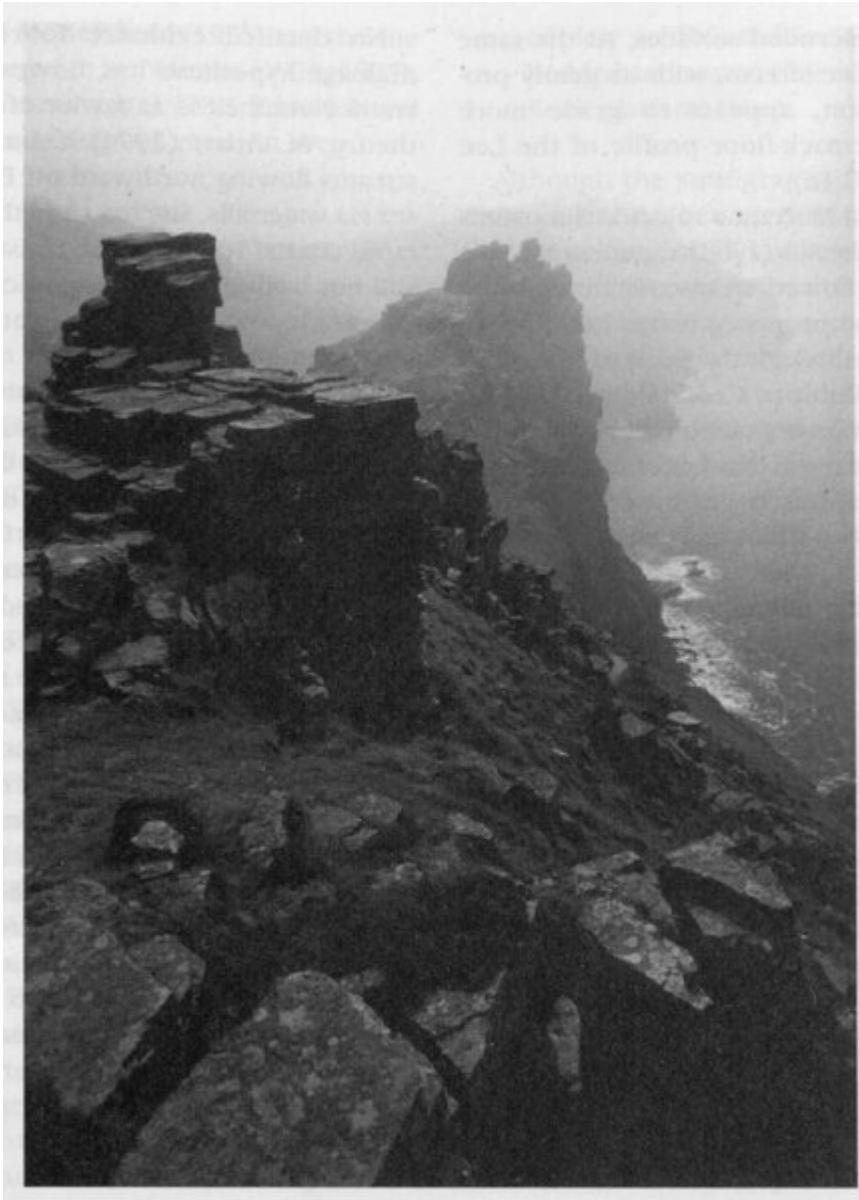
(Figure 7.18) (a) Landforms and Pleistocene deposits between Lynmouth and Woody Bay. (b) Profile of Pleistocene deposits within the Valley of Rocks and at Lee Abbey. (Adapted from Dalzell and Durrance, 1980.)



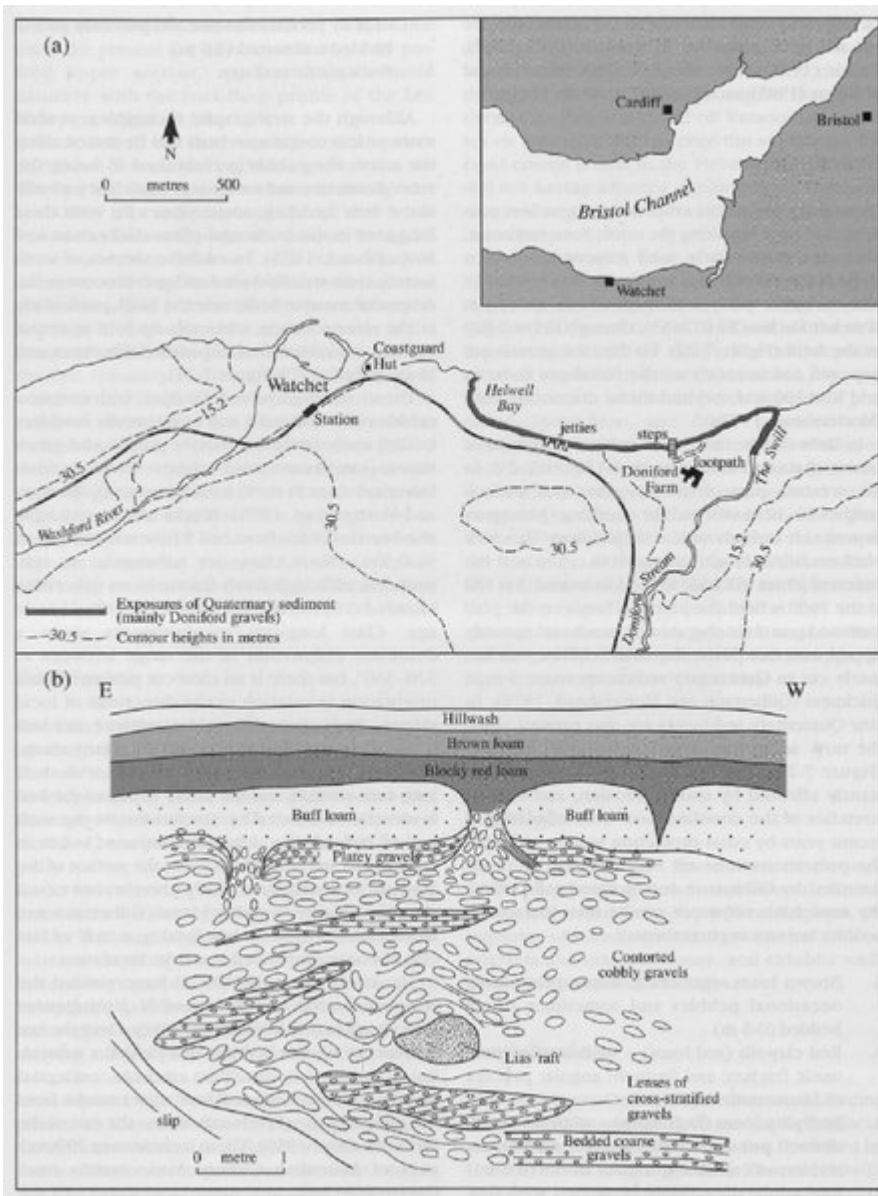
(Figure 7.19) The Valley of Rocks, looking east from Wringcliff Bay. (Photo: S. Campbell.)



(Figure 7.20) The evolution of the Valley of Rocks by: (a) Pre-Devensian glacial meltwaters; (b) Marine erosion and river capture. (Adapted from Mottershead, 1967, 1977c.)

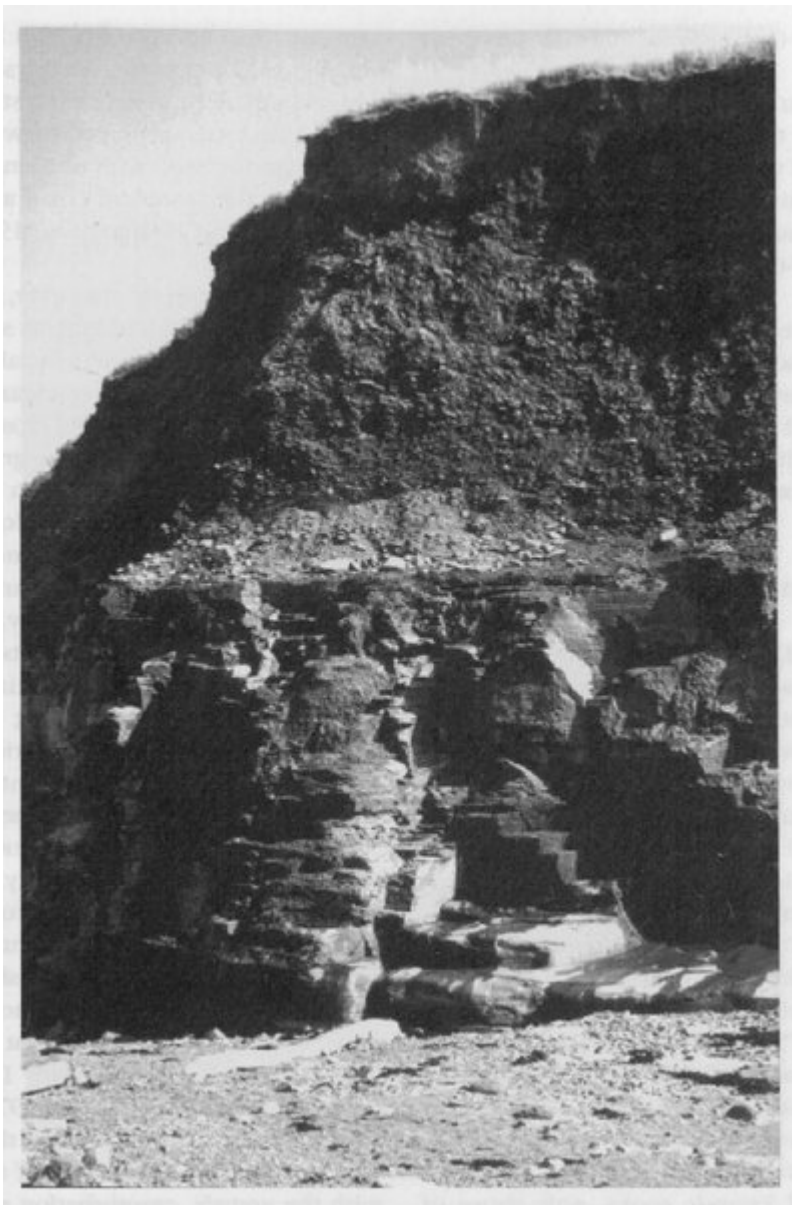


*(Figure 7.21) Tor-like buttresses and precipitous rock slopes on the northern margin of the Valley of Rocks, looking west.  
(Photo: S. Campbell.)*



(Figure 7.22) (a) The location of the Doniford gravels. (b) Typical section through the Doniford gravels west of the footpath. (Adapted from Gilbertson and Mottershead, 1975.)

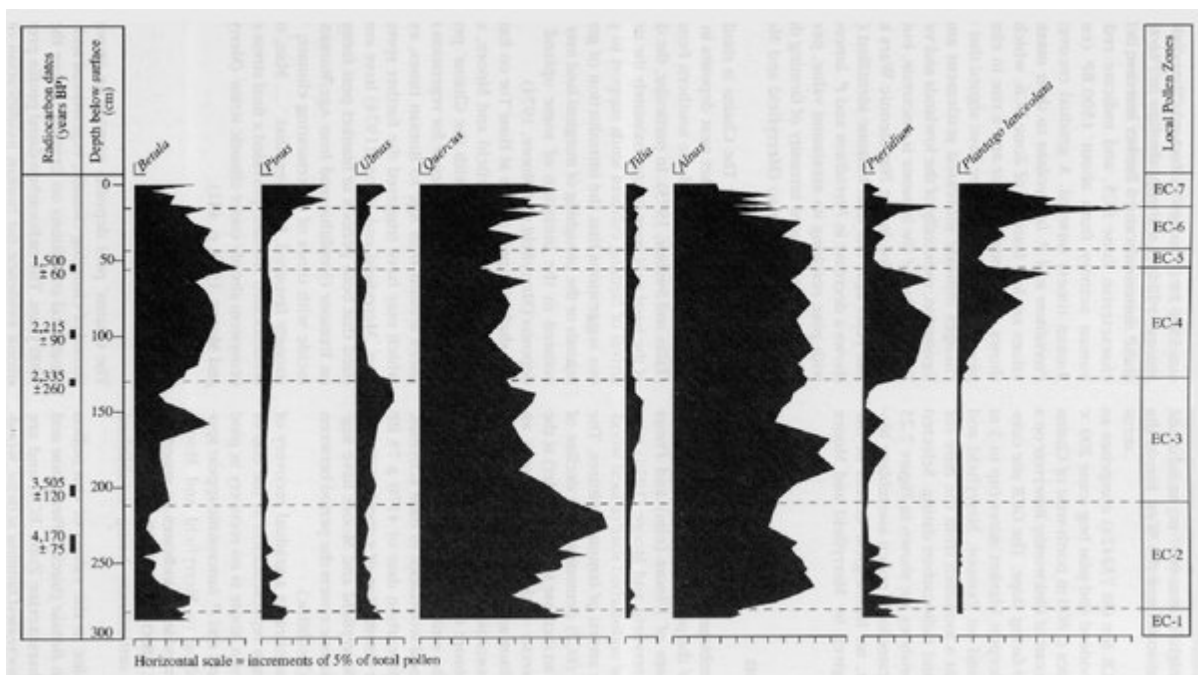




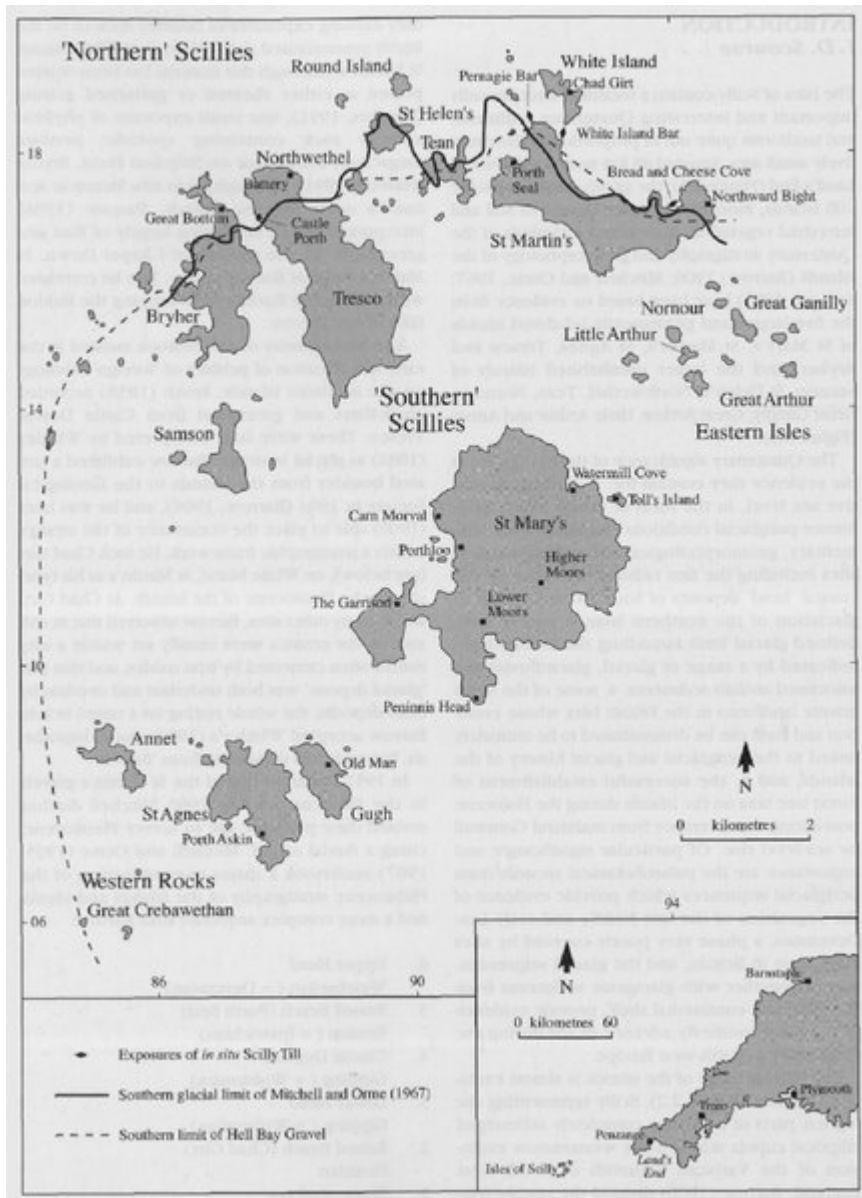
*(Figure 7.23) The Doniford gravels overlying Liassic bedrock at the eastern end of Helwell Bay. (Photo: S. Campbell.)*



(Figure 7.24) Quaternary deposits (mainly fluvial cobbly gravels; bed 2) exposed on the western bank of the Swill in 1980. (Photo: S. Campbell.)



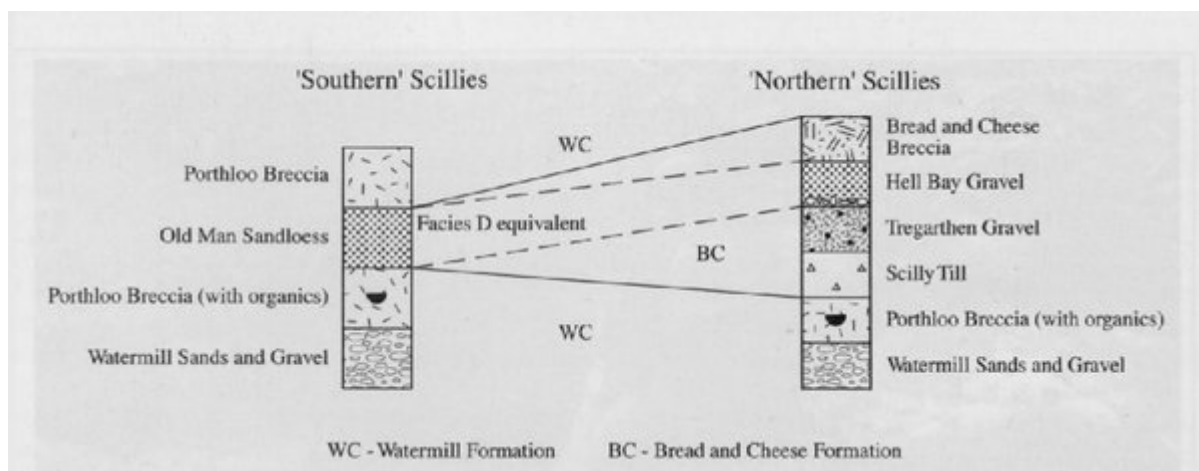
(Figure 7.25) Selected pollen data and radiocarbon dates from a peat profile at The Chains, Exmoor. (Adapted from Merryfield and Moore 1974.)



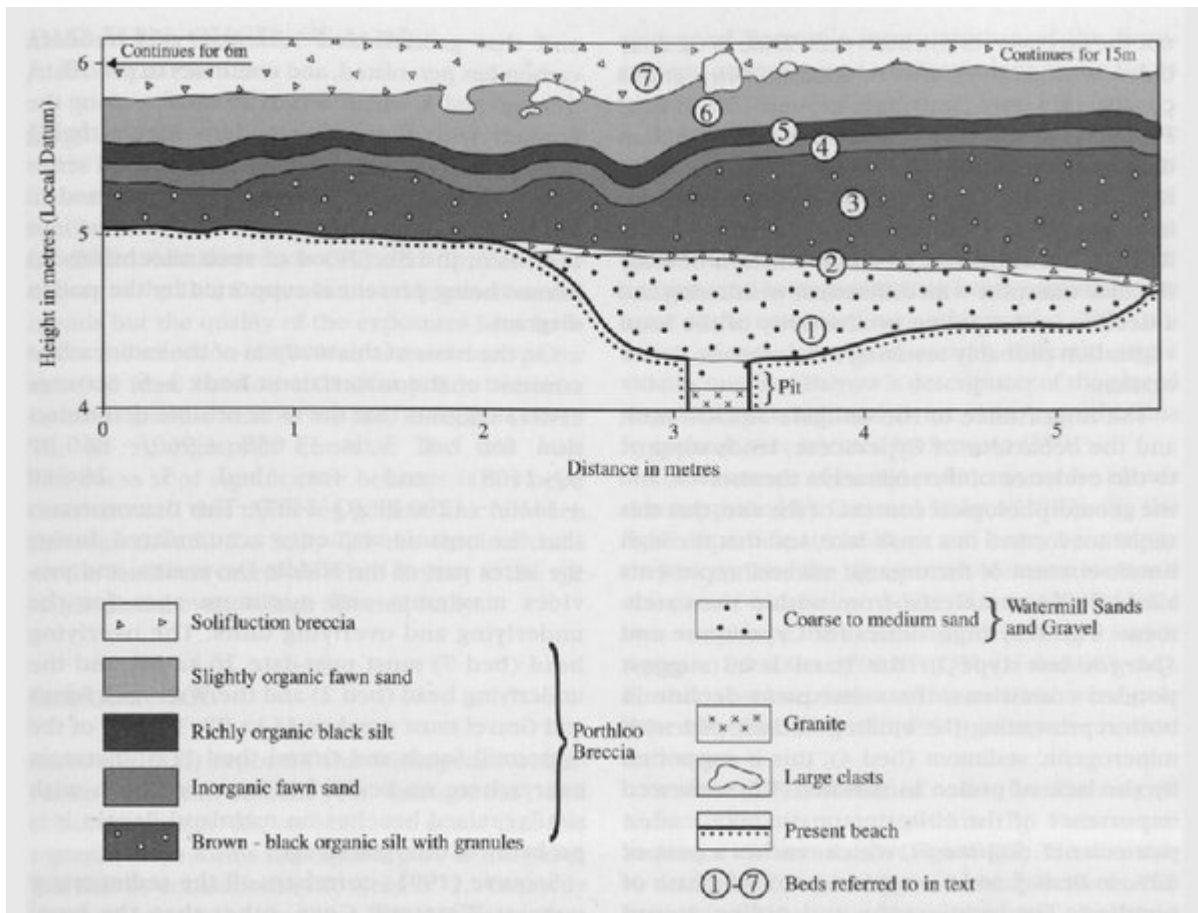
(Figure 8.1) The Isles of Scilly: critical sites, exposures of the Scilly Till, the southern limit of the Hell Bay Gravel and Mitchell and Orme's (1967) glacial limit. (Adapted from Scourse, 1991.)



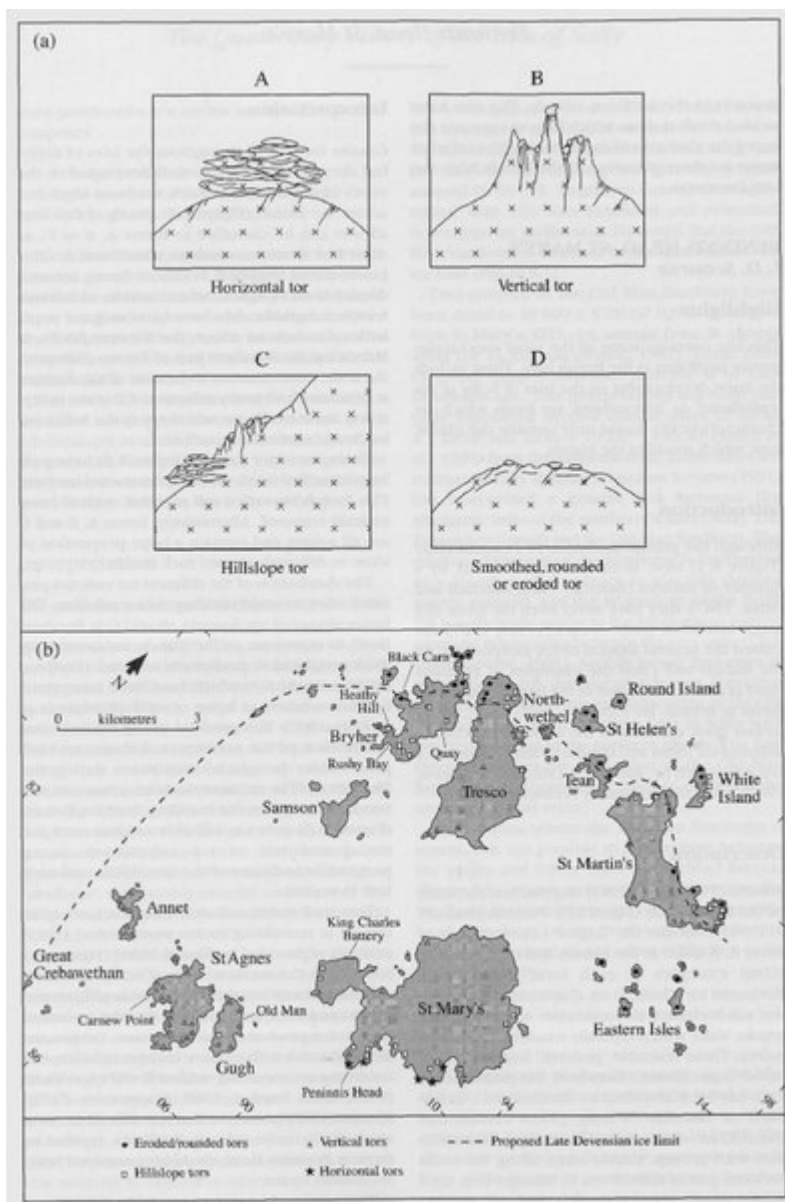
(Figure 8.2) Carn Morval on St Mary's (Figure 8.1) is one of five sites on the Isles of Scilly where organic sediments, which have yielded pollen evidence and radiocarbon dates, lie beneath or interbedded with periglacial head. Although yielding the most detailed of these palaeoenvironmental records, Carn Morval was not selected as a GCR site because coastal erosion has since removed much of the critical organic sequence. (Photo: J.D. Scourse.)



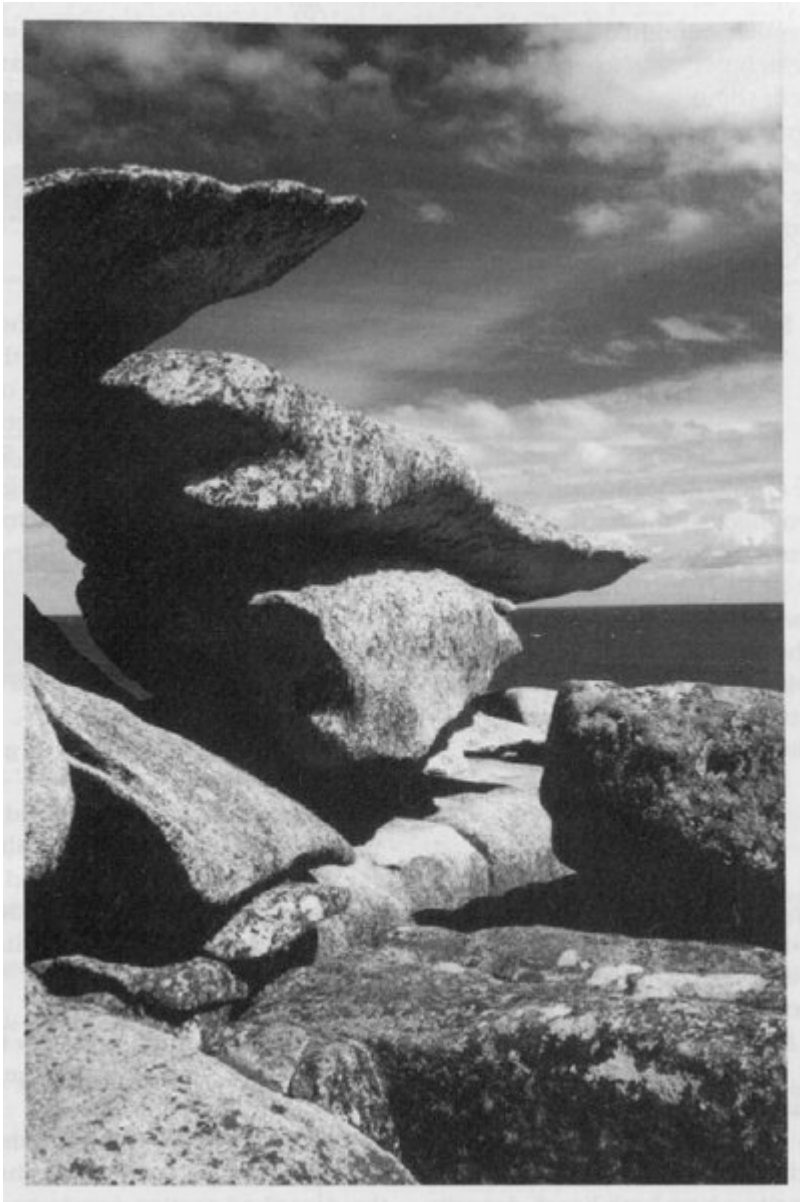
(Figure 8.3) A lithostratigraphic model for the Isles of Scilly. (Adapted from Scourse, 1991.)



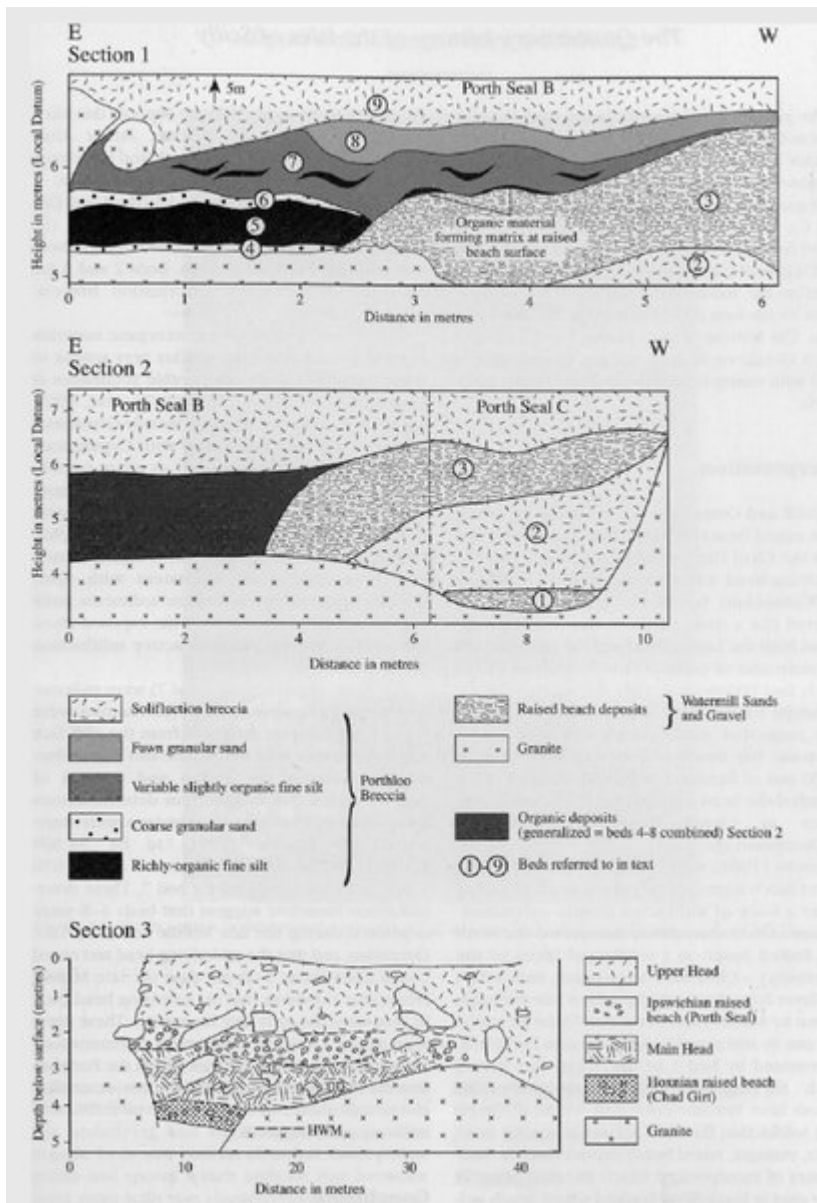
(Figure 8.5) The Pleistocene sequence at Watermill Cove. (Adapted from Scourse 1991.)



(Figure 8.6) (a) Variations in tor morphology. (b) Their distribution across the Isles of Scilly. (Adapted from Scourse 1986.)

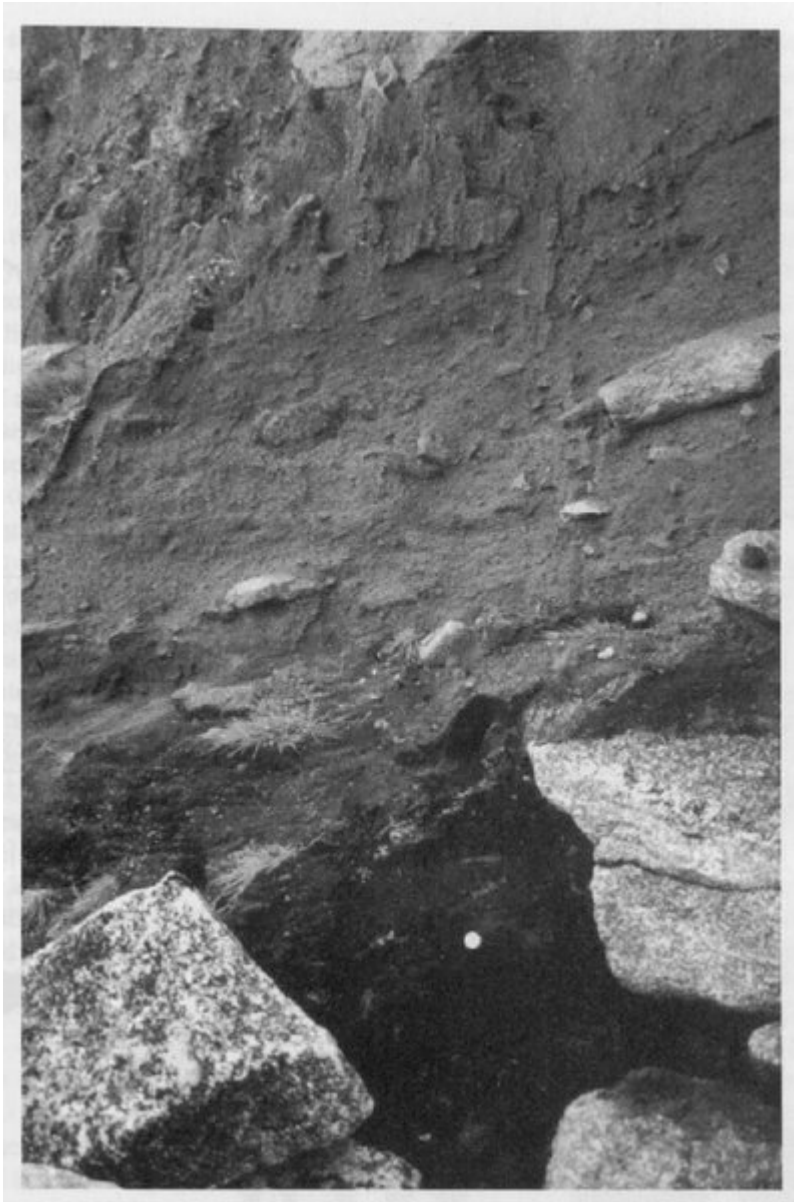


*(Figure 8.7) The spectacular development of horizontal tors (form (a); (Figure 8.6)) on the eastern side of Peninnis Head.  
(Photo: S. Campbell.)*

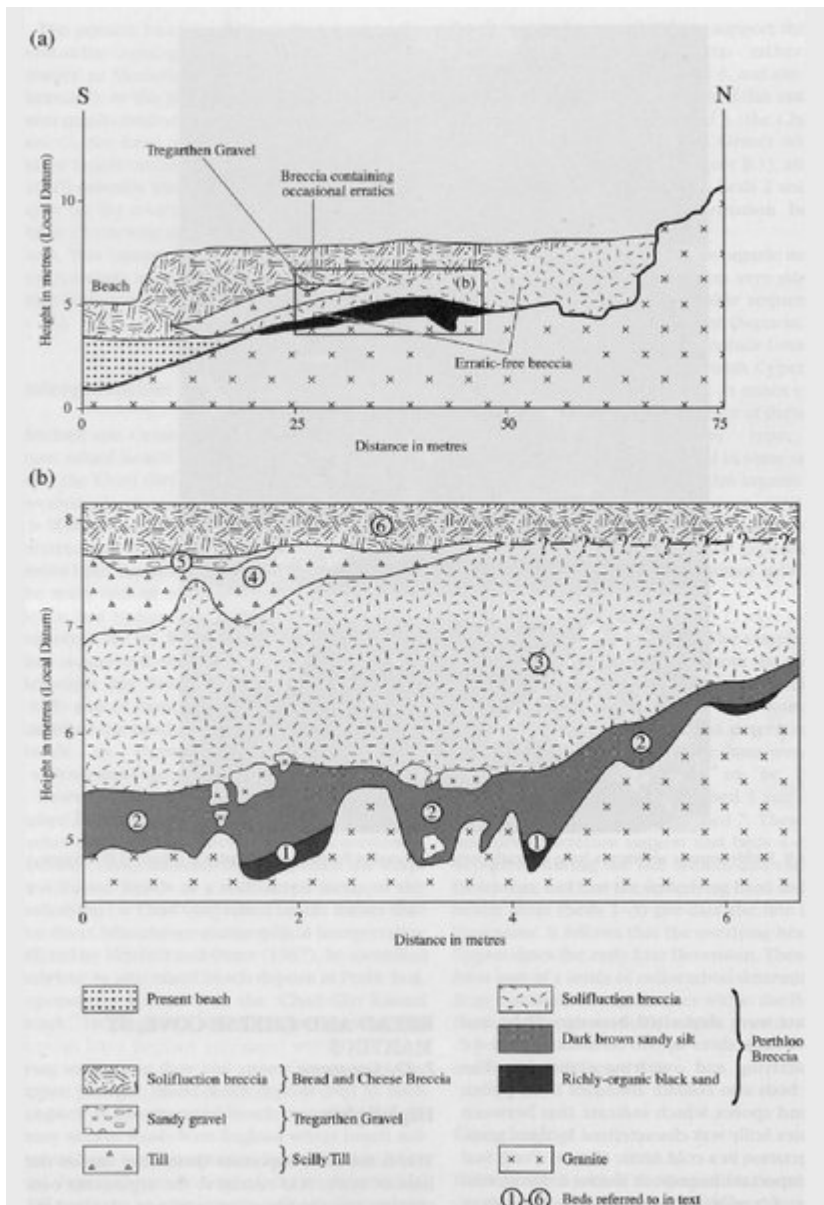


(Figure 8.8) The Pleistocene sequence at Porth Seal: Sections 1 and 2 adapted from Scourse (1991); Section 3 is based on a field sketch made in 1965 by F.M. Syngé and subsequently figured in Stephens (1970a) and Kidson (1977).

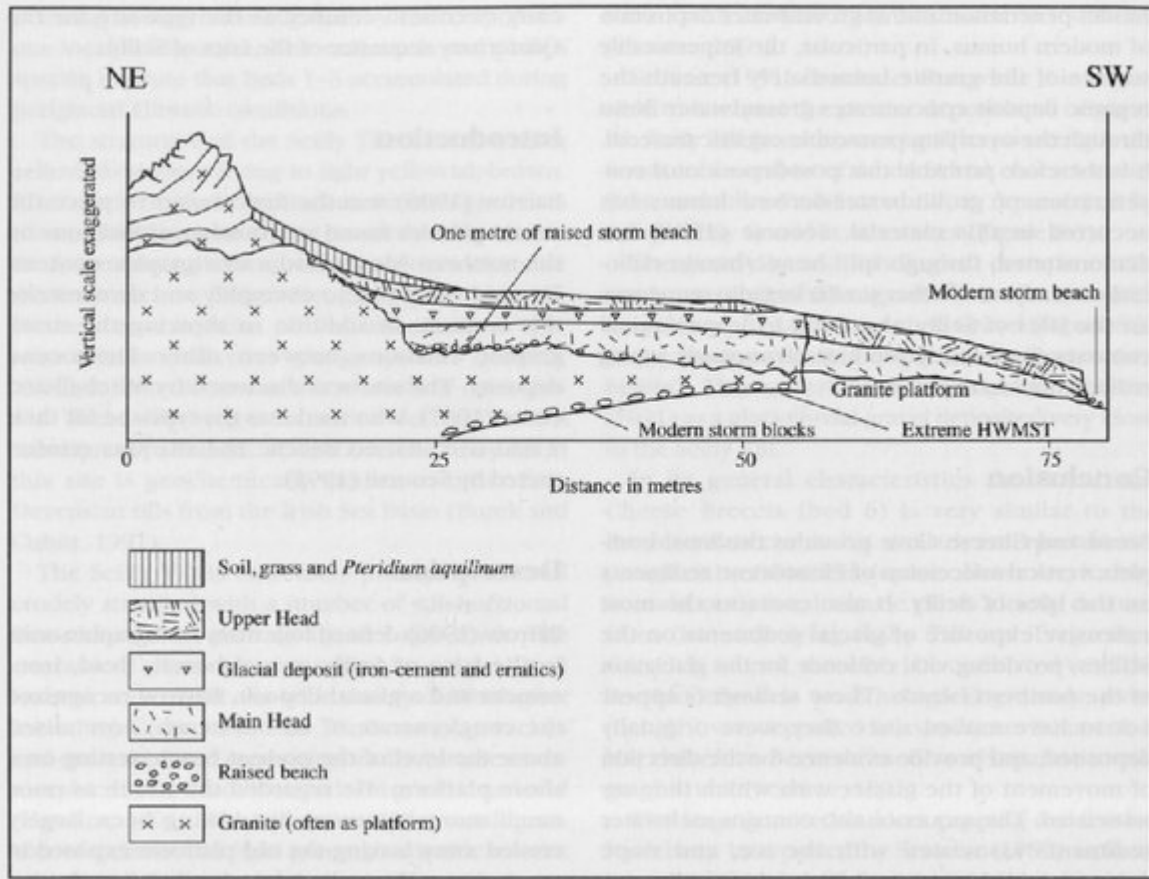




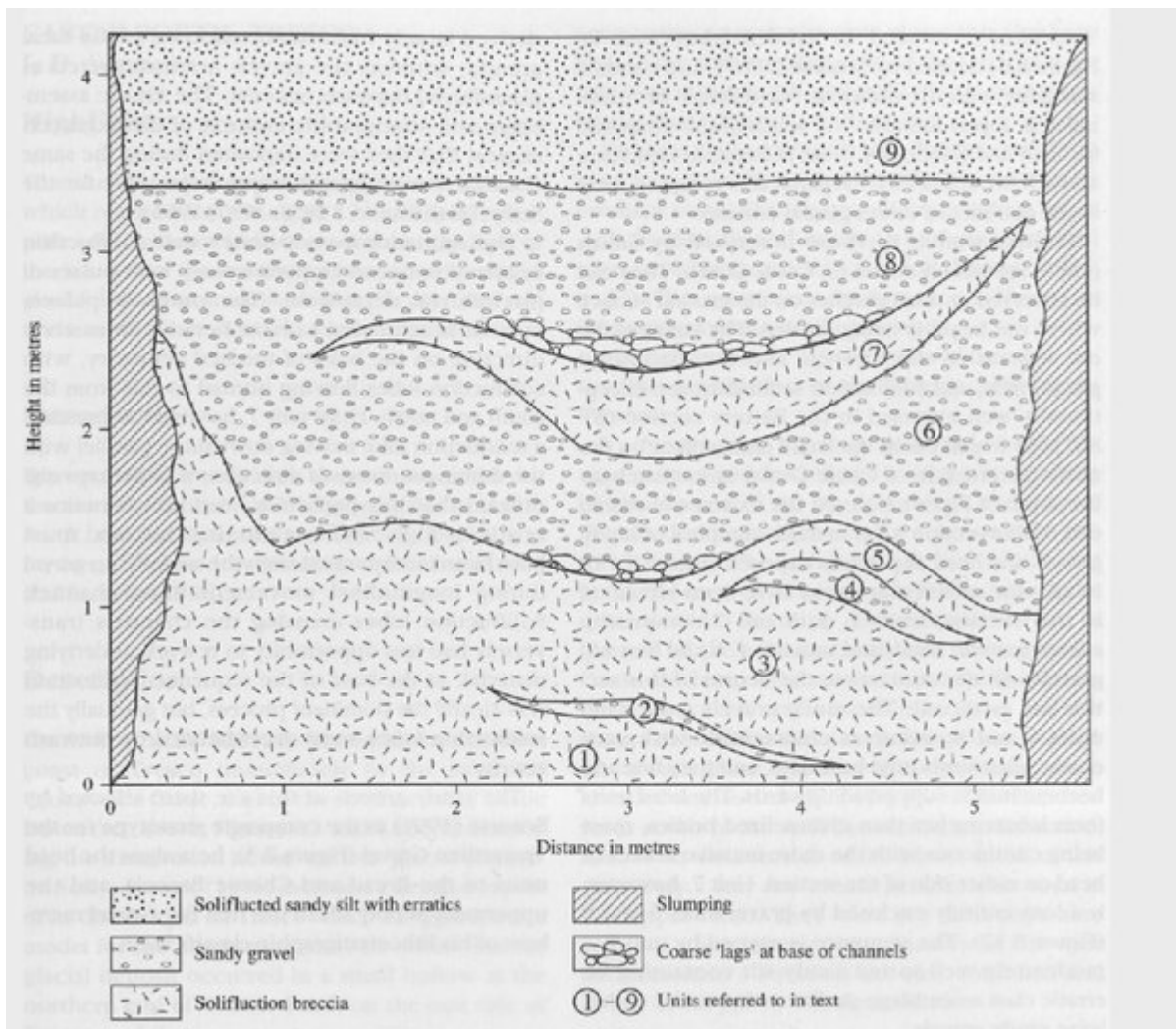
*(Figure 8.9) Richly organic sediments lying beneath periglacial head at Porth Seal, St Martin's. (Photo: J.D. Scourse.)*



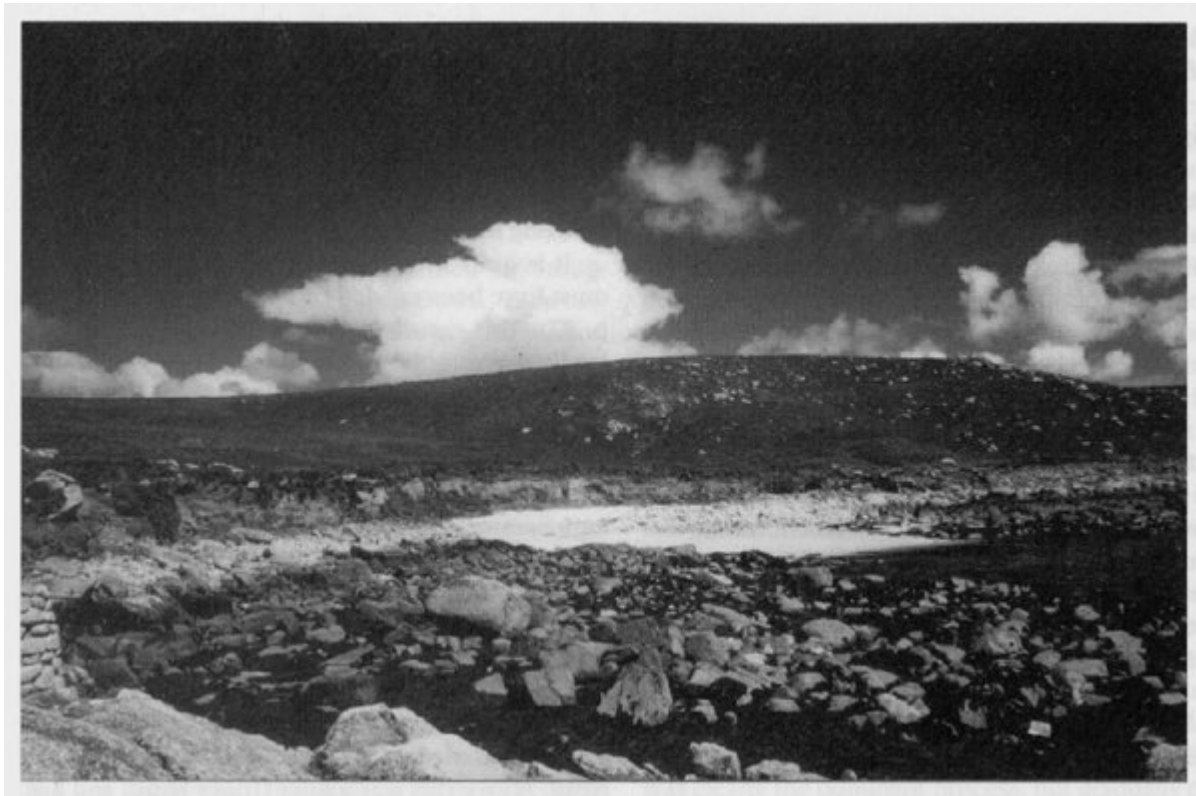
(Figure 8.10) The Pleistocene sequence at Bread and Cheese Cove. (Adapted from Scourse, 1991.)



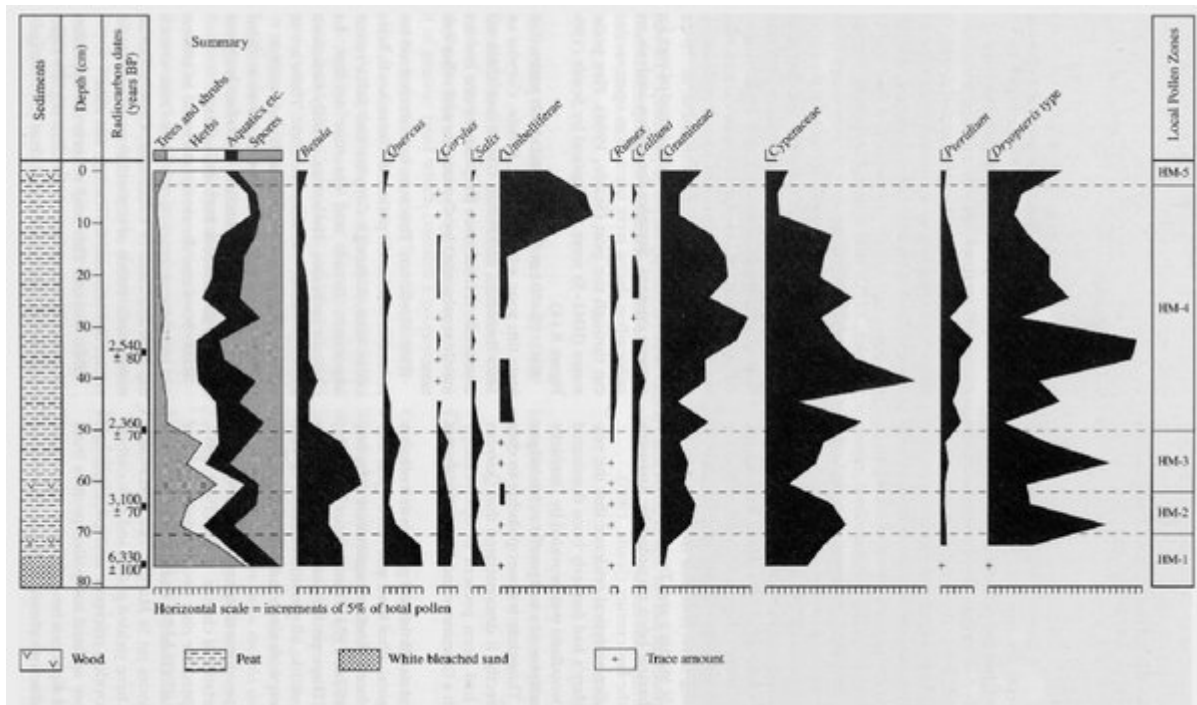
(Figure 8.11) The Quaternary sequence at Chad Girt according to Barrow (1906). (Adapted from Scourse, 1986.)



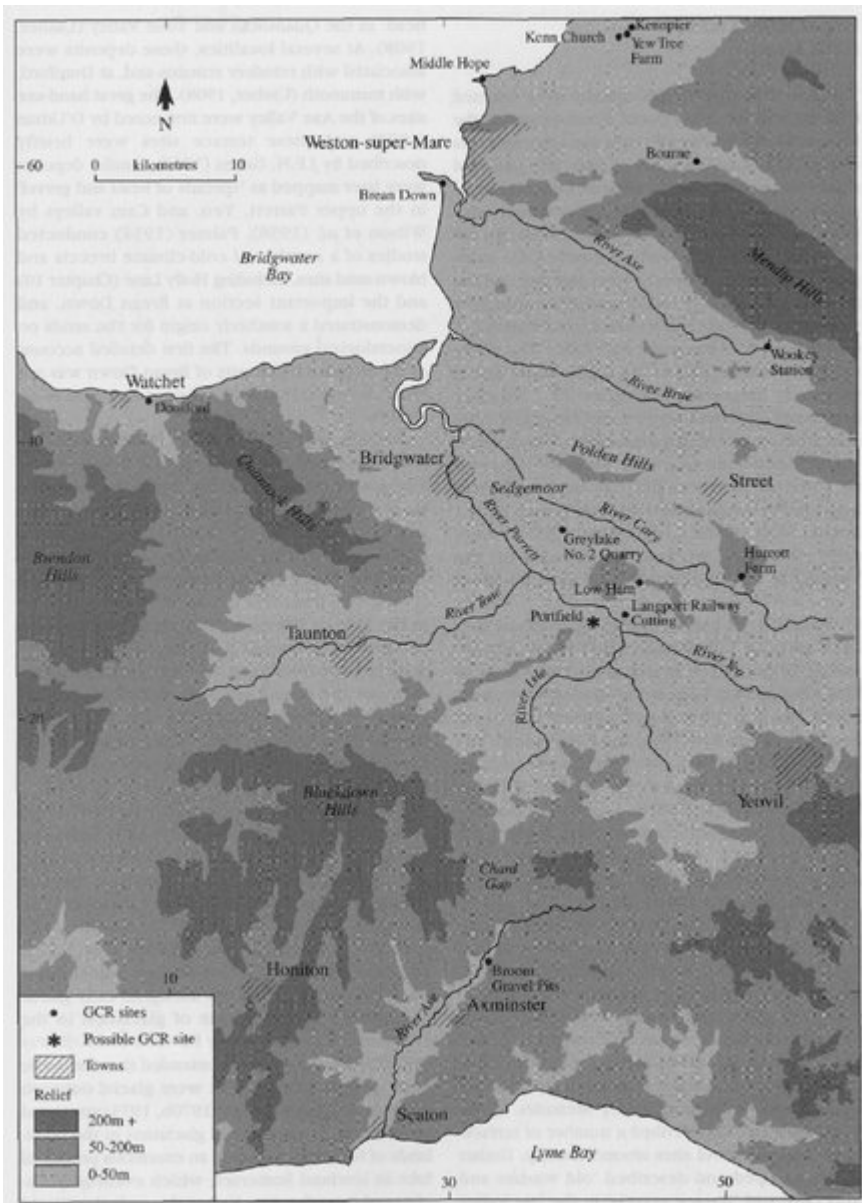
(Figure 8.12) The Pleistocene Sequence at the Battery section. (Adapted from Scourse, 1986.)



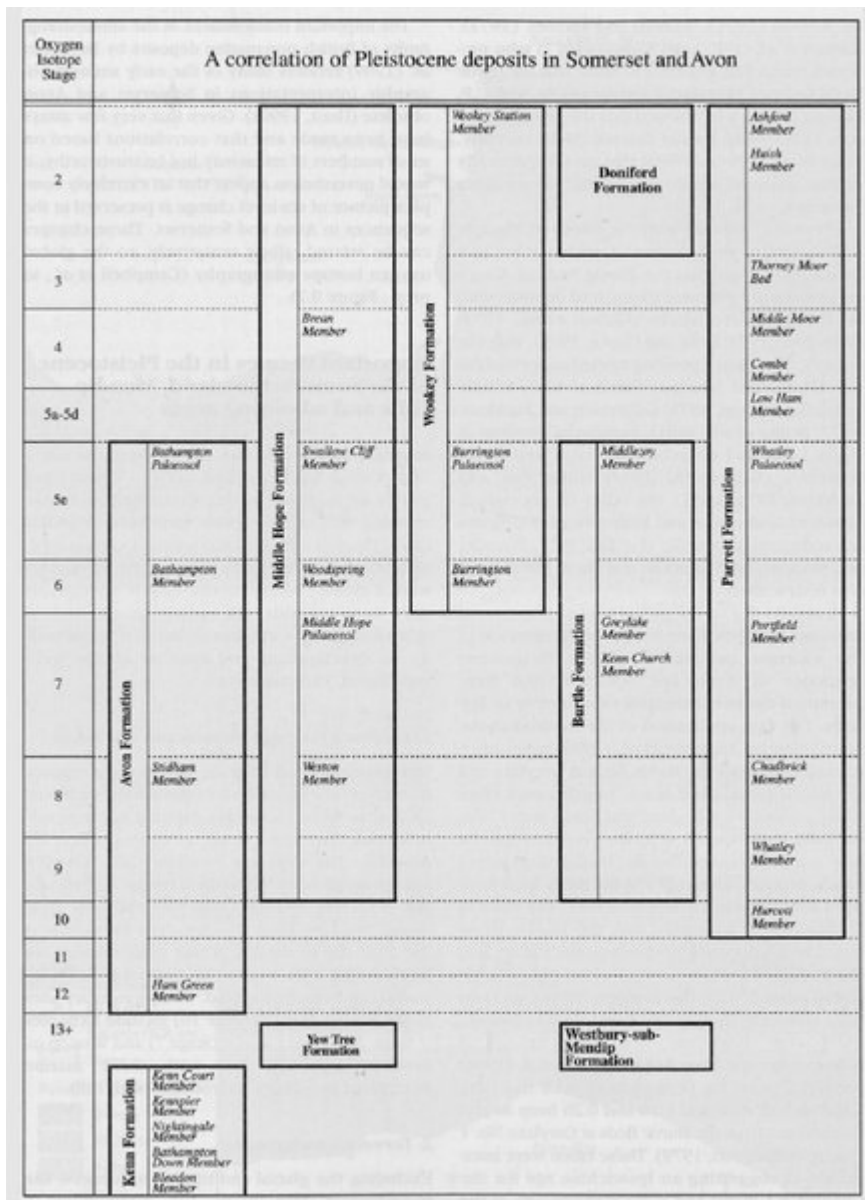
(Figure 8.13) Quaternary sediments exposed in coastal cliffs at Castle Porth, Treco. The Hell Bay Gravel at the northern end of the exposure (left) is rich in erratics, whereas erratics are absent at the southern end (right) of the section. (Photo: S. Campbell.)



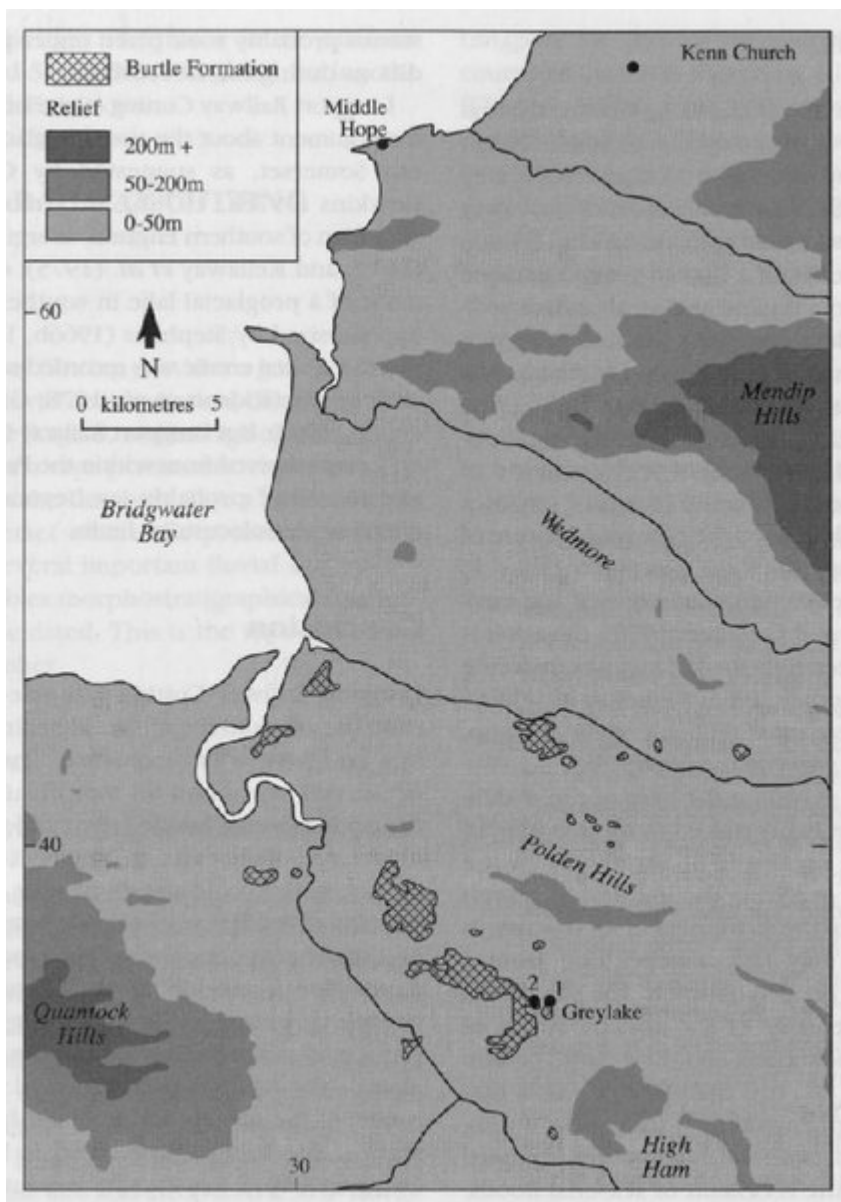
(Figure 8.14) Selected pollen data and radiocarbon dates for a peat profile at Higher Moors, St Mary's. (Adapted from Scaife, 1984.)



(Figure 9.1) The Mendips and Somerset lowland, showing GCR sites described in this chapter, and selected GCR sites described in Chapters 7 and 10.

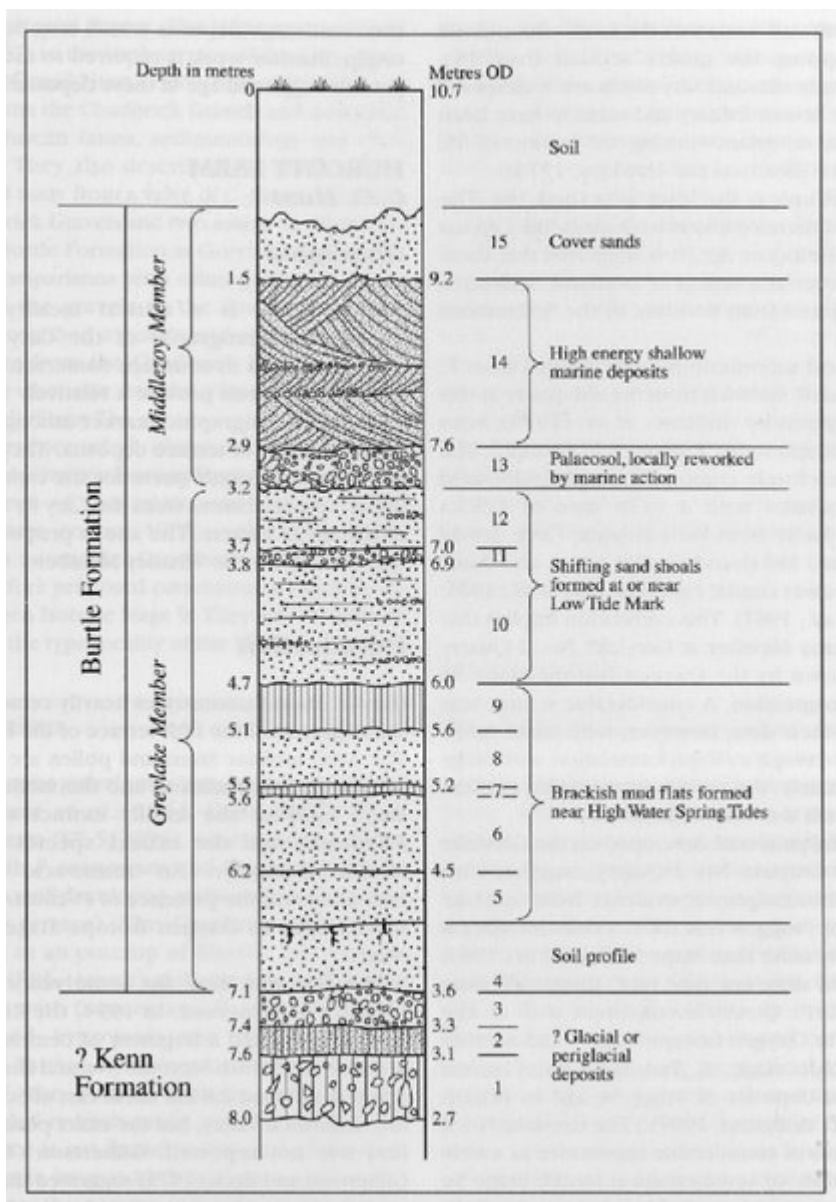


(Figure 9.2) A correlation of Pleistocene deposits in the Somerset lowland, Mendips, Bristol district and Avon Valley. (Adapted from Campbell et al., in prep.)

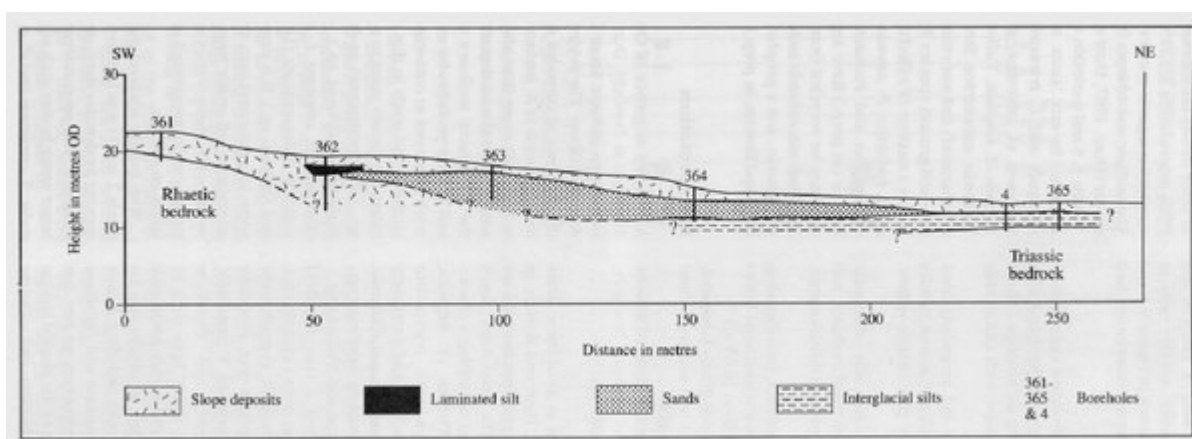


(Figure 9.3) The Burtle Formation of the Somerset lowland. (Adapted from Kidson et al., 1978 and Hunt, 1987.)



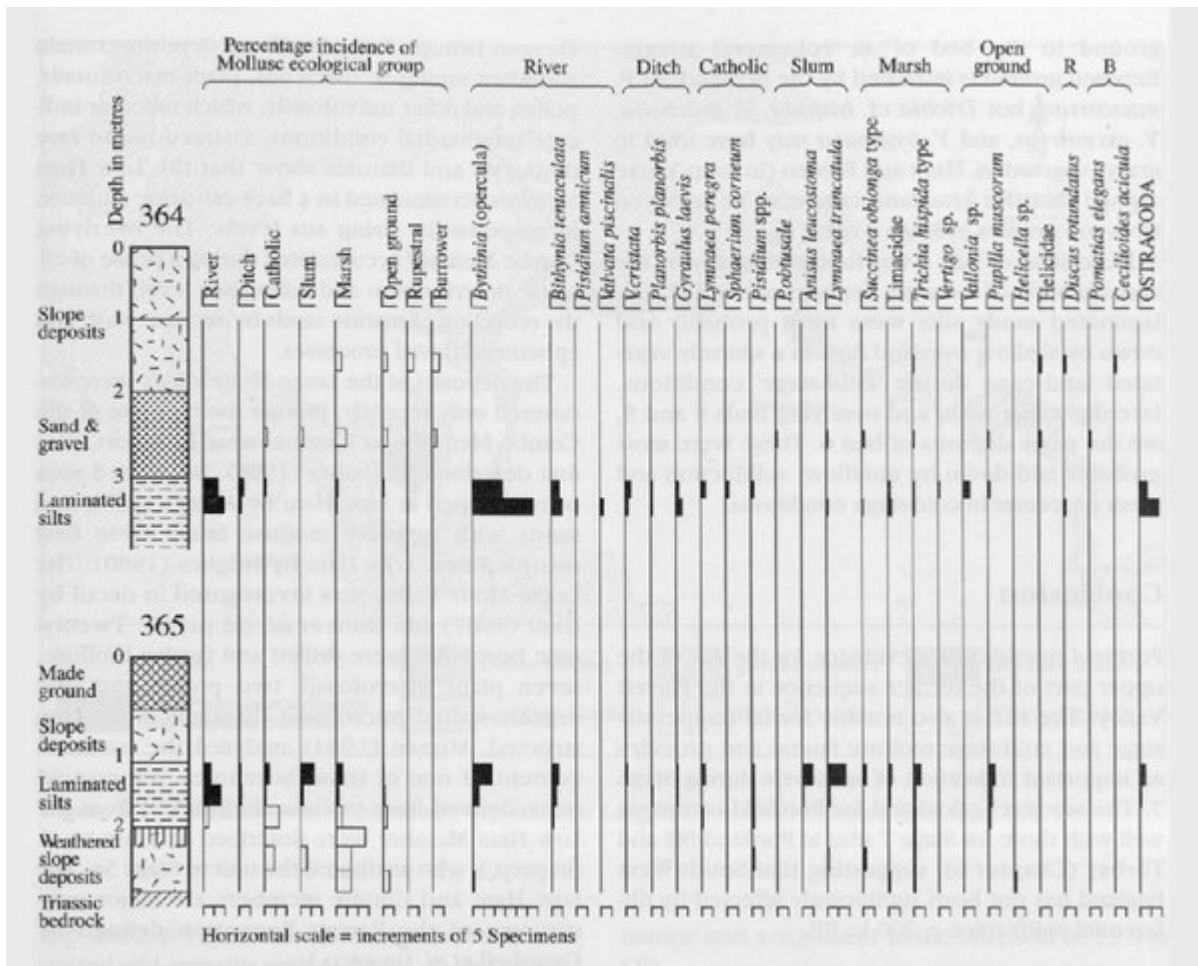


(Figure 9.4) An interpretation of the Quaternary sequence at Greylake No. 2 Quarry, adapted from Hughes (1980). Beds 1–15 are described in more detail in the text.

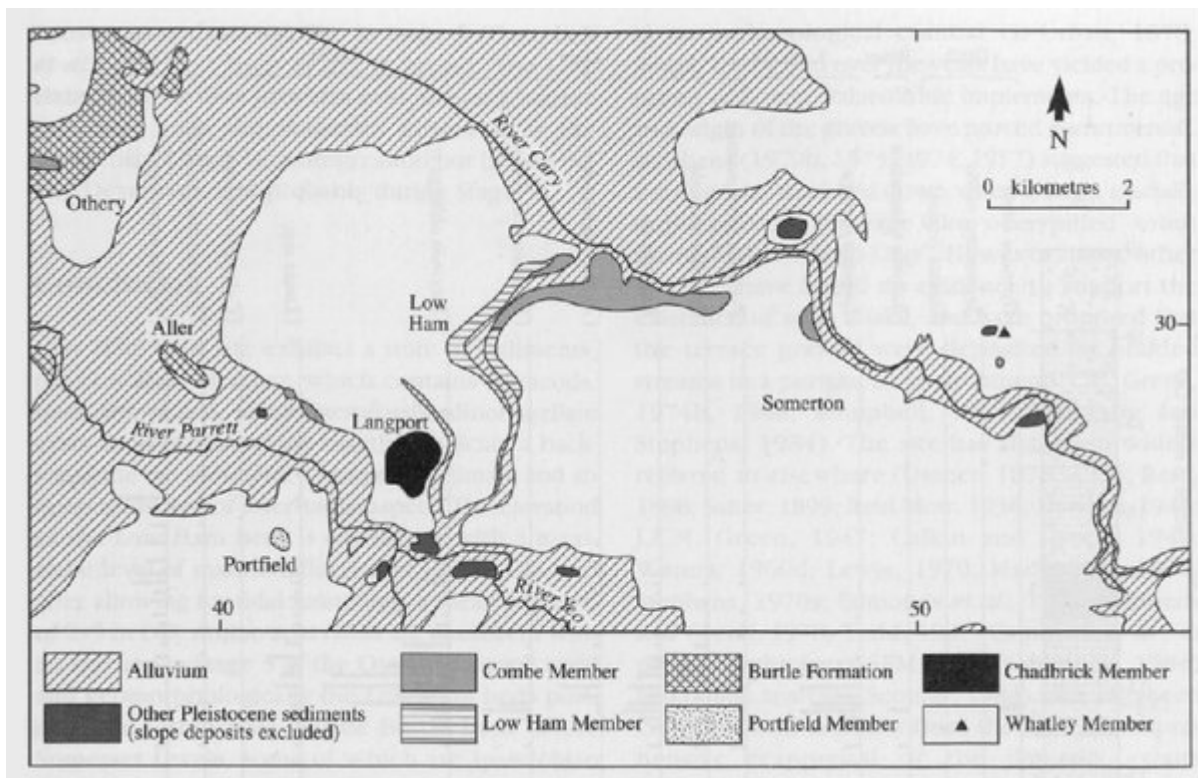


(Figure 9.5) A cross-section of the Pleistocene deposits at Portfield. (Adapted from Hunt, 1987.)

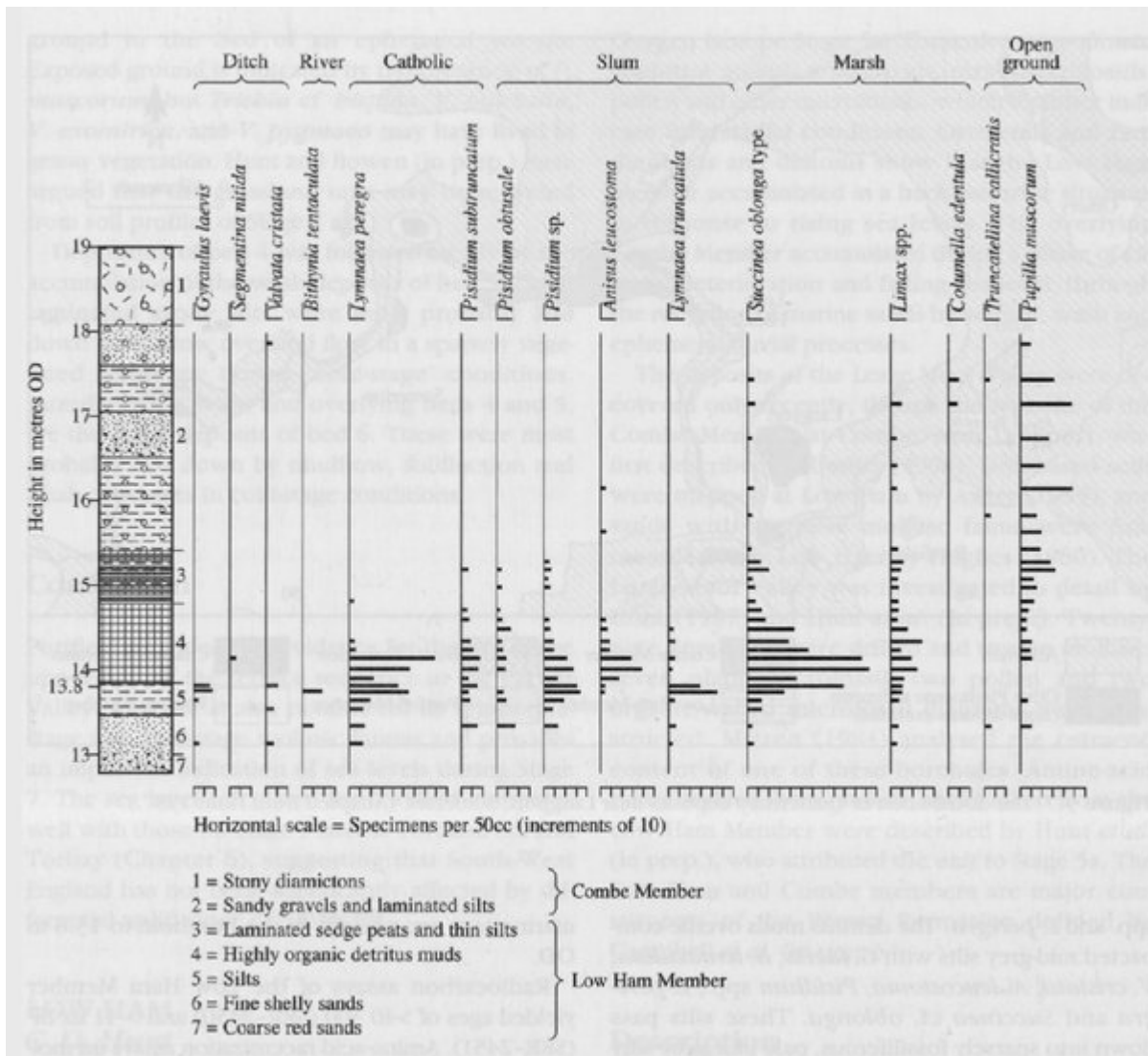




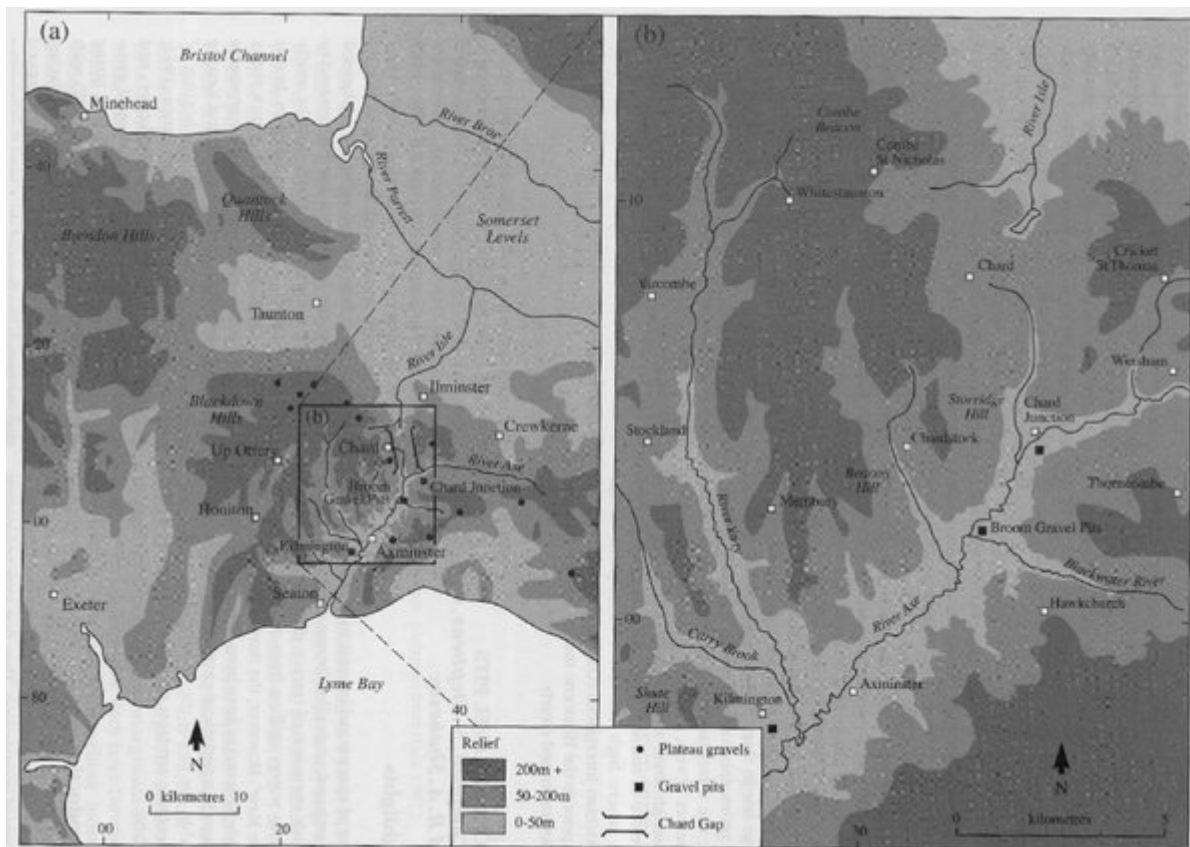
(Figure 9.6) The molluscan biostratigraphy of Pleistocene deposits at Portfield, adapted from Hunt (1987). Numbers 364 and 365 refer to boreholes shown in (Figure 9.5).



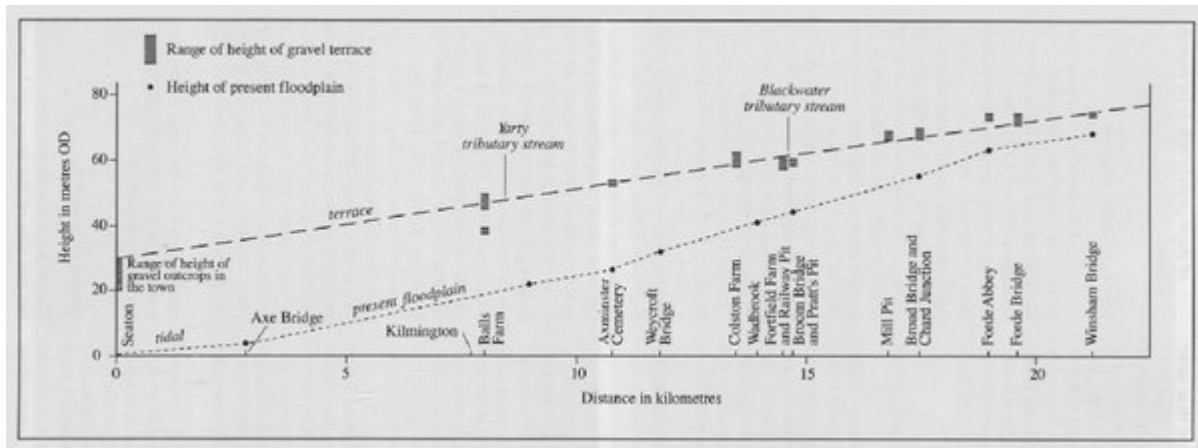
(Figure 9.7) The distribution of Quaternary deposits near Langport, Somerset. (Adapted from Hunt 1987.)



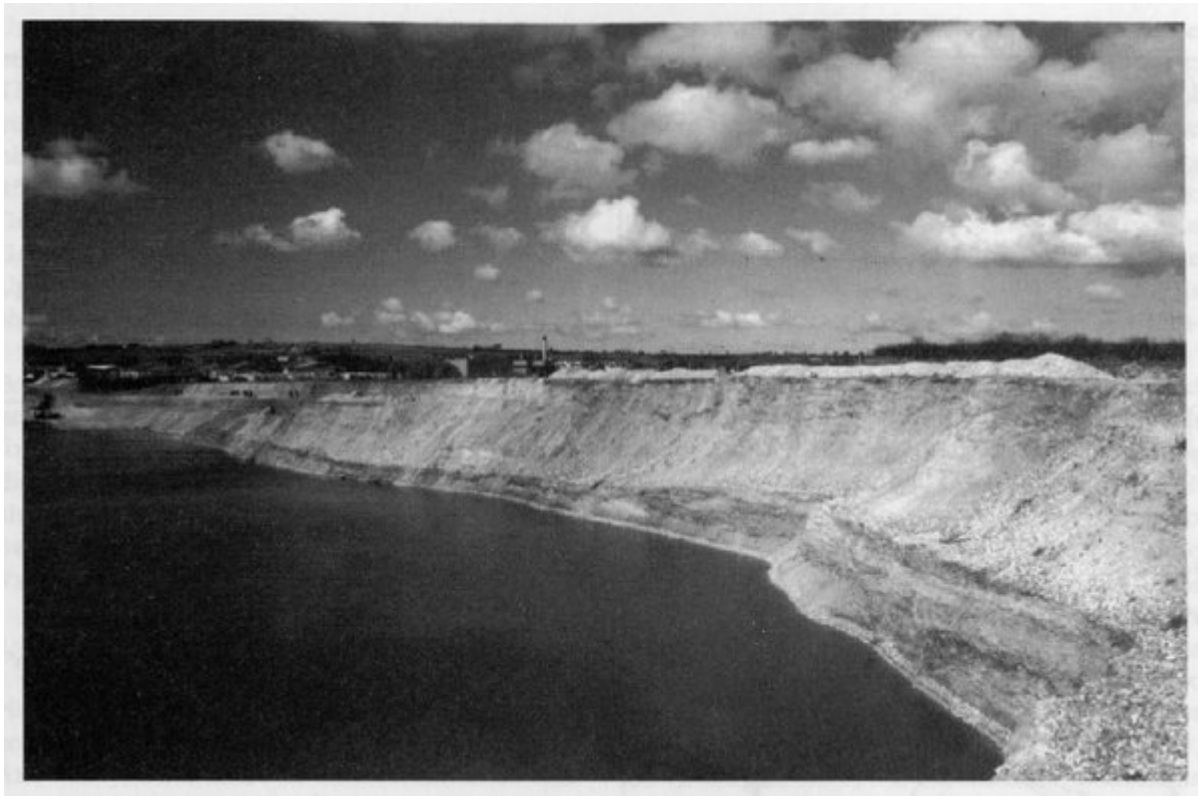
(Figure 9.8) The molluscan biostratigraphy of Pleistocene deposits at Low Ham. (Adapted from Hunt 1987.)



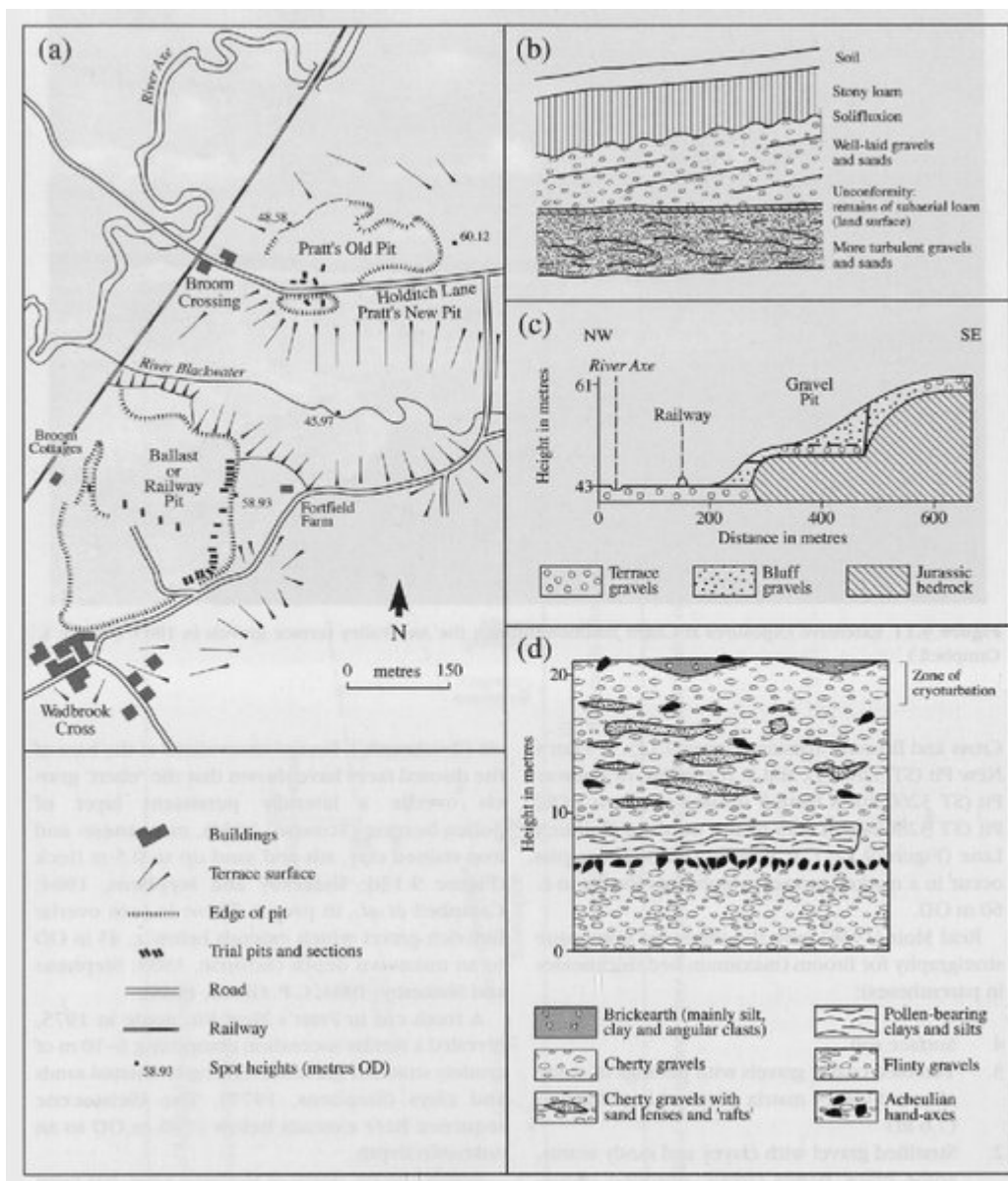
(Figure 9.9) (a) The topographic setting of the Axe Valley and the distribution of plateau-gravel sites. (b) The principal exposures of the Axe Valley terrace gravels. (Adapted from Stephens, 1977 and Green et al., in prep.)



(Figure 9.10) The long-profile of the modern River Axe, and the height-range and distribution of the principal terrace gravel outcrops. (Adapted from Green et al., in prep.)



(Figure 9.11) Extensive exposures at Chard Junction through the Axe Valley terrace gravels in 1985. (Photo: S. Campbell.)



(Figure 9.12) (a) Location of the Broom Gravel Pits, adapted from Green et al. (in prep.). (b) Schematic section of the Broom gravels, adapted from Reid Moir (1936) and Hawkes (1943). (c) An interpretation of a section of the Broom gravels, adapted from J.F.N. Green (1947) and Calkin and Green (1949). (d) A schematic composite section of the Broom gravels, adapted from Shakesby and Stephens (1984).

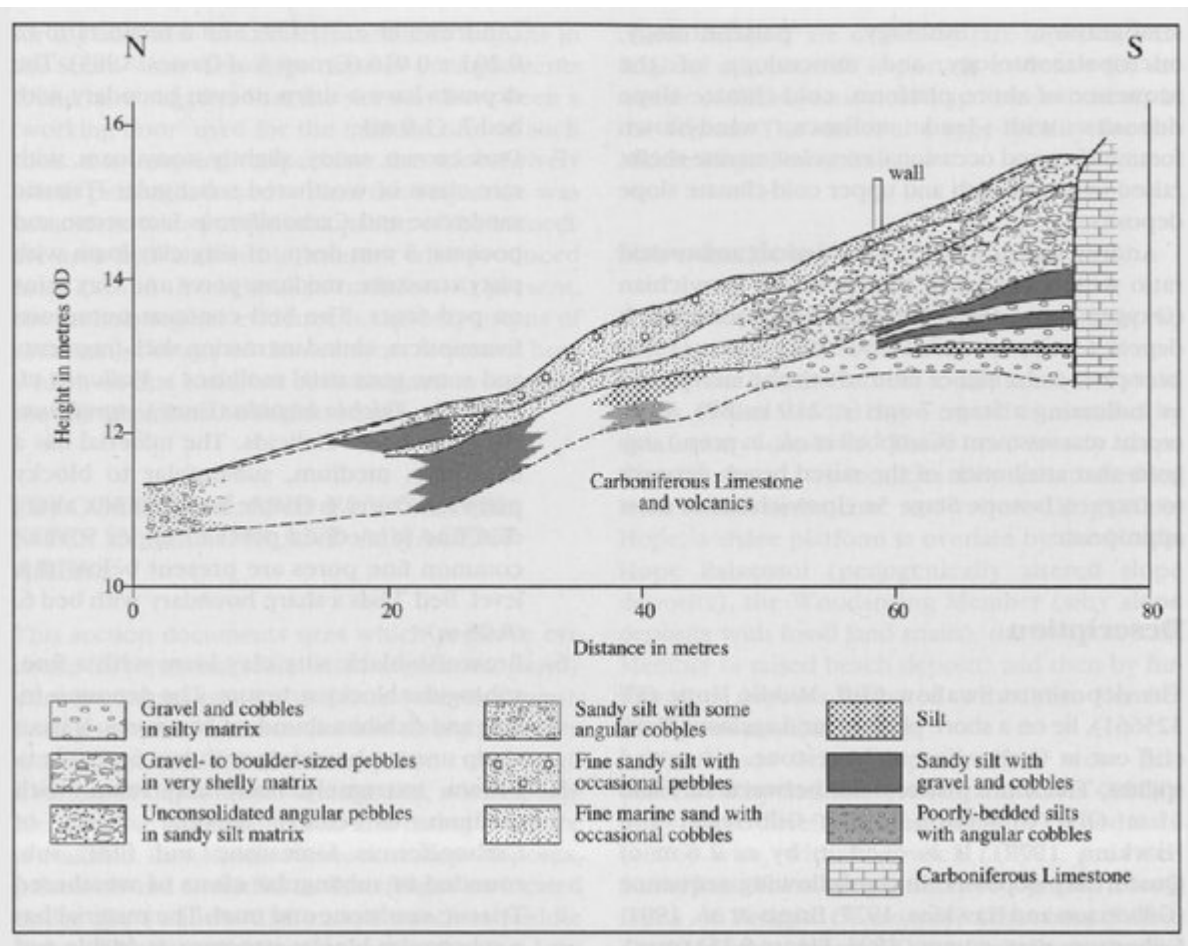


(Figure 9.13) 'Cherry' gravels with sand lenses, seen in the south-east faces of the disused Railway Pit at Broom in 1985. (Photo: S. Campbell.)

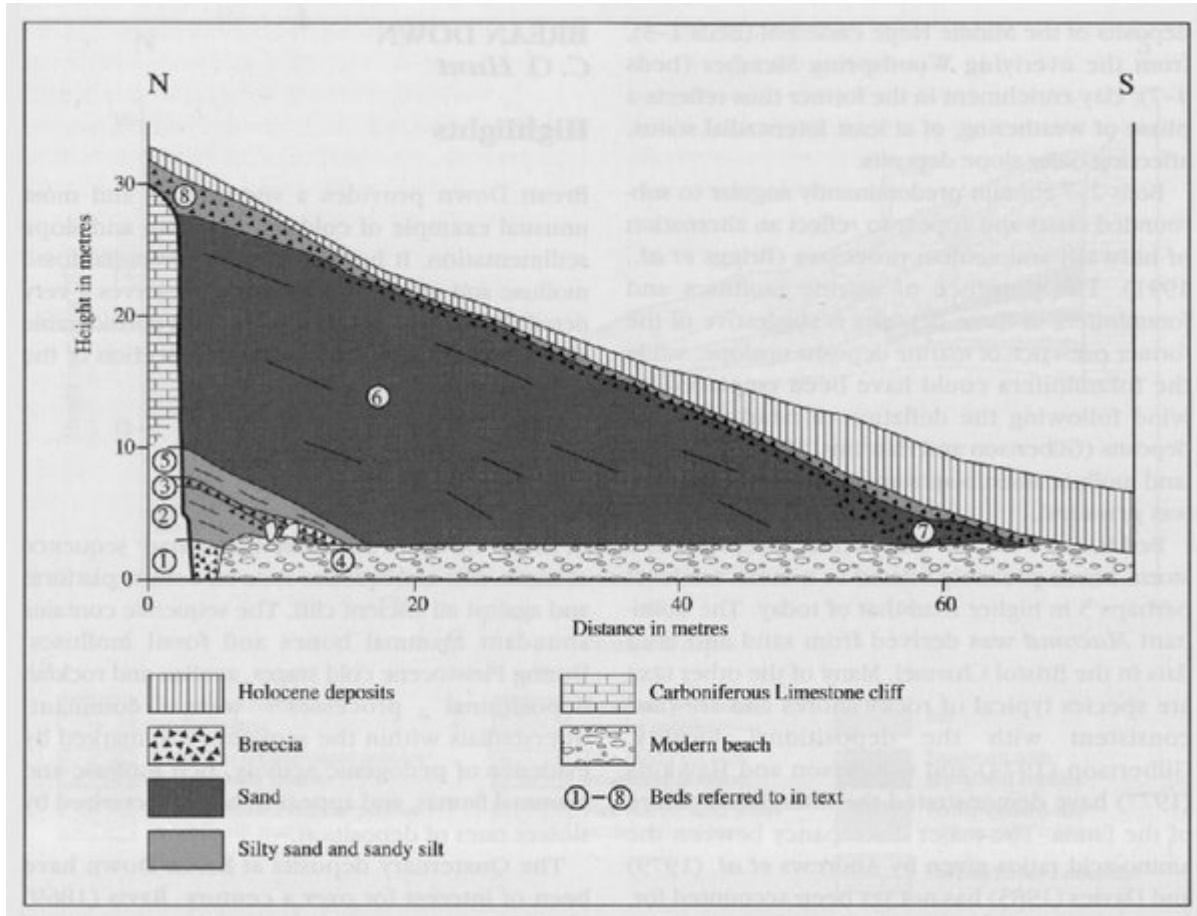


(Figure 9.14) Acheulian hand-axes from Broom, seen during the 1977 INQUA visit to South-West England. (Photo: N. Stephens.)

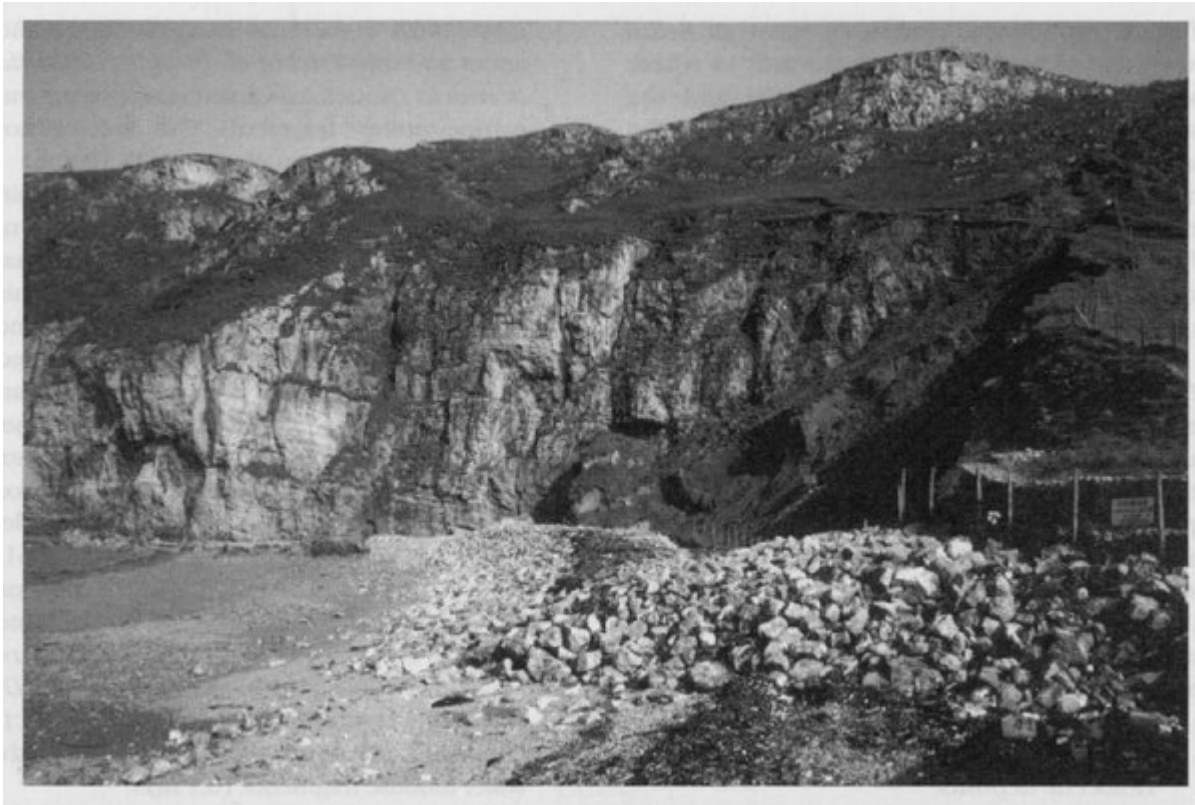




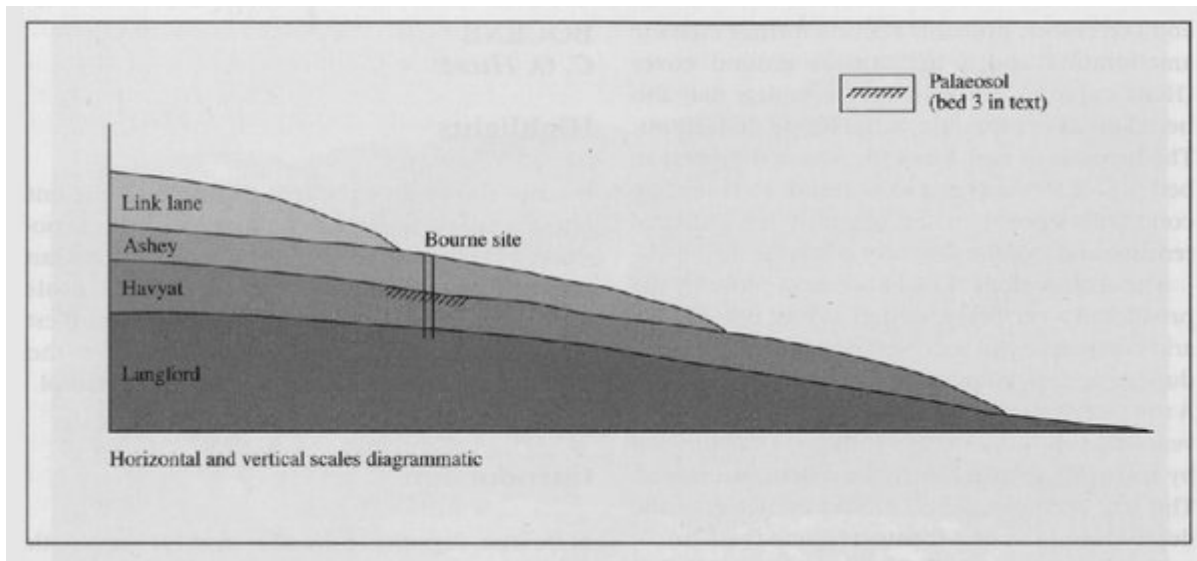
(Figure 9.15) Quaternary deposits at Swallow Cliff, Middle Hope, simplified from Gilbertson and Hawkins (1977).



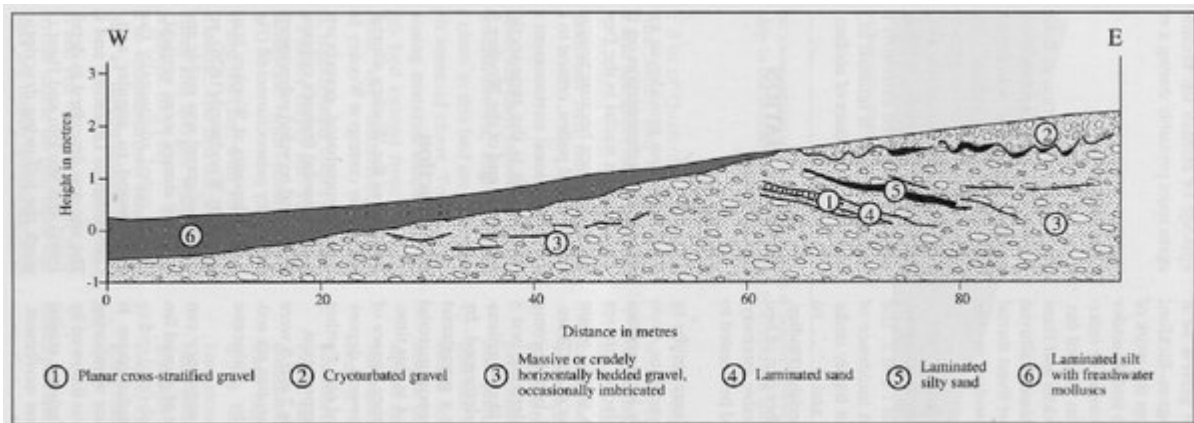
(Figure 9.16) The Quaternary sequence at Brean Down, simplified from ApSimon et al. (1961).



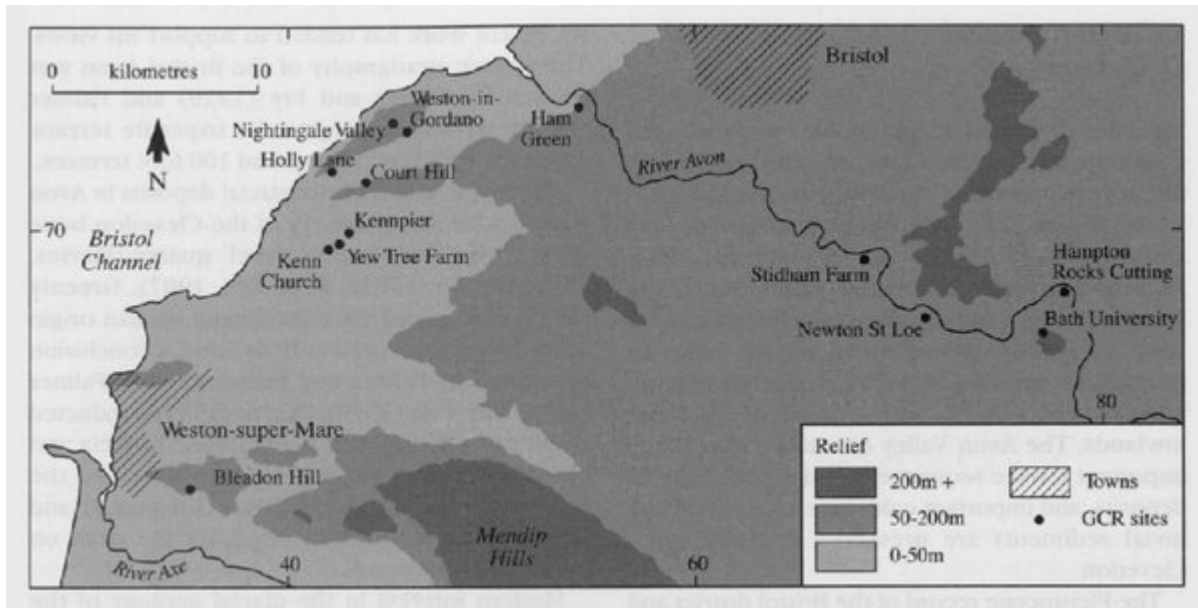
(Figure 9.17) The Pleistocene sequence at Brean Down. (Photo: S. Campbell.)



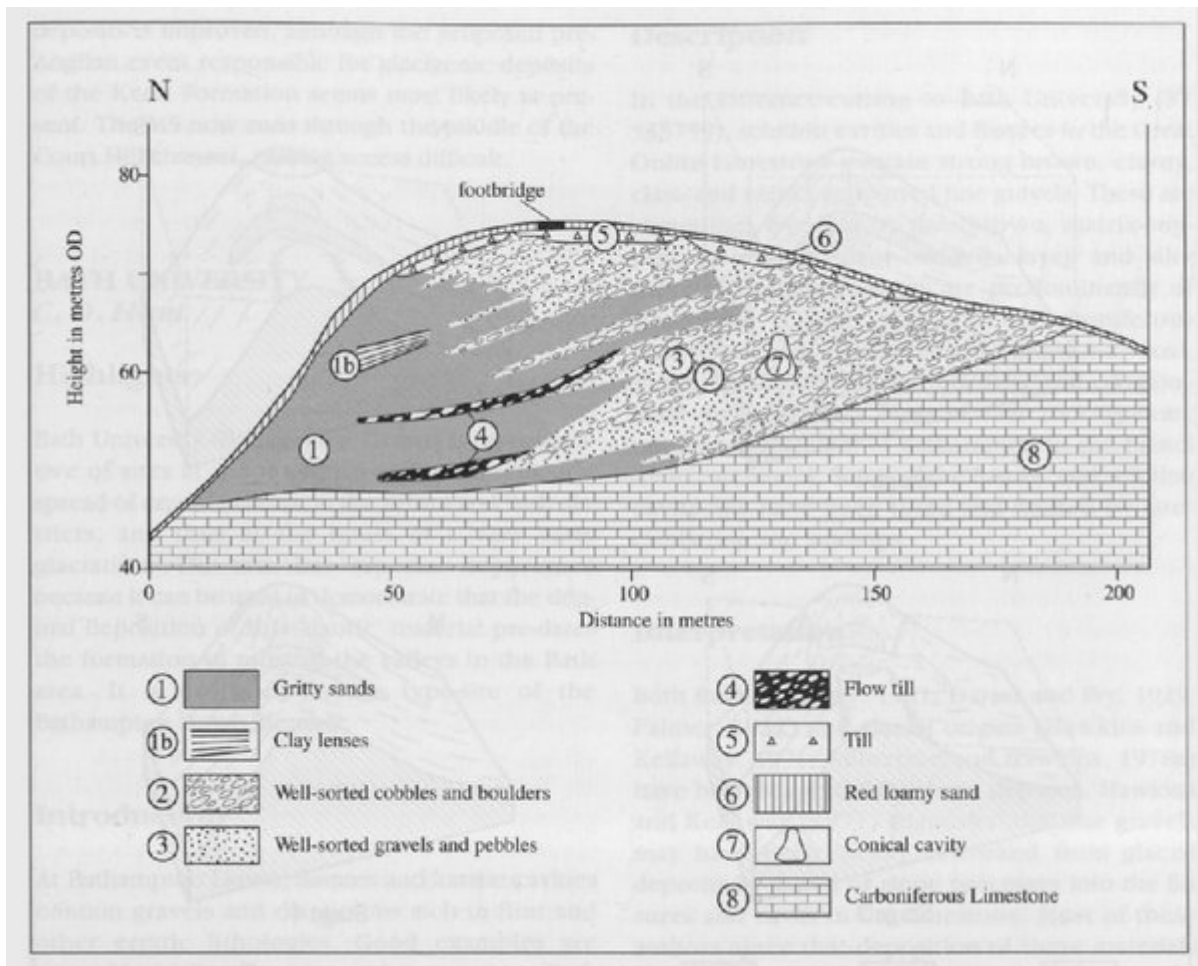
(Figure 9.18) Schematic cross-section of the Buffington fan at Bourne, showing the aggradational components of the fan and their relationship to the Bourne section. (Adapted from Pounder and Macklin, 1985.)



(Figure 9.19) The Quaternary sequence exposed in the old railway cutting at Wookey Station. (Adapted from Macklin and Hunt, 1988.)

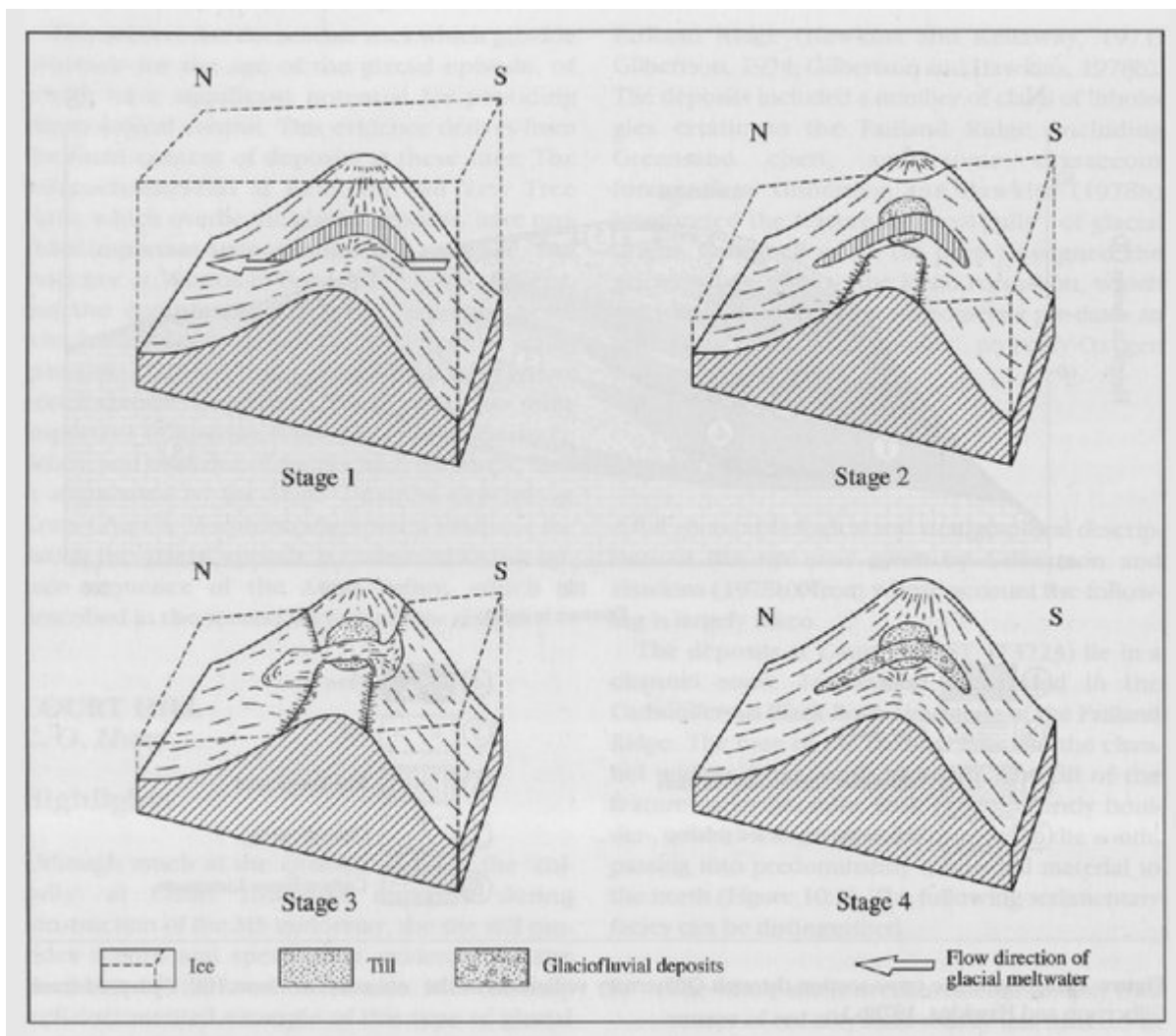


(Figure 10.1) The Avon Valley and Bristol district, showing GCR sites described in this chapter.

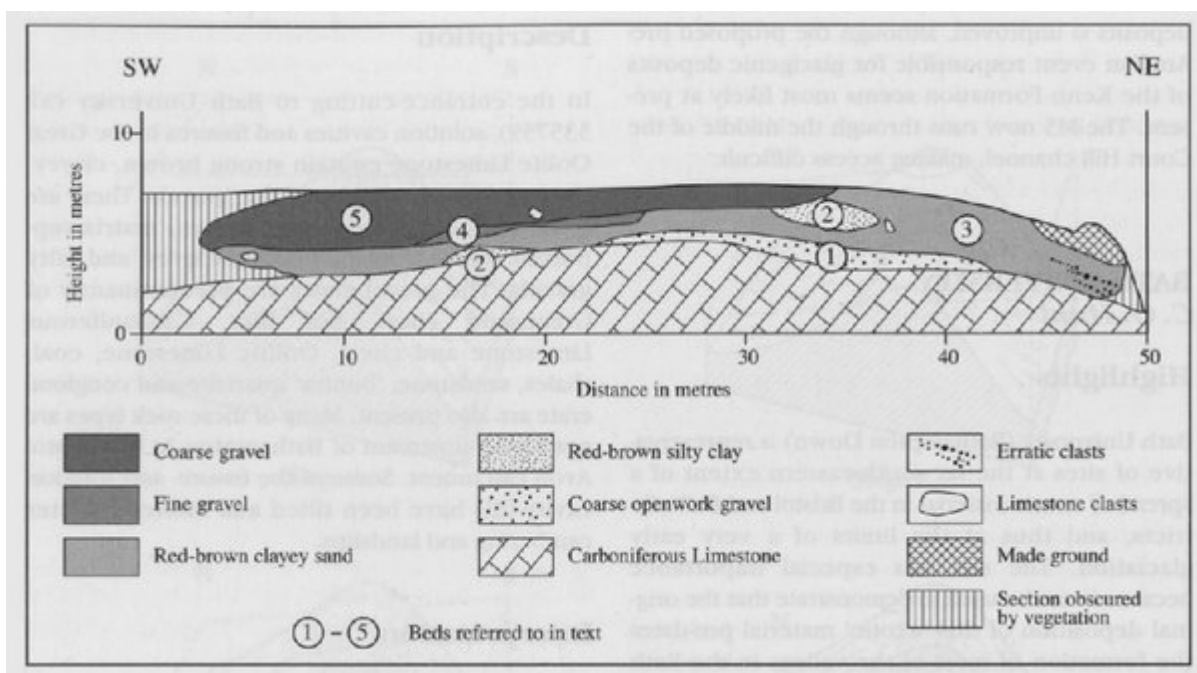


(Figure 10.2) Schematic cross-section through Quaternary sediments in the 'col-gully' at Court Hill. (Adapted from Gilbertson and Hawkins, 1978b.)

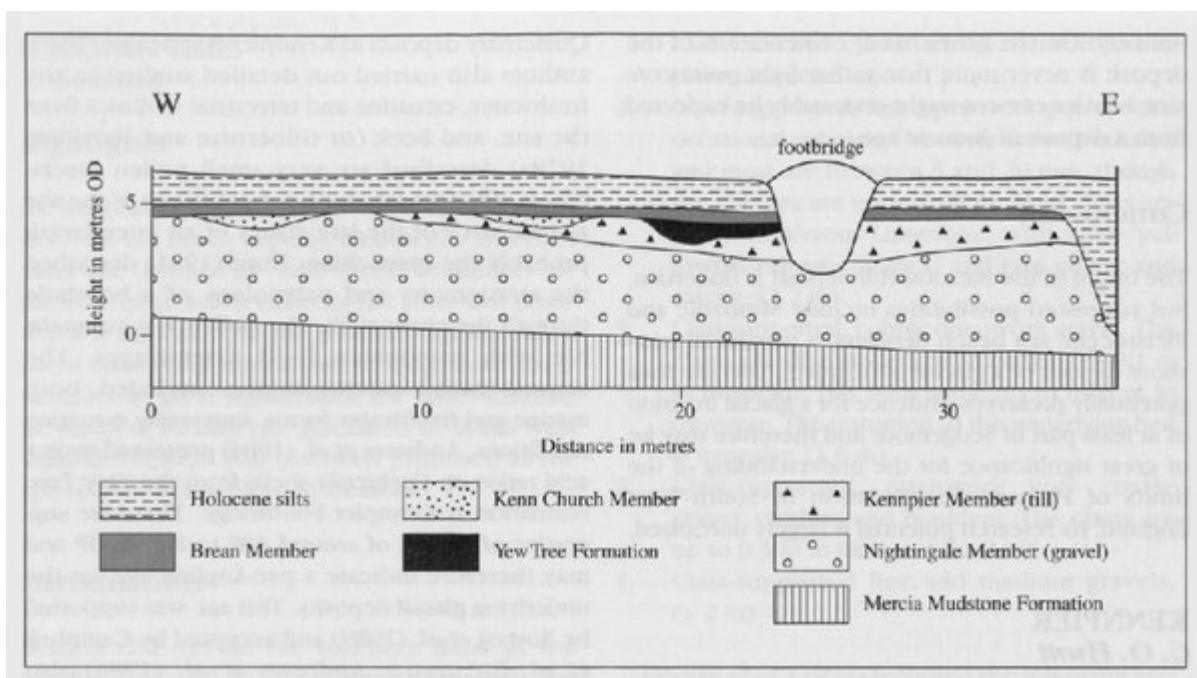




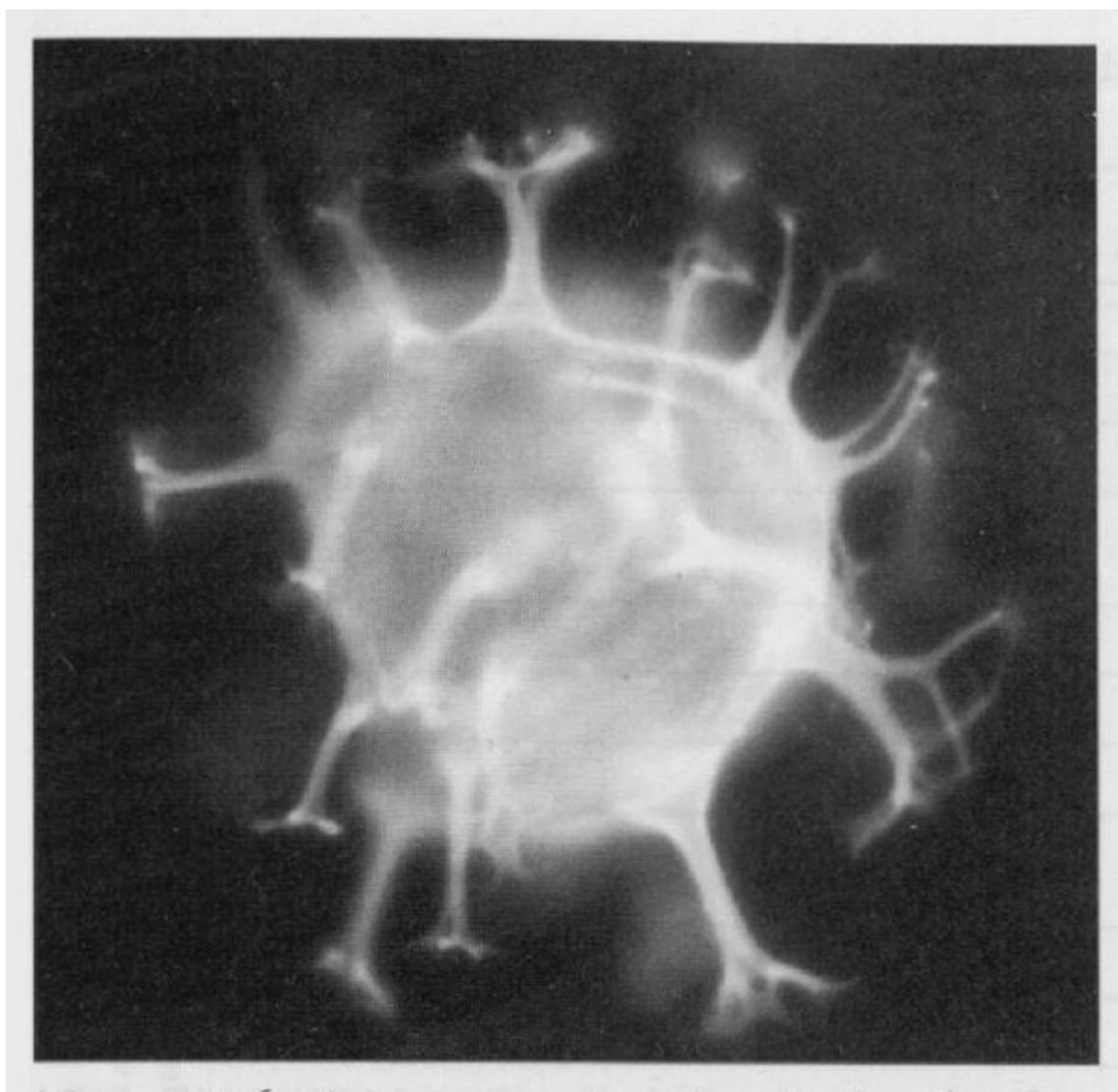
(Figure 10.3) A four-stage model to explain the formation of the Court Hill 'col-gully'. (Adapted from Gilbertson and Hawkins, 1978b.)



(Figure 10.4) The Pleistocene sequence at Nightingale Valley, adapted from Hunt (in prep.).

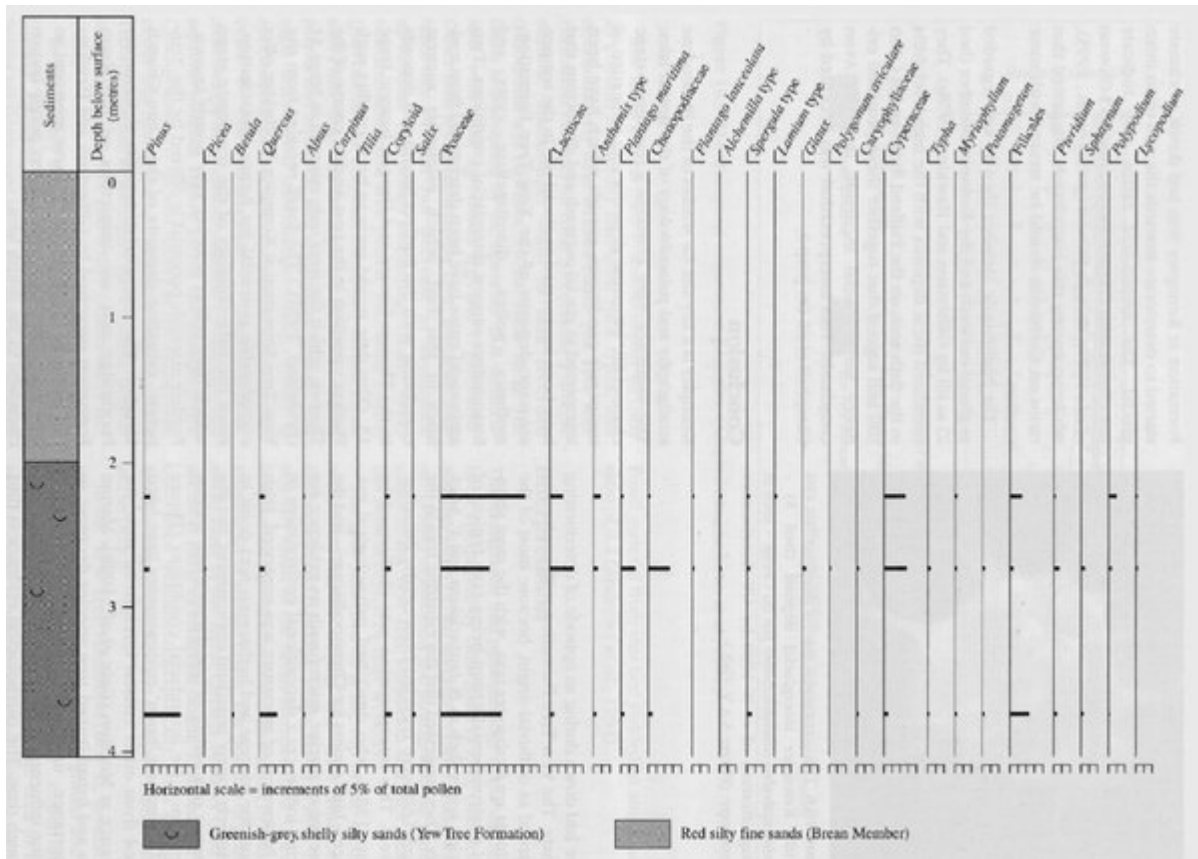


(Figure 10.5) The Quaternary sequence at Kennpier. (Adapted from Andrews et al., 1984.)

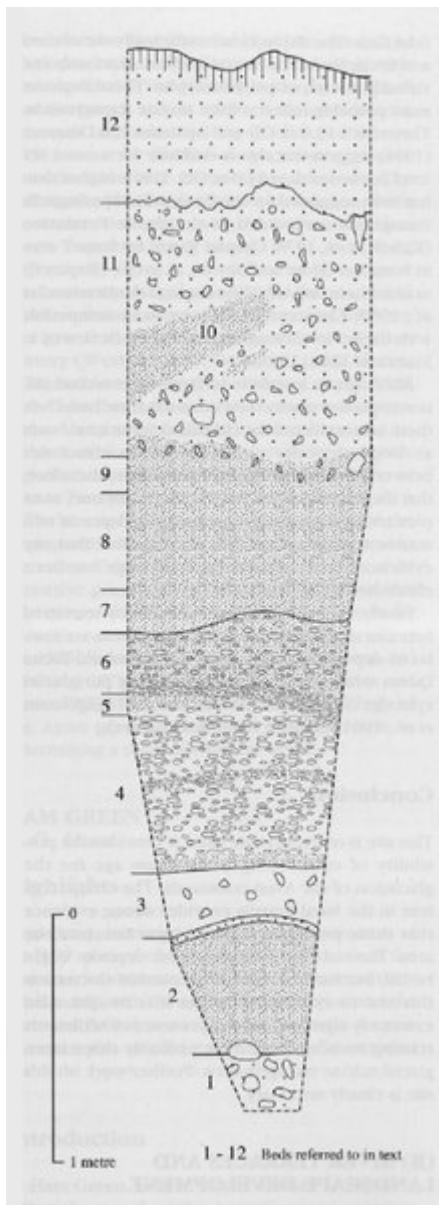


(Figure 10.6) The commonest marine dinoflagellate cyst in the Kennpier interglacial deposit (bed 3) - *Achomosphaera andalusiense* Jan du Chene — seen at a magnification of c. x 1000 by UV fluorescence microscopy. (Photo: S.A.V.)

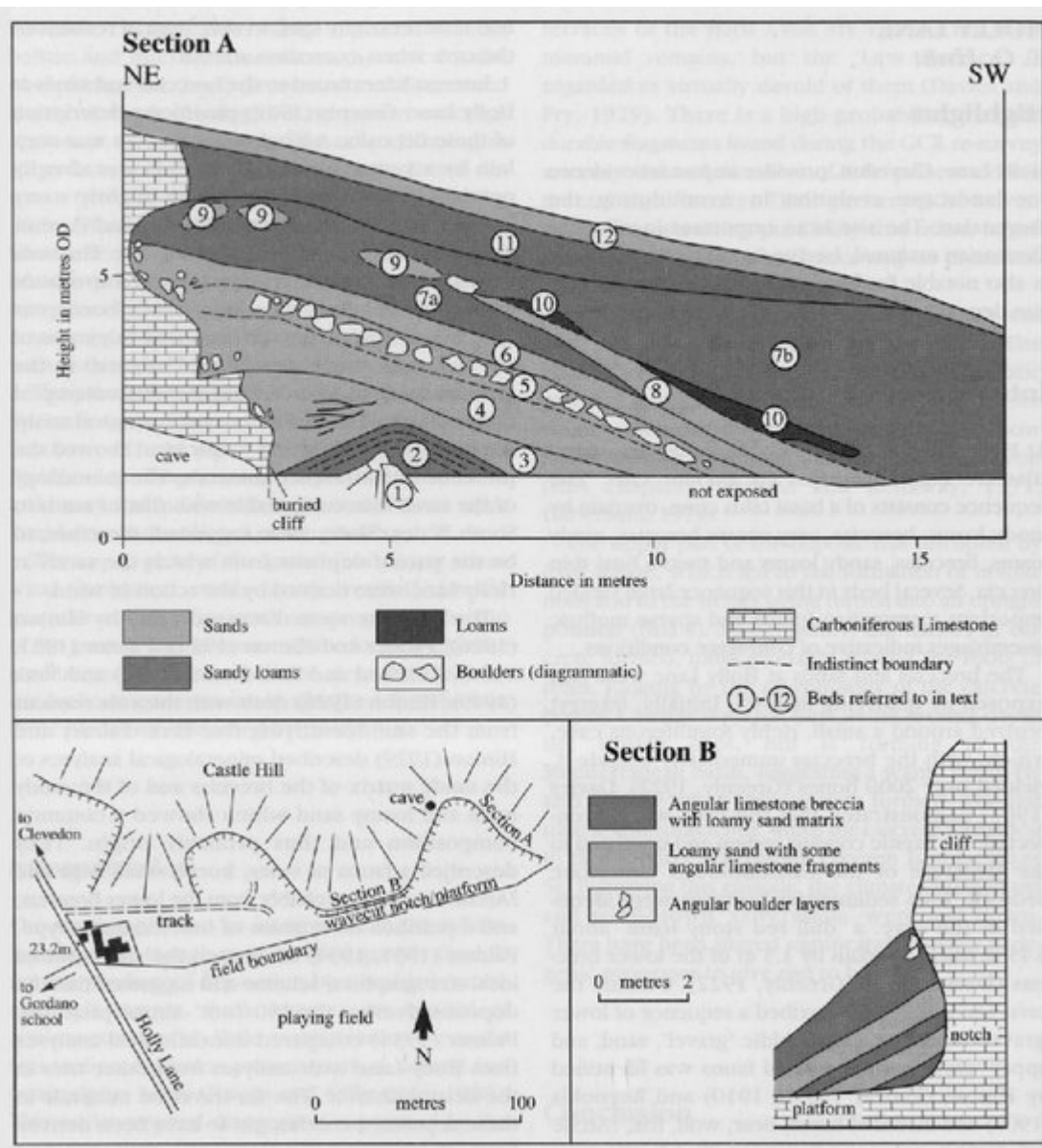
Hall.)



(Figure 10.7) Pollen diagram for Kennpier. (Adapted from Hunt, 1981.)



(Figure 10.8) The Quaternary sequence at Weston-in-Gordano. (Adapted from ApSimon and Donovan, 1956.)



(Figure 10.9) The Quaternary sequence at Holly Lane, Clevedon. (Adapted from Gilbertson and Hawkins, 1974.)

<i>Material</i>	<i>Lab. Ref.</i>	<i>Result (years BP)</i>	<i>Height (metres OD)</i>
wood	HAR-5642	4840 ± 70	-1.0
peat	HAR-6363	5190 ± 80	—
peat	HAR-5640	5200 ± 120	-2.1
wood	HAR-5631	6100 ± 100	-2.0
wood	HAR-5630	5630 ± 80	-2.0
peat	HAR-5641	5740 ± 100	-2.2

(Table 7.1) Radiocarbon dates from the outer peat.

<i>Species</i>	<i>Number</i>	<i>Percentage</i>
<i>Valvata cristata</i> (Müller)	1	0.4
<i>Valvata piscinalis</i> (Müller)	88	35.5
<i>Bithynia tentaculata</i> (Linné)	24	9.6
<i>Physa fontinalis</i> (Linné)	1	0.4
<i>Lymnaea stagnalis</i> (Linné)	1	0.4
<i>Lymnaea peregra</i> (Müller)	41	16.5
<i>Planorbis</i> spp.	2	0.8
<i>Gyraulus laevis</i> (Alder)	7	2.8
<i>Ancylus fluviatilis</i> (Müller)	1	0.4
<i>Unio</i> sp.	3	1.2
<i>Corbicula fluminalis</i> (Müller)	18	7.3
? <i>Sphaerium</i> sp.	1	0.4
<i>Pisidium amnicum</i> (Müller)	9	3.6
<i>Pisidium clessini</i> Neumayr	5	2.0
<i>Pisidium benslowanum</i> (Sheppard)	5	2.0
<i>Pisidium nitidum</i> Jenyns	1	0.4
<i>Pisidium subtruncatum</i> Malm	4	1.6
<i>Pisidium</i> spp.	22	8.9
<i>Oxyloma</i> cf. <i>pfeifferi</i>	5	2.0
<i>Cochlicopa</i> cf. <i>lubrica</i>	1	0.4
<i>Vallonia</i> cf. <i>pulchella</i>	1	0.4
<i>Discus rotundatus</i> (Müller)	1	0.4
? <i>Helicella</i> sp.	1	0.4
<i>Trichia</i> cf. <i>hispida</i>	6	2.4
<b>Total</b>	<b>248</b>	

(Table 9.1) Fossil molluscs from the Chadbrick Gravel.

Species	Profiles		
	KPA	KPB	KPD
<b>Marine</b>			
<i>Littorina littorea</i> (Linné)	3	-	1
<i>Littorina saxatilis</i> (Olivi)	1	-	-
<i>Littorina littoralis</i> (Linné)	5	1	-
<i>Littorina</i> spp.	13	1	2
<i>Retusa</i> sp.	-	-	1
<i>Nucella lapillus</i> (Linné)	3	-	-
<i>Ostrea</i> sp.	1	-	2
<i>Cerastoderma</i> spp.	2	-	frags
<i>Macoma balthica</i> (Linné)	36	1	16
<b>Land and freshwater</b>			
<i>Valvata piscinalis</i> (Müller)	127	72	423
<i>Belgrandia marginata</i> (Michaud)	14	-	13
<i>Bitbynia tentaculata</i> (Linné) shells	3	-	4
<i>Bitbynia tentaculata</i> (Linné) opercula	1092	3579	5619
<i>Lymnaea peregra</i> (Müller)	12	-	65
<i>Anisus leucostoma</i> Müller	-	-	1
<i>Gyraulus laevis</i> Alder	4	-	1
<i>Armiger crista</i> (Linné)	1	-	1
<i>Planorbis</i> spp.	-	-	1
<i>Ancylus fluviatilis</i> Müller	2	-	-
<i>Tricbita bispida</i> (Linné)	-	-	15
<i>Zonitoides nitidus</i> (Müller)	-	-	1
<i>Agrolimax</i> cf. <i>agrestis</i> (Linné)	70	70	128
<i>Agrolimax</i> cf. <i>reticulatus</i> (Müller)	30	43	35
<i>Agrolimax</i> cf. <i>laevis</i> (Müller)	6	-	22
<i>Agrolimax</i> spp.	65	56	162
<i>Corbicula fluminalis</i> (Müller)	-	20	24
<i>Pisidium amnicum</i> (Müller)	4	6	7
<i>Pisidium obtusale</i> (Lamarck)	-	-	1
<i>Pisidium subtruncatum</i> Malm	5	-	1
<i>Pisidium henslowanum</i> (Sheppard)	1	-	-
<i>Pisidium nitidum</i> Jcnyns	5	-	1
<i>Pisidium moltessierianum</i> Paladilhe	-	-	1
<i>Pisidium</i> spp.	13	4	13
<b>Total</b>	<b>1560</b>	<b>3854</b>	<b>6564</b>

(Table 10.1) Fossil molluscs from three profiles through the interglacial channel-fill at Kennpier Footbridge (after Gilbertson and Hawkins, 1978a).

<i>Species</i>	<i>Number</i>
<i>Valvata cristata</i> Müller	12
<i>Valvata piscinalis</i> (Müller)	3324
<i>Belgrandia marginata</i> (Michaud)	970
<i>Bitbynia tentaculata</i> (Linné) shells	1039
<i>Bitbynia tentaculata</i> (Linné) opercula	1755
<i>Carychium minimum</i> Müller	2
<i>Lymnaea truncatula</i> (Müller)	192
<i>Lymnaea palustris</i> (Müller)	1
<i>Lymnaea peregra</i> (Müller)	886
<i>Planorbis planorbis</i> (Linné)	25
<i>Anisus vorticulus</i> Troschel	147
<i>Anisus leucostoma</i> Müller	141
<i>Gyraulus laevis</i> Alder	1613
<i>Armiger crista</i> (Linné)	615
<i>Planorbis</i> spp.	3
<i>Hippentis complanata</i> (Linné)	21
<i>Acroloxus lacustris</i> (Linné)	8
<i>Oxytoma</i> cf. <i>pfeifferi</i> Rossmässler	6
<i>Cochlicopa lubrica</i> (Müller)	2
<i>Pupilla muscorum</i> (Linné)	2
<i>Vallonia costata</i> (Müller)	4
<i>Vallonia pulchella</i> (Müller)	6
<i>Vallonia</i> spp.	1
<i>Cepaea nemoralis</i> (Linné)	1
<i>Trichia bispida</i> (Linné)	3
<i>Punctum pygmaeum</i> Draparnaud	1
<i>Zonitoides nitidus</i> (Müller)	4
<i>Agrolimax</i> cf. <i>agrestis</i> (Linné)	6
<i>Agrolimax</i> spp.	42
<i>Spbaerium corneum</i> (Linné)	1
<i>Corbicula fluminalis</i> (Müller)	72
<i>Pisidium amnicum</i> (Müller)	44
<i>Pisidium casertanum</i> (Poli)	7
<i>Pisidium obtusale</i> (Lamarck)	10
<i>Pisidium milium</i> Held	56
<i>Pisidium subtruncatum</i> Malm	138
<i>Pisidium benslowanum</i> (Sheppard)	24
<i>Pisidium nitidum</i> Jenyns	270
<i>Pisidium pulchellum</i> Jenyns	2
<i>Pisidium moltessterianum</i> Paladilhe	3
<i>Pisidium</i> spp.	190
Total	11 649

(Table 10.2) Fossil molluscs from the interglacial deposit at Yew Tree Farm (after Gilbertson and Hawkins, 1978a).



Sample	A	B	C	D	E	G	J	O
Sample depth (m)	2.7	2.2	1.7	1.5	1.2	0.8	unstratified	
<b>Marine/estuarine taxa</b>								
<i>Patella vulgata</i> Linné						2		
<i>Gibbula</i> sp.							1	
<i>Littorina littorea</i> (Linné)	1						2	
<i>Littorina saxatilis</i> (Olivi)	2						1	
<i>Littorina littoralis</i> (Linné)	1				1	1		
<i>Littorina</i> sp.	2f	f	2f	1f		f	f	f
<i>Nucella lapillus</i> (Linné)							1	2
<i>Ocenebra erinacea</i> (Linné)						1	1	
<i>Buccinum undatum</i> (Linné)							1	3
<i>Nassarius reticulatus</i> (Linné)							1	
<i>Cerastoderma</i> spp.	3f	8f	1f	f		f	f	1f
<i>Macoma balthica</i> (Linné)	7f	16f	23f	2f		6f	90f	50f
<b>Brackish-water taxa</b>								
<i>Hydrobia ventrosa</i> Montagu	163	125	16	2		1		
<i>Hydrobia ulvae</i> (Pennant)	103	75	19	4		2	1	
<b>Freshwater taxa</b>								
<i>Valvata piscinalis</i> (Müller)	6	2						
<i>Belgrandia marginata</i> (Michaud)	1							
<i>Bitbyntia tentaculata</i> (Linné)	3							
<i>Lymnaea peregra</i> (Müller)	20	14	5					
<i>Planorbis planorbis</i> (Linné)	1	2						
<i>Anisus vorticulus</i> Troschel	2							
<i>Gyraulus laevis</i> (Alder)	11	15	1					
<i>Corbicula fluminalis</i> (Müller)						2		
<i>Pisidium subtruncatum</i> Malm	1							
<i>Pisidium nitidum</i> Jenyns	1							
<i>Pisidium moltesstertanum</i> Paladilhe	1							
<i>Pisidium</i> spp.	2	2						
<b>Terrestrial taxa</b>								
<i>Vallonia pulchella</i> (Müller)	1							
<i>Vallonia enntensis</i> (Gredler)		1						
<i>Trichia striolata</i> Pfeiffer	1							
<i>Helicella virgata</i> (Da Costa)						1		
<i>Discus rotundatus</i> (Müller)						1		

(Table 10.3) Molluscs from the interglacial deposit at Kenn Church (after Gilbertson, 1974; Gilbertson and Hawkins, 1978a).